STUDIES ON THERMAL CHARACTERISTICS OF NANOFLUIDS IN HEAT PIPE

A thesis submitted in fulfilment of the requirements for the Degree of

DOCTOR OF PHILOSOPHY

By

BHUPINDER SINGH BHULLAR
Registration Number: 950801001

Under the supervision of

Dr. D. GANGACHARYULU
Professor
Department of Chemical Engineering
Thapar University

and

Dr. SARIT KUMAR DAS
Professor
Department of Mechanical Engineering
Indian Institute of Technology Madras
(Presently, Director - IIT Ropar)

DEPARTMENT OF CHEMICAL ENGINEERING
THAPAR UNIVERSITY, PATIALA 147004, INDIA

May 2016

THESIS CERTIFICATE

This is to certify that the thesis entitled **"STUDIES ON THERMAL CHARACTERISTICS OF NANOFLUIDS IN HEAT PIPE"** submitted by **BHUPINDER SINGH BHULLAR,** in fulfillment of the requirements for the award of the Degree of **Doctor of Philosophy** in the Department of Chemical Engineering, **Thapar University, Patiala (INDIA)** is a bonafide record of research work carried out by him under our supervision and guidance. The contents of this thesis, in full or in parts, have not been submitted to any other Institute or University for the award of any degree or diploma.

D. Gangacharyulu
Professor
Department of Chemical Engineering
Thapar University, Patiala,
Punjab, INDIA

(Supervisor)

Sarit Kumar Das
Professor
Indian Institute of Technology -Madras
Chennai, INDIA
(Presently Director-IIT Ropar)

(Co- Supervisor)

DECLARATION

I, **Bhupinder Singh Bhullar,** hereby declare that the thesis, entitled **"STUDIES ON THERMAL CHARACTERISTICS OF NANOFLUIDS IN HEAT PIPE"**, submitted to the **Thapar University**, in partial fulfillment of the requirements for the award of the Degree of Doctor of Philosophy in Chemical Engineering is a record of original and independent research work done by me during the period 2009 – 2016, under the supervision and guidance of **Dr. D. Gangacharyulu**, Professor, Department of Chemical Engineering, Thapar University and under the Joint Supervision of **Dr. Sarit Kumar Das**, Professor, Department of Mechanical Engineering, IIT-Madras (Presently, Director- IIT Ropar). The work contained in this thesis has not been previously submitted to meet the requirements for a degree or diploma at this or any other higher education institution.

(Bhupinder Singh Bhullar)
Regd. No 950801001

ACKNOWLEDGEMENTS

I would like to express my gratitude to my supervisor Dr. D. Gangacharyulu and joint supervisor Dr. Sarit Kumar Das for the useful comments, remarks and engagement through the learning stages of this doctorate work.

The day, I along with Dr. Gangacharyulu thought of taking up the research activity with the nanoparticles, it seems as if fighting a war without ammunition. It was an area of research we had never thought of and the local initial expertise and guidance was way ahead. Dr. Gangacharyulu inspiration and motivation helped me to stay focused on this particular subject. The use of nanoparticles in the fluids as an excellent heat transfer carrier stormed our brains further in exploring its potential use in heat pipes. We become passionate in exploring the use of nanoparticles in the working fluid of heat pipes. I owe particular thanks to Dr. Gangacharyulu, whose penetrating questions taught me to question more deeply.

While surfing the research publications and the worldwide eminent personalities who already travelled the nano-research path in the domain of nanofluids, Dr.Sarit Kumar Das was found to be one of the leading researchers known worldwide for his marvelous and in depth contribution in understanding the anomalous enhancement in thermal conductivity of nanofluids.

I am kind enough to Dr. Sarit Kumar Das who had given me space in his research group and had shown me the challenges ahead as applicative to nanofluids. His multidimensional approach in solving a particular problem is worth mentioning.

I am also thankful to research scholars Mr. Pawan, Mr. Manoj and Mr. Anoop who while working in the HTTP laboratory at IITM Chennai facilitated me in carrying out the initial research work and guidance.

I am indebted to Dr. Baldev Raj, former Director IGCAR-Kalpakkam who facilitated my visits to the newly setup Center for Nanoscience and Nanotechnology (CNSNT). The visit acquainted me with the latest equipments and testing facilities available in the state of the art laboratory.

I would like to express my special appreciation and thanks to PhD coordinator Dr. Bhunia, you have been a tremendous mentor for me. I would like to thank you for encouraging and motivating me to complete my research workwithin bounded timelines.

I would also like to thank Dr.Bajpai, Dr. Mohapatra and Dr. Raj Kumar Gupta fortheir brilliant comments and suggestions showered during the interim research evaluations and presentations.

The research work carried by me involves frequent visit to various research laboratories and testing facilities spending hours to understand the science behind the nanofluids. This has become possible due to the support of my family members. Words cannot express how grateful I am to my father S. Kashmir Singh Bhullar, my mother Smt. Jasbir Kaur Bhullar, my wife Dr. Randeep Bhullar and my lovable children Gurman and Sukhman for all the sacrifices that they have made to keep me harmonious and helping me putting pieces together. Your prayer for me was what sustained me thus far. I will be grateful forever for their contribution.

(Bhupinder Singh Bhullar)

:

ABSTRACT

High heat fluxes due to densification of electronic components in integrated circuits pose a challenge in their heat dissipation rates. Use of forced convective or micro conductive fin attached to the integrated circuits limit their performance at high heat flux loads. Phase change heat transfer devices play an excellent role in dissipating the heat from the highly concentrated heat sources, thus providing superior cooling capabilities.

Over the past decade, comprehensive research work has been carried out on the operating characteristics of heat pipe using conventional working fluids. The heat pipes using nano-suspensions of metallic and oxide particles in the base fluid termed as "nanofluids" have attracted the attention of researchers worldwide because of enhanced thermophysical properties of the nanofluids.

In the present work, the potential of using Al_2O_3 / Deionised (DI) water based nanofluids as working fluids in heat pipe has been investigated at various orientations. The nanofluids prepared by two step method without the use of any surfactant are stabilized by ultrasonication. Structural modifications in the manufacturing of heat pipe have been made to delineate any vapor velocity fluctuation effects. A heating chamber has been constructed around the evaporator section of the heat pipe for uniform heat flux and the condenser section has been cooled by natural convection.

The thermal conductivity enhancement of Al_2O_3 / DI water nanofluids measured by transient hot wire (THW) method demonstrates a nonlinear relationship with increase in volume fraction of dispersed nanoparticles and attains a maximum enhancement of 15 % for 1 vol. % of Al_2O_3 loading in distilled water at 70°C.

The thermal performance of heat pipe has been investigated at increasing concentrations of Al_2O_3 / DI water nanofluids (0.005 %, 0.05 %, 0.5 % and 1 %) and Watt loads of heat inputs (12 W, 32 W & 72 W) to cover the operating temperature range of the electronic equipments ($< 70^oC$). Achieving favorable results, the average wall temperature along the length of the heat pipe reduces with the use of nanofluids as compared to conventional fluids i.e. DI water. Interestingly, the wall temperature decreases further with the increase in the Al_2O_3 volume concentration from

0.005 to 1 vol.% in the base fluid. The effective thermal conductivity of heat pipe increases with the increase in the nanoparticle concentration. An increase of 28 %, 22.6 % and 23.21 % has been achieved in the effective thermal conductivity of heat pipe tested at 12 W, 32 W and 72 W heat input respectively when loaded with 1 vol. % of Al_2O_3 nanoparticles as compared to DI water.

Secondly, the heat pipe tested at various favorable tilt angles in the range 0^o to 90^o demonstrates an optimum thermal performance at 30^o favorable tilt angle using DI water as working fluid. Interestingly, the use of nanofluids as working fluid has shifted the optimum favorable tilt angle from 30^o to 45^o irrespective of the selected concentration level (0.005 & 0.05 vol. %) of nanofluids and given heat inputs.

Thirdly, the operational limitations of modified heat pipe are calculated based on the thermophysical properties of Al_2O_3/ DI water nanofluids. The changed properties of nanofluids show an enhancement in the boiling, entrainment, viscous and sonic limit except the capillary limit of heat pipe. The surfactant free nanofluids provide higher margin of safety to the boiling limit of the heat pipe, simultaneously eliminating possibility of vapor lock. The capillary limit decreases with the use of nanofluids due to increase in the vapor and liquid flow path resistance rather than capillary pressure in the evaporator section of heat pipe.

Lastly, the nanofluids are prone to sedimentation and clogging with respect to time. The study will be incomplete without conducting the temporal study on the thermal performance of heat pipe. The heat pipes loaded with different volume concentrations (0.005, 0.05, 0.5, 1 vol. %) of Al_2O_3 / DI water nanofluids is investigated after 0, 3, 6 and 9 months from the date of manufacturing. The heat pipes are kept non-operational in between the specified durations. The consistency in the heat pipe performance is compared at different Watt loads (12 W, 32 W & 72 W) of heat input. The results indicate temporal deterioration in the thermal performance of heat pipe at low volume concentration in the selected range of heat inputs. The consistency in the operating characteristics of heat pipe has been observed at high vol. % concentration (1 vol. %) and high heat input of 72 W. The optical microscope images of the used mesh in the heat pipe reveal and authenticate our observations.

TABLE OF CONTENTS

LIST OF FIGURES

LIST OF TABLES

NOMENCLATURE

English Symbol	Description	Unit
v	Velocity	m/s
m	mass	Kg
Q	Heat	W
W	Weight	Kg
g	Acceleration due to gravity	m/s^2
V	Voltage	Volts
I	Current	Amperes
E	Energy	J
r	Radius	M
k	Thermal conductivity	W/(m.K)
$k_{e,e}$	Effective thermal conductivity of liquid saturated wick at evaporator	W/(m.K)
$k_{e,c}$	Effective thermal conductivity of liquid saturated wick at condenser	W/(m.K)
F_v	Frictional coefficient for vapor	Pa/(W-m)
x	Interparticle surface to surface distance	M
A	Area of cross section	m^2
L	Length	M
P	Pressure	N/m^2
t	Time	Secs
T	Temperature	^oC
q	Heat flux	W/m^2
d	diameter	M
t	thickness	M
N	Screen mesh number	-----
K	Wick permeability	m^2
K	Temperature	Kelvin
R	Thermal resistance	$^oC/W$
C_p	Specific heat	J/(kg.K)
J	Mechanical heat equivalent	J/cal

Greek Letters

ϵ	Dielectric constant
Ψ	Dimensionless surface potential
ε	Wick porosity

Greek Letters	Description	Unit
λ	Latent heat of vaporization	kJ/kg
δ	X-ray wavelength	Å
ρ	Density	kg/m^3
μ	Viscosity	kg/(m.s)
κ	Inverse Debye screening length	
ψ	Sphericity	
α β	Empirical fitting parameters	
φ	Volume fraction	
n	Shape factor	
σ	Surface tension	N/m
λ	Latent heat of vaporization	J/kg

Constants

$\mathbf{A_{132}}$	Hamaker constant of metal oxide 10^{-20} J

Subscripts

avg.	average
p	particle
pi	Pipe
l	liquid
el	electrostatic repulsion
A	van der Waals attraction
Total	Total
eff	effective
bf	base fluid
nf	Nanofluid
np	nanoparticle
wi	Wire
w	wire wick
T	tube (Heat Pipe)
v	vapor
ph,e	phase transition in evaporator
ph,c	phase transition in condenser
g	acceleration due to gravity
ca	capillary
h,s	wick surface pore hydraulic radius

Subscripts	Description
en	Entrainment
b	Boiling
s	sonic limit
vi	viscous limit
e	evaporator
a	adiabatic
o	Outer
c	Condenser
in	Input
r	relative
n	nucleation
i	inner

CHAPTER 1

INTRODUCTION

1.1 Thermal management challenges in electronics industry

The phrase “thermal management” involves the controlled generation and dissipation of heat for efficient working of electronic devices. Heat being inevitable by-product of every electronic device is usually disadvantageous to the performance and of the desired reliability. According to the BCC research report on semiconductor manufacturing [1], the global market trend heads north for thermal management products and is expected to touch $14.7 billion by 2019 with an annual growth rate of 6.8% between 2014 and 2019.

Today after 50 years of the reign of Moore's law [2], the transistor density doubles roughly every two years as projected in Figure 1.1. Transistor densities accelerated from 50 components per square centimeter in 2004 and will touch a million per square centimeter in 2020 [3].

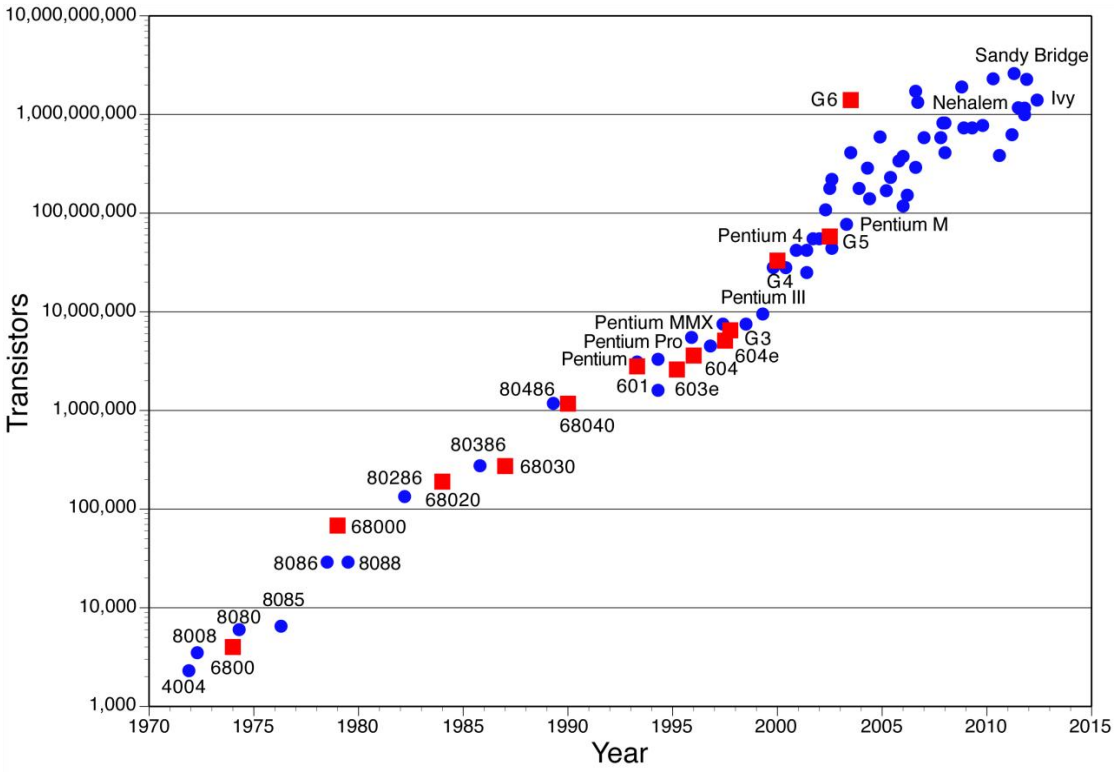

Figure 1.1 Moore’s law for transistors count per CPU in electronics industry [2]

This increase in the chip density together with size miniaturization is approaching the fundamental limit and has challenged the thermal fraternity for its heat dissipation solutions.

As per the International Technology Roadmap for Semiconductors (ITRS) [4] recent report, power management has become a primary issue due to two times increase in transistor count per generation while cost-effective heat removal from packaged chips remains almost flat.

The science and technology journalist, Geoff Koch recently reports [5], "Widely available microprocessors in 1993 had around three million transistors while the Intel itanium processor currently has nearly one billion transistors with size miniaturization. If this rate continued, "Intel processors would soon be producing more heat per square centimeter than the surface of the sun – which is why the problem of heat is already setting hard limits to frequency (clock speed) increases".

The technological shift from bipolar to CMOS circuit technology does promise thermal management by air cooling due to high operating speeds and efficient usage of energy. Despite decrease in the power consumption per gate in CMOS, the heat dissipation problem further aggravated after 1990 due to increase in the number of gates per feature size and faster clock speed.

The race for the size miniaturization, multiple uses and faster response time further aggravated the heat dissipation problem and has demanded for the development of new materials and cooling strategies to be adopted for the efficient working of the electronic gadgets.

1.1.1 Electronics thermal management solutions

Several heat dissipation technologies have been incorporated from time to time to meet the increasing cooling demand of power electronics. The prevailing cooling technologies at the chip level functionality are summarized in Table 1.1.

Typical heat transfer coefficients using air and dielectric cooling liquids under the natural convection conditions are 5 – 12 W/m^2K and 200 – 500 W/m^2K respectively.

Table 1.1 Summary of electronic cooling technologies [6,7]

Single-Phase Technology	Two-Phase Technology	Special Technology
• Natural convection (air or liquid) • Forced convection (air or liquid)	• Pool boiling • Falling film • Liquid jet impingement cooling • Flow boiling	• Thermoelectric& Refrigeration devices • Phase change material based cooling • Heat pipes, various designs • **Heat pipe using nanofluids**

At higher altitudes, the reduced atmospheric density leads to less effective heat transfer to the surroundings resulting in higher device operating temperatures [8]. The forced convection can enhance the heat transfer coefficient by a factor ranging from 5-12 compared to cooling by natural convection depending on the configuration [9]. The heat transfer process involving the latent heat gives 10-50 times more heat transfer coefficient than that for single phase forced convection with the same working fluid [10].

Overcoming these limitations, the use of heat pipe working on phase change process allows the rapid exchange of heat transfer through evaporation and condensation. The heat pipes can be integrated into complex geometries to extract heat without the need of temperature gradient. The nanofluids due to their enhanced thermophysical properties find replacement of conventional working fluids in heat pipes.

1.1.2 Motivation for the present research

Microprocessor design has recently encountered many architectural and thermal constraints. Among these challenging issues, temperature has become a first order processor design constraint and has proven to be a key limiter in performance, throttling, clock skew, leakage power, reliability, variability, and cooling costs for modern processors. The International Technology Roadmap for Semiconductors (ITRS) also projects an exponential increase in power dissipation in microprocessor in coming years.

Taking a case study, the power density of the Freescale 8640 Processor is about11 W/cm^2 and the 2^{nd} generation Intel Core i7 is greater than 20 W/cm^2 and close to 50 W/cm^2in localized areas of CPU. A conduction cooled card typically has an 85^oC card edge specification whereas the CPU have maximum die temperature reliability limit in the range 100^oC to 105^oC. Therefore the thermal design has a 15 to 20^oC total

temperature rise budget from die to card edge. This increased power density means that a greater proportion of this temperature budget is expended in the interface between the CPU and the heat sink, making the design of the cooling solution critical to the performance that can be attained at elevated temperatures.

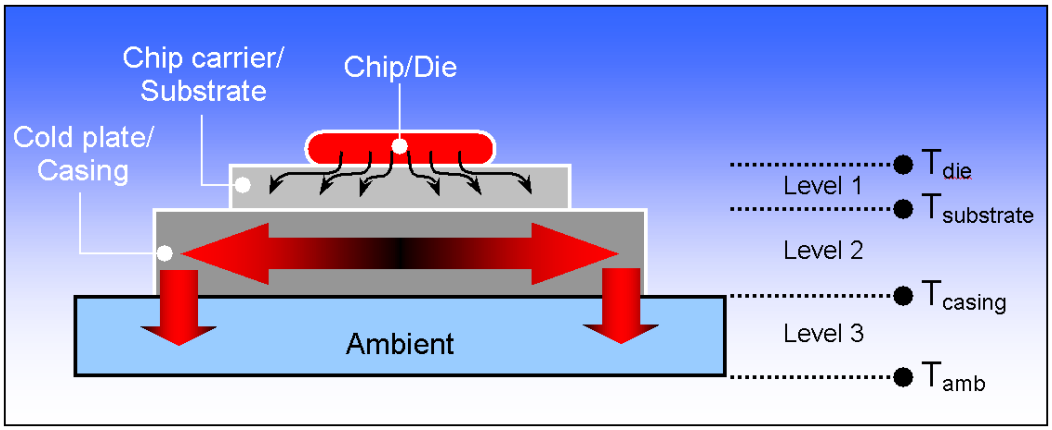

Figure 1.2 Heat paths in a typical package (Khandekar, 2004) [11]

The present day chip level cooling problems can be broadly divided into three levels as illustrated in Figure 1.2 [11]. First, second and third level cooling covers heat dissipation from chip to chip carrier, chip carrier to cold plate and cold plate to ambient, respectively. The chip temperature must be maintained despite high local heat flux. These thermal management challenges together with the combination of speed, compactness and system features challenge the thermal fraternity for innovative solutions.

The focus in this study is on cooling of power electronic modules on the base plate level. Historically, the current cooling technologies were primarily based on natural convection or forced convection and it is essential to continue research and develop superior technology capable of dissipating high heat flux rates [12].

Till today, heat pipes with high heat flux capability and low thermal resistance are already used in processors for heat spreading, creating isothermal surfaces, temperature control, and allowing independent placement of heat source and sink. The thermo physical properties of conventional working fluids used in the heat pipe have limited their heat transport capability. The replacement of conventional working fluids with the nanofluids can surpass the operational limitations of heat pipe due to improved thermo physical properties of nanofluids used as working fluids.

Accepting the challenge, an attempt has been made to experimentally investigate the heat transfer characteristics of heat pipe using nanofluids as working fluids. The study is further extended to investigate the temporal impact of sedimentation and agglomeration of nanofluids on the efficiency of heat pipe.

1.2 Fundamental working principle of heat pipe

Heat pipe, an excellent passive heat transfer device using latent heat of vaporization, found widespread application in microelectronics thermal management systems [13]. Heat pipes are hollow metal pipes comprising of evaporator, adiabatic and condenser section. When filled with a working fluid, it transfers heat by evaporating and condensing in an endless cycle.

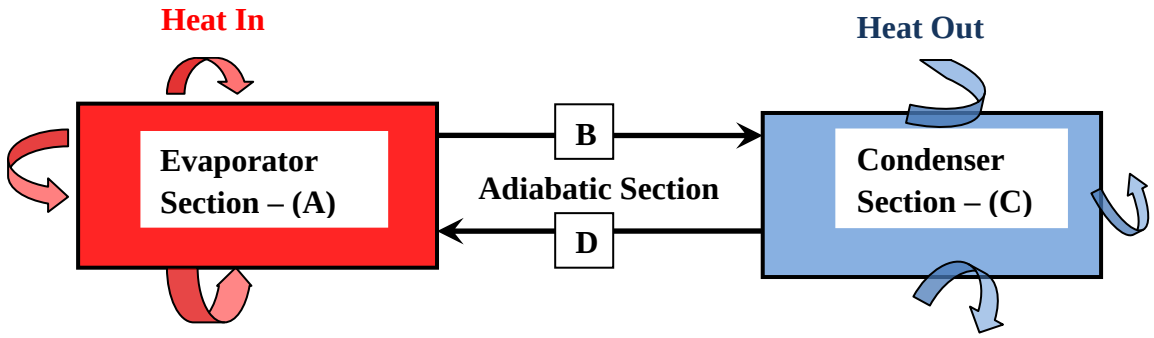

A: Working fluid is vaporized **B: The vapor flow**
C: Vapor is condensed **D: Liquid returns through capillary structure**

Figure 1.3 Block diagram of heat pipe (Reid and Merrigan, 1997) [13]

The heat input to the evaporator section vaporizes the working fluid, resulting in increase of specific volume to about 1600 times (at standard pressure). This dramatic increase in volume results in an increase of local pressure in the evaporator region. This increased pressure drives the vapor through the adiabatic region to the lower pressure condenser region. If the surface temperature of the condenser section of heat pipe is held below the saturation temperature of the vapor, condensation will occur. The condensate will flow back to the evaporator section due to the capillary effect of the wick structure.

In this way, heat pipe works on a closed two-phase cycle utilizes the latent heat to transfer heat with a very small temperature gradient. Block diagram depicting working principle of heat pipe is shown in Figure 1.3.

1.3 Heat pipes using nanofluids as working fluids

The use of nanofluids as working fluids in heat pipe is in the nascent stage of investigation and needs to further validate before its commercialization. The open literature indicates the positive impact of the use of nanofluids on the thermal performance of heat pipe. This has been credited due to the improved thermal conductivity of nanofluids as compared to conventional fluids. The results of open literature have shown that:

a) The studies are limited to cylindrical profiled heat pipes with end caps brazed to conceal the pipe.
b) The average wall temperature along the length of heat pipe decreases with the use of nanofluids as compared to conventional fluids.
c) The use of nanofluids decreases the thermal resistance of heat pipe.
d) There exists an optimum volume concentration and filling ratio of nanofluids for the maximum thermal performance of heat pipe.
e) The operational limitations of heat pipes improve with the use of nanofluids in heat pipe.

1.4 Closure

The volumetric heat dissipation by densely packed electronic equipment at each level of the package from chip to chassis is having a tremendous impact on the thermal management strategies. The insatiable human desire for gadget miniaturization has challenged the thermal engineers for innovative cooling solutions. The prevailing heat pipes with regular geometrical configurations and conventional working fluids have limited the application use and heat transport capabilities.

The development of nanofluids exhibiting excellent heat transfer capabilities has shown positive results in its use in heat pipes. From the literature review, it has been found that the use of nanofluids as working fluids in heat pipes improves the operational limitations. But the research is in the nascent state with inconsistency in findings and needs further consolidation and validation of results.

Secondly, the thermal performance of heat pipes is gravity sensitive and needs to be explored at different tilt angles using nanofluids as working fluid. The results need to be investigated and compared with the base fluid i.e. DI water.

Thirdly, the nanofluids prepared by two step method are prone to agglomeration, cluster formation and finally sedimentation with respect to time. Very rare studies are available on the temporal performance of heat pipe using nanofluids as working fluid. So an attempt is made to analyse the heat pipe performance with respect to designed time frame in months. This feature will highlight the practical applicability of heat pipe.

CHAPTER 2

LITERATURE REVIEW

2.1 Introduction

This chapter compiles the relevant information obtained from the literature on the thermophysical properties of nanofluids and the merits and demerits of using the nanofluids in heat pipes. The literature has been thoroughly studied and presented in the most lucid manner to interpret the research findings as per the following objectives:

a) To study the thermophysical properties of nanofluids with more emphasis on Al_2O_3/ DI water nanofluids.
b) The thermal conductivity being the dominating thermophysical property is to be exhaustively investigated.
c) To identify the effects of size, shape, concentration, pH and other parameters on the thermal conductivity of nanofluids.
d) To study the thermal conductivity measurement techniques for nanofluids.
e) To investigate the performance parameters of heat pipe at different nanofluid concentrations and orientations.
f) To study temporal consistency in the performance of heat pipe using nanofluids.

The details are presented in the following section.

2.2 Nanofluids and its preparation

The "Nanofluids" have proved both experimentally and theoretically to be enhanced heat transfer fluids as compared to base fluid and find applications in thermal exchange systems for different industrial and medical applications as shown in Figure 2.1.

The nanofluids are prepared by two methods, ***one step method*** and *two* ***step method***. In ***One step method,*** the making and dispersing of the nanoparticles in the fluid occurs simultaneously. In ***two step method, the*** dry nanoparticles are dispersed into suitable liquid host.

One step method has the advantage in controlling and reducing the particle agglomeration. ***Two step method*** gives better stability results for the preparation of nanofluids which contains oxide nanoparticles suspended in de-ionised water [14, 15].

The different techniques studied in the literature for the preparation of nanofluids by one step method have been shown in Figure 2.2 and the two-step method process has been shown in Figure 2.3. The summarized information pertaining to nanofluid preparation methods and their observations by various researchers is summarized in Table 2.1.

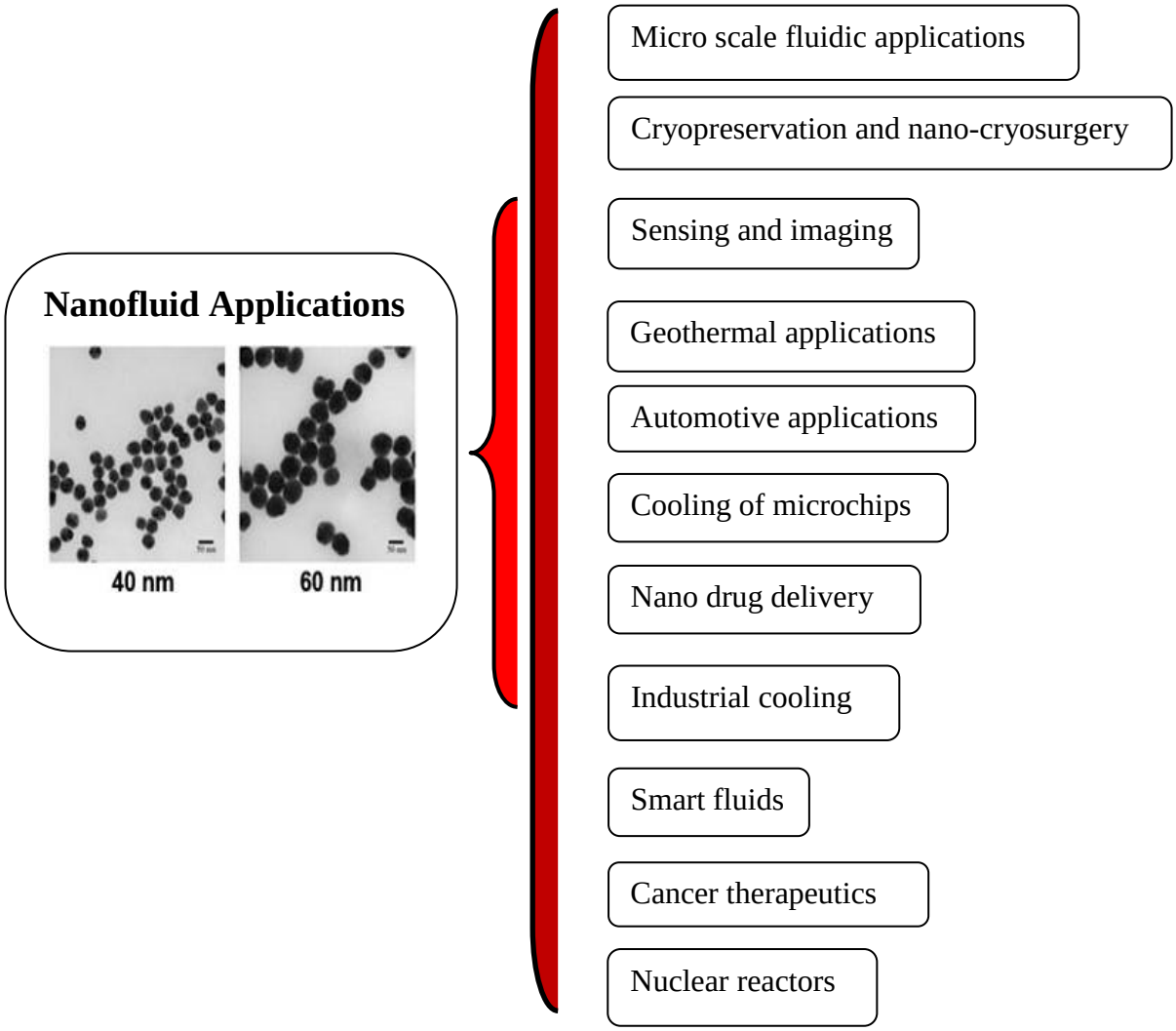

Figure 2.1 Application of nanofluids

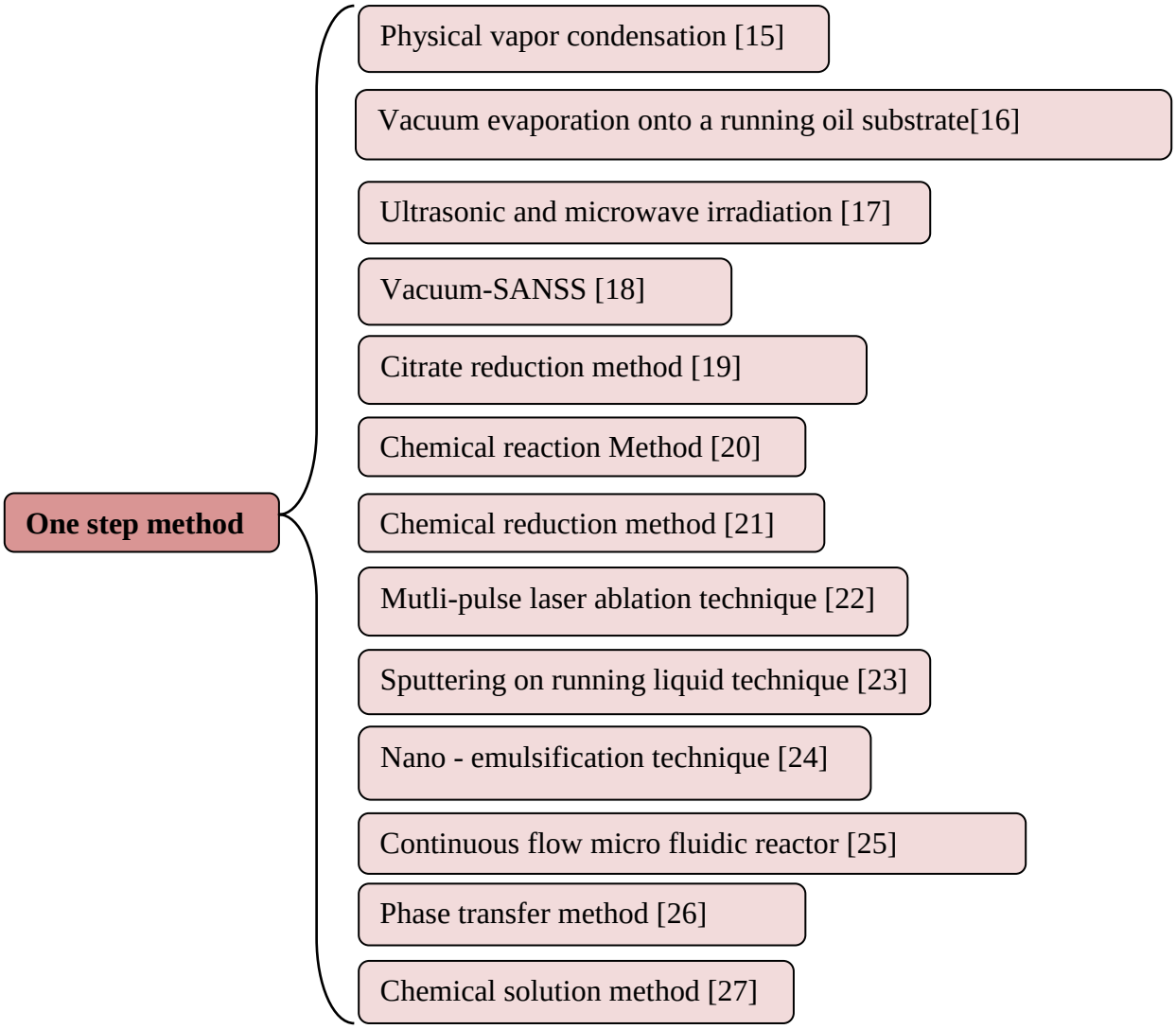

Figure 2.2 Synthesis of nanofluids by one step method

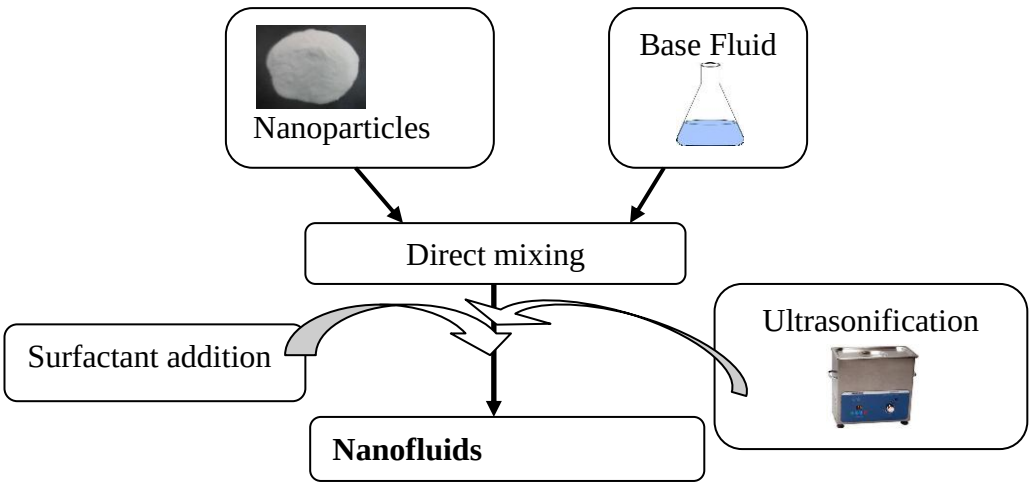

Figure 2.3 Two-step method

2.3 Stability of nanofluids

The strong van der Waals' interaction between the nanoparticles promotes the formation of aggregates. Various chemical and physical treatments are mentioned in the literature for the stability of nanofluids. They are categorized as the addition of surfactants, surface modification techniques and force application on the aggregated nanoparticles. In the literature, there exists a theory that cluster formation and agglomeration of nanoparticles promotes the thermal conductivity of nanofluids [28]. But contrary to it, another theory shows that the decline in the thermal conductivity due to clustering and agglomeration of nanoparticles.

The settling velocity of small spherical particles dispersed in a stationary liquid follows the Stokes law [29].

$$v = \frac{2gr^2}{9\mu}(\rho_p - \rho_l) \qquad \text{.....(2.1)}$$

Where v is the sedimentation velocity of particle, r is the spherical particle radius, ρ_p and ρ_l are the density of particle and liquid and μ is the viscosity of the liquid medium. As per the equation (1), the sedimentation velocity of particle is directly proportional to square of the particle size dispersed in the base fluid. The decrease in the particle size results in the Brownian motion of nanoparticles but there exists an optimum size called critical size beyond which the surface energy of the particle increases and will result in the agglomeration of nanoparticles [30].

The literature unfolds various techniques for the enhancement and evaluation of nanofluids which are summarized in the Figure 2.4.

2.4 Enhancement Methods

2.4.1 Surfactant or activator adding

The surfactants play a vital role in the stability of nanofluids by lowering the surface tension of the base fluids and changing the hydrophobic surfaces of nanoparticles to hydrophilic surfaces for aqueous fluids and reverse for non-aqueous fluids. They increase the wettability by increasing the contact angle between the materials.

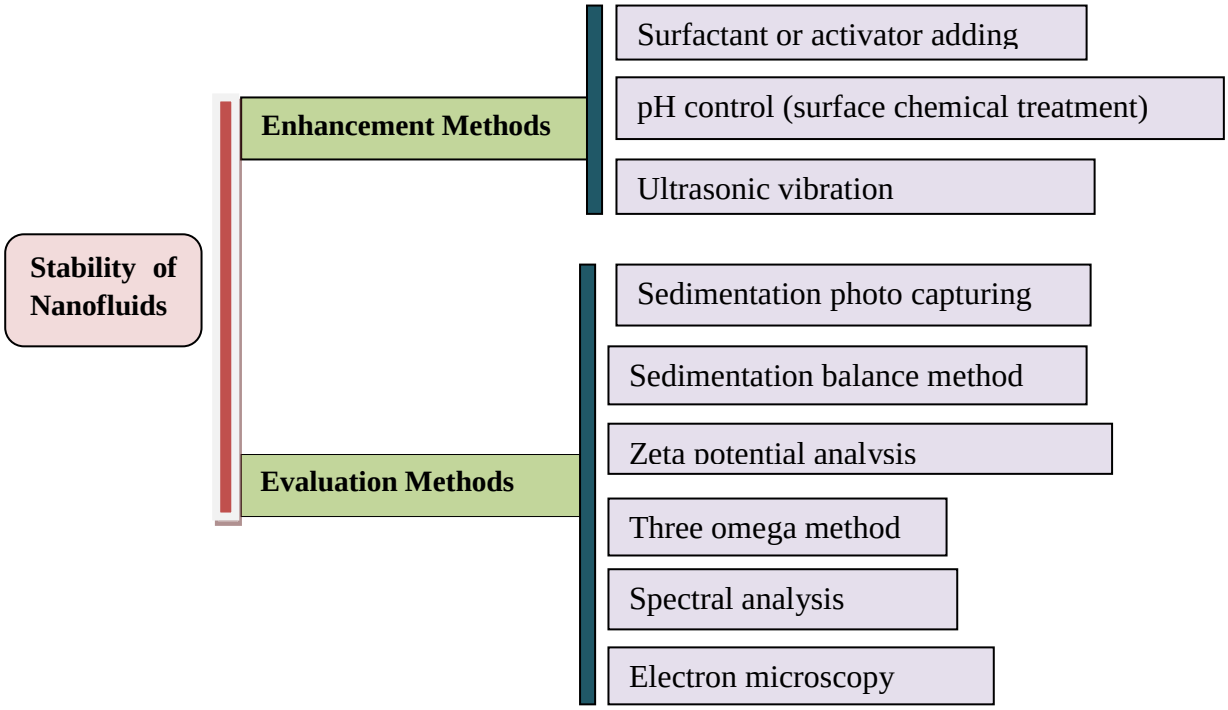

Figure 2.4 Nanofluids stability methods

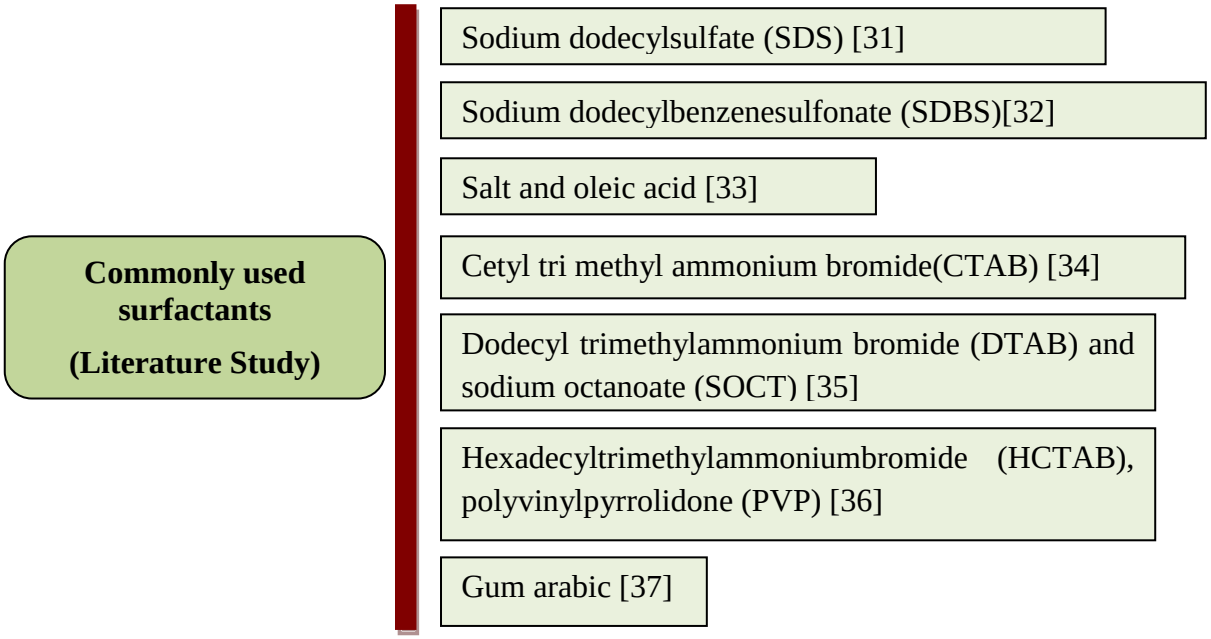

Figure 2.5 Commonly used surfactants (Literature Study)

In a two-phase system, a dispersant introduces a degree of continuity between the nanoparticles and fluids by locating at the interface. The force of repulsion between the suspended nanoparticles is measured by the zeta potential which is dependent on the surface charge of the particles suspended in the base fluid [31, 32].The most commonly

used surfactants in the literature are listed in Figure 2.5. The use of surfactants at high temperature applications (> 60^{o}C) is disadvantageous due to the damaging of the bonding between the surfactant and the nanoparticles [38, 39]. Therefore, the nanofluid will be prone to sedimentation and will lose its stability [41].Citing the other side effects of using surfactants, it may contaminate the heat transfer media by producing foams during heating in heat exchange systems.

2.4.2 Control of pH (Surface chemical treatment)

The electro-kinetic properties of aqueous solution nanofluids define its stability. Strong repulsive forces among the suspended nanoparticles will result in a stabilized solution due to high surface charge density [33, 34, 42, 43, 44].

Xie et al. [45] reported good stability of carbon nanotube in water by simple acid treatment. This happens due to conversion of hydrophobic surface to hydrophilic surface due to generation of hydroxyl group. A larger zeta potential is required for the stable suspension of small sized particles because of small repulsive forces on the surface of particles [46]. The departure of pH value of the solution from the iso-electric point is indicative of the stability of the solution but results in the alteration of thermo physical properties of nanofluids [44].In a liquid suspension system, the force of attraction and repulsion depends on the distance between the particles and the total interface energy E_{total} which is the sum of van der Waals' attraction E_A and the electrostatic repulsion E_{el} between them. The electrostatic repulsion between two charged particles having surface potentials Ψ_{d1} and Ψ_{d2} is approximated by the Derjaguin, Verway, Landau, and Overbeek (DVLO) theory [47, 48].

$$\mathrm{E}_{el} = \frac{\epsilon_0 \epsilon_r r_1 r_2}{r_1 + r_2}\left\{2\Psi_{d1}\Psi_{d2}\mathrm{In}\left[\frac{1+\exp(-\kappa x)}{1+\exp(-\kappa x)}\right] + (\Psi_{d1}^2 + \Psi_{d1}^2)\mathrm{In}[1-\exp(-2\kappa x)]\right\} \quad (2.2)$$

Wherer_1 and r_2 are the radii of two particles, x is an interparticle surface to surface distance.

From the Hamakar equation,

$$\mathrm{E_A} = -\frac{\mathrm{A_{132}\,r}}{12\,\mathrm{x}} \quad \text{…….. (2.3)}$$

A_{132} is the Hamaker constant for metal oxide and its value is of the order 10^{-20} J

$$E_{Total} = E_{el} + E_A \quad (2.4)$$

Therefore enhancement of repulsive forces over attractive forces can prevent particle aggregation and ensure stability.

Lee et al. [49] investigated various pH values for Al_2O_3 nanofluid and observed decrease or increase of agglomeration by changing pH. Different nanoparticles have different pH values of base fluids for stability. Taking a case study, alumina nanoparticles exhibit stability at pH of 8 and copper nanoparticles exhibit stability at 9.5 [50]. For Al_2O_3 /DI water nanofluids at pH ≈ 8.0 and for copper pH ≈ 9.5, a good dispersion of nanoparticles can be obtained which is attributed to charge build up on the surface of nanoparticles due to the addition of dispersants [32].

2.4.3 Ultrasonic vibration

With a high surface area to volume ratio, the nanoparticles dispersed in the base fluid tend to agglomerate with each other due to high surface energy. The resulting agglomerated nanoparticles can be broken down efficiently using the ultrasonic vibrations as compared to magnetic and high shear stirrer action. The frequency; power and duration of the ultrasonic process have a positive impact on the cluster formation.

Another method of passing the nanofluid through microchannels produces stabilized nanofluids. As a nanofluid flows through a microchannel, the increase in velocity results in cavitation. The particle clusters are broken down by the strong shockwaves produced on the inside wall of the chamber, formation of micro bubbles and high shear rate of flow [51]. The high energy of the cavitation helps in breaking down the cluster formation. Researchers have experimented with different procedures and methods to optimize the stabilization results. The compiled information from the literature as relevant to the present research work on Al_2O_3/ water nanofluids using ultrasonic with diverse durations is given in Table 2.2.

2.5 Thermophysical properties of nanofluids

The enhancement in the thermophysical properties of nanofluids justifies their use in the heat transfer applications. But the literature reflects ambiguous picture in declaring the percentage change of the thermophysical properties of nanofluids with change in the

volume concentration, temperature, size, shape of nanoparticles and chemical properties of base fluid. The literature indicates strong dependency of these parameters on the thermal conductivity of nanofluids and is considered in detail separately. The literature values of various researchers are plotted and the results are compared to gain an insight of the influence of individual parameters. The factors affecting the nanofluid properties are shown in Figure 2.6.

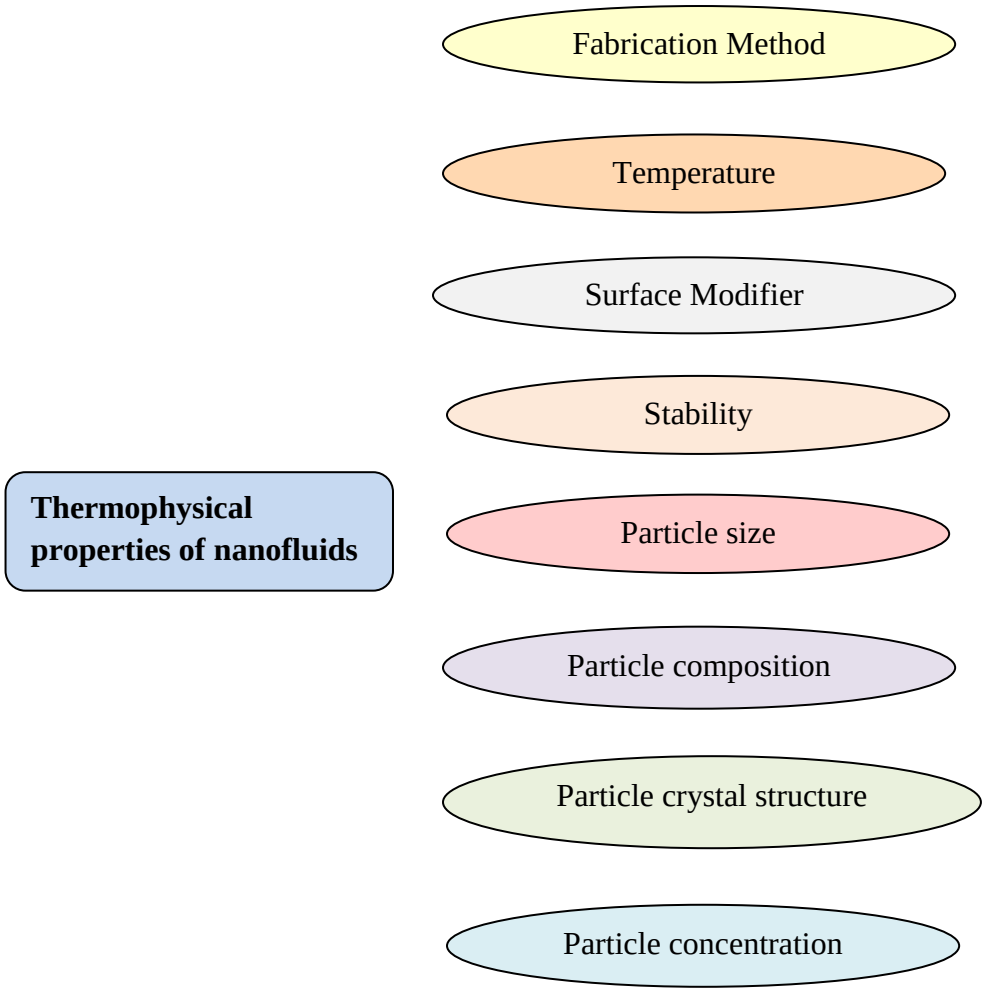

Figure 2.6 Parameters affecting the properties of nanofluids

2.5.1 Thermal conductivity of nanofluids

The thermal conductivity of a nanofluid increases with increase in the volume concentration and the literature data shown in Figure 2.4 exhibits a linear relationship without taking in to consideration the physical and chemical parameters [41]. Some exceptions have shown a non-linear relationship in the value of thermal conductivity due

to increase in volume fraction. But these inconsistencies are even reflected for the same base fluid, nominal size, shape and composition of the nanoparticles.

Anomalous variation in the thermal conductivity enhancement due to volume fraction, testing methodology and temperature as reported by more than 300 leading researchers resulted in the standardization study coordinated and conducted by Massachusetts Institute of Technology [52].In this bench marking exercise, identical samples of stable nanofluids were distributed among 30 organizations worldwide for the measurement of thermal conductivity using different experimental approaches.

This exercise unfolds various myths which are documented in the literature by various individual researchers. The study concludes that the thermal conductivity of nanofluids increases with the increase in particle concentration and aspect ratio but the enhancement is only between 5 to 10% of the base fluid. The systematic differences in the obtained values of thermal conductivity among the various experimental approaches tend to disappear when the data is normalized to the measured thermal conductivity of the base fluid. Breaking the unusual enhancement myth in the thermal conductivity of nanofluids, this exercise ends with no anomalous enhancement.

With heaps of efforts put on to avoid the agglomeration of nanoparticles, the studies conducted by some researchers benefitted from agglomeration effect [38, 53, 54].Furthermore, this enhancement resulted due to long chain of cluster formation associated with radius of gyration and dimension of aggregates as depicted in Figure 2.8.

Contrary to above findings, Hong et al. [55, 56] demonstrated experimentally from the light scattering of Fe nanoparticles aggregate, the negative impact of particle aggregation on the thermal conductivity of nanofluids.

2.5.1.1 Effect of Shape of nanoparticles

Timofeeva et al. [57] investigated the impact of alumina nanoparticle shape on the thermal conductivity of alumina nanofluids. Different shapes of the nanoparticles (i.e. blades, platelets, cylindrical, bricks, and spherical) were used during the experimental study. The study concludes that if the surface area and surface heat resistance of solid

liquid interface are high, the thermal conductivity of nanofluids will be reduced due to the negative contribution of interfacial effects.

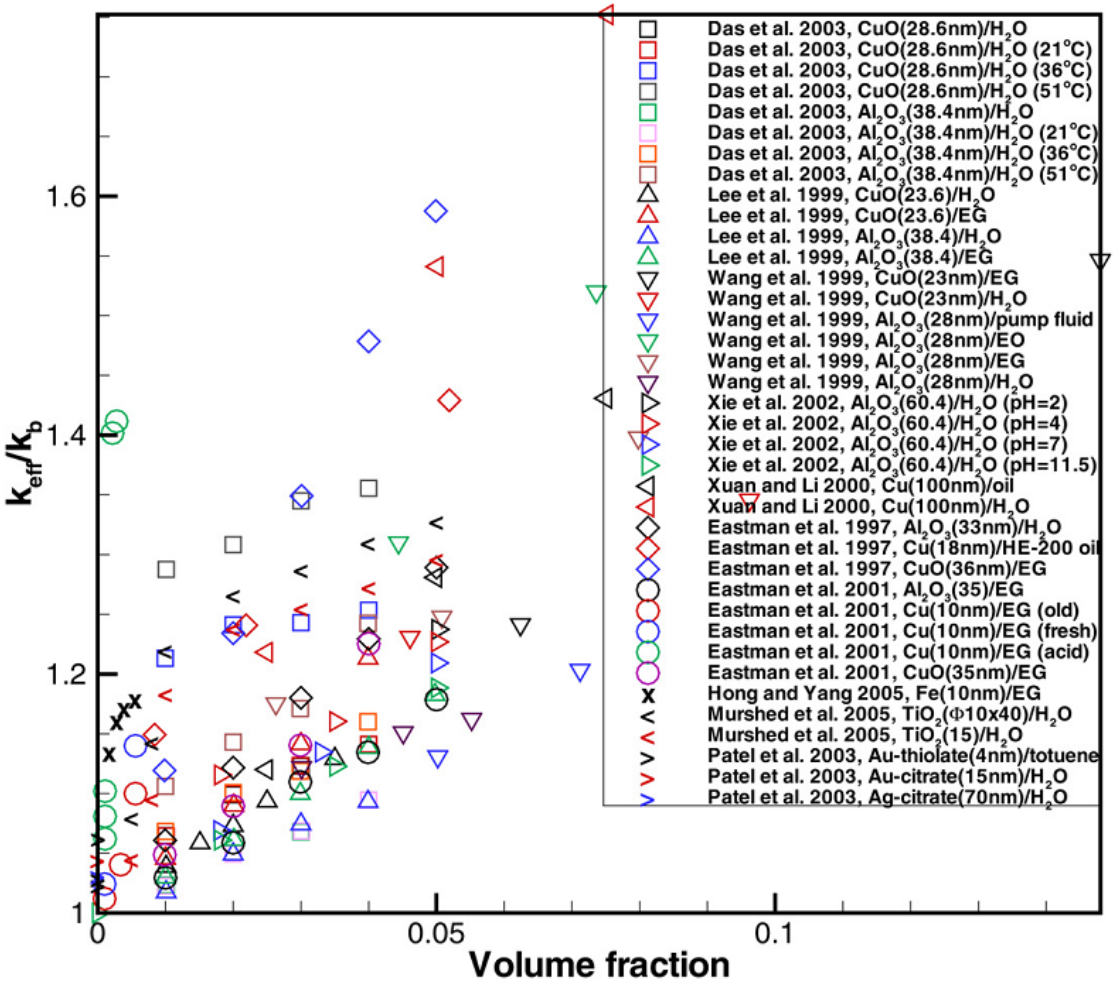

Figure 2.7 Enhancement in thermal conductivity ratio of various nanofluids with the increase in nanoparticles concentration [41]

Xie et al. [58] were the first to investigate effect of size and shape of the nanoparticles in to suspension on the thermal conductivity enhancement. Later on Murshed et al. [59] performed the thermal conductivity experiments by transient hot wire method by using cylindrical and spherical shaped TiO_2 nanoparticles dispersed in water. An enhancement of 33 % and 30 % percent has been reported for rod and spherical shaped nanoparticles dispersed in water at 5% volumetric loading.

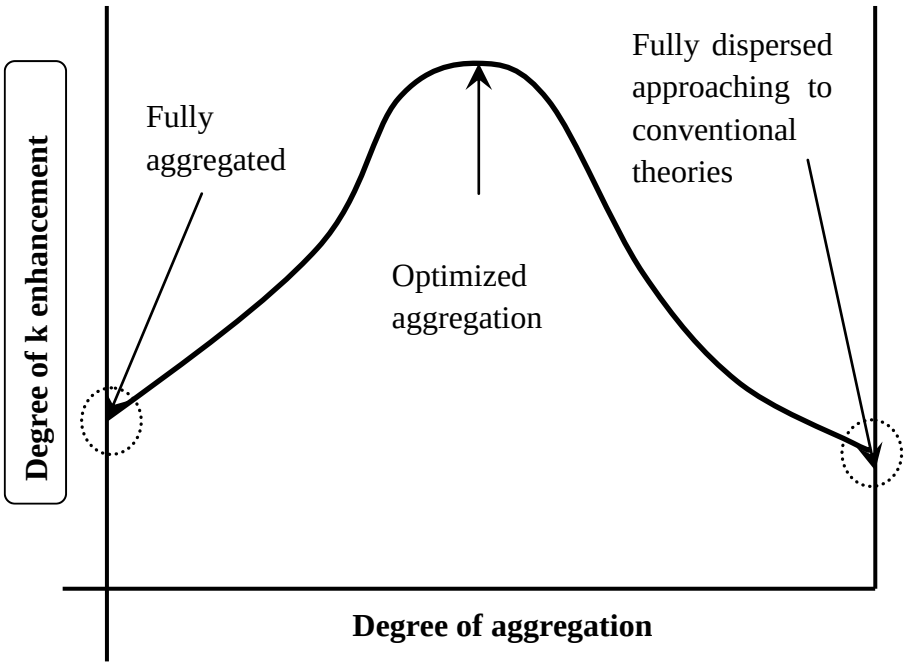

Figure 2.8 Effect of degree of aggregation on thermal conductivity [54]

Jeong et al. [60] experimentally studied the thermal conductivity enhancement of ZnO nanofluids with rectangular and spherical nanoparticles having concentration level ranging from 0.05 to 5.0 vol. %. The thermal conductivity shows an enhancement of 12% and 18% at 5.0 vol. % for the spherical and the nearly rectangular shape nanoparticles, respectively, compared to the base fluid conductivity. Similarly, Singh et al. [61] investigated the effect of disc or platelet shaped silicon carbide (SiC) nanoparticles dispersed in water on the mechanical properties and thermal conductivity enhancement.

Zhou and Gao [62] numerically investigated the effects of interfacial thermal resistance and aspect ratio on the thermal conductivity of nanofluids. The adjustment of the particle shape plays a vital role to achieve appreciable increase in the effective thermal conductivity of nanofluids. A small volume fraction of non-spherical nanoparticles results in large enhancement of effective thermal conductivity.

2.5.1.2 Effect of size of nanoparticles

The literature demonstrates ample experimental and theoretical studies projecting a considerable effect of nanoparticle size on the thermal conductivity of nanofluids. In two separate studies conducted by Das et al.[63] and Lee et al.[14], with an average size of alumina nanoparticles (38.4 nm) dispersed in DI water, an enhancement in the range of 2% to 10% has been reported in the thermal conductivity values. Another similar study

performed by Xie et al. [64], an enhancement of 21 % has been reported with the same size of nanoparticles. The research conducted by various research groups on the thermal conductivity of Al_2O_3/water based nanofluids with the nanoparticles size in the range 13 to 150 nm has been graphically shown in Figure 2.9.

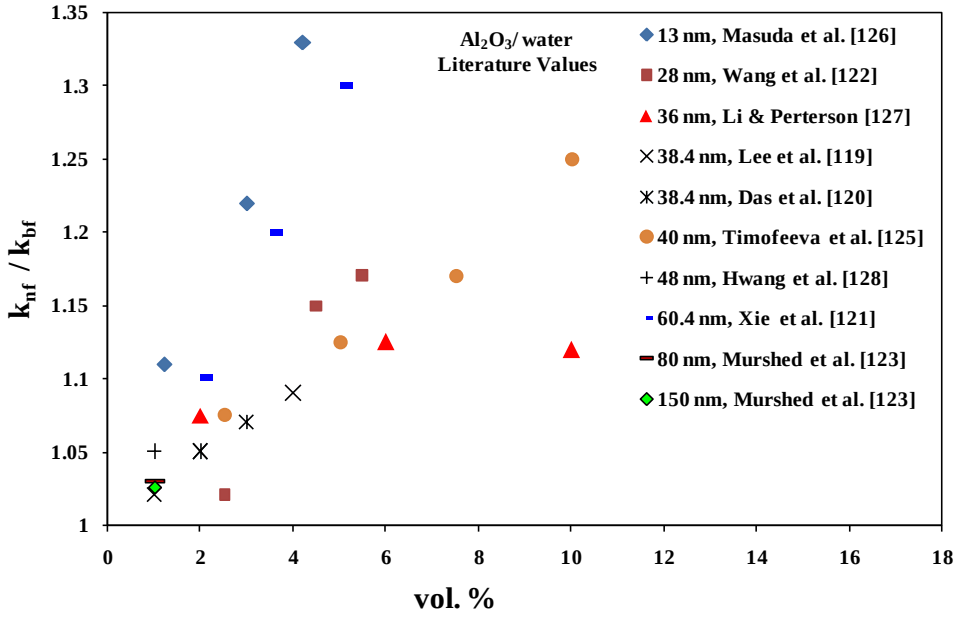

Figure 2.9 Effect of volume concentration and particle size on the thermal conductivity ratio of Al_2O_3/ water nanofluids

With wide variation in the thermal conductivity values with respect to the size of the nanoparticles, it has become ambiguous to draw a clear picture on the size dependency. Li & Peterson [127] indicated an increase and then decrease in the thermal conductivity ratio with the increase in the volume concentration from1 to 10 vol. % whereas Timofeeva et al. [125] showed an increase in same concentration range with merely a small size difference of 4nm in nanoparticles. This haphazard deviation fails to conclude a relational theory and needs to be further investigated. Using 13 nm size of nanoparticles, Masuda et al.[126] observed maximum enhancement from 10 % to 34% in thermal conductivity when the volume concentration increases from 1 to 4 %.

2.5.1.3 Effect of temperature

As compared to base fluids, the dispersion of nanoparticles in base fluid makes the 'nanofluids' more temperature sensitive. The plotted thermal conductivity values at different temperatures performed by various researchers are shown in Figure 2.10. It is observed that Das et al. [63] working in the temperature range of 21 to 51°C, demonstrated an enhancement of 2to10.8% when loaded with 2 vol. % of nanoparticles.

The results obtained by Masuda et al. [69] are not in synchronization with the results reported by other research groups as indicated in Figure 2.10. Even with the same concentration of 1 vol. % Das et al. [63] and Murshed et al.[40] differ in their findings. On seeing the results, the temperature does have an effect on the thermal conductivity but the results obtained do not reflect any clear trends.

From the literature studies, it is concluded that the thermal conductivity of nanofluids increases with the increase in temperature. Various mechanisms resulting in the enhancements have been quoted by researchers. But inconsistency in the data has become a big hurdle in the commercialization for this product.

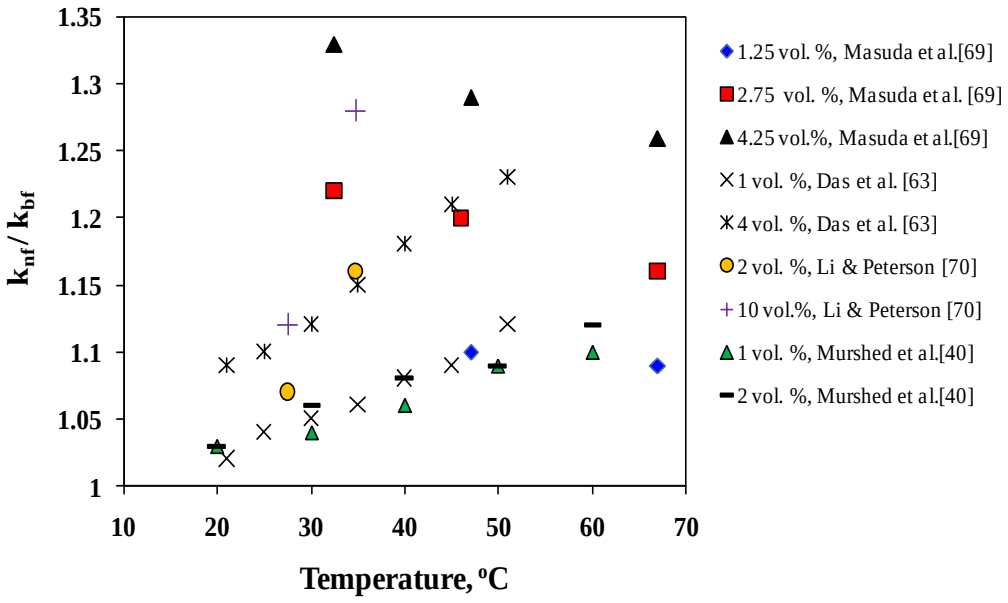

Figure 2.10 Enhancement in the thermal conductivity ratio of Al_2O_3/ DI water nanofluids with temperature

2.5.1.4 Effect of volume fraction

Figure 2.11 shows the compiled results obtained by various researchers on the effect of volume concentration of nanofluids on the thermal conductivity ratios. Despite different sizes of the nanoparticles, the thermal conductivity increases with increase in volume concentration. Masuda et al. [69] demonstrate an enhancement of 32 % in the thermal conductivity value obtained at 4 vol. % loading of alumina nanoparticles in water-based nanofluid. Whereas Hwang et al. [71] in an experimental study observed 4% enhancement in thermal conductivity when loaded at 1 vol.% concentration [14, 67,15].

Lee et al. [49] at a lower volume percent of 0.5 % using 35 nm sized Al_2O_3nanoparticles observed an enhancement of 2% enhancement. Li and Peterson [70] observed the reverse trend in the thermal conductivity enhancement as the concentration jumps from 6% to 10%. It is concluded that within the same volume concentration range, different research groups obtained different enhancement values in the thermal conductivity. It reflects inconsistency in the enhanced values.

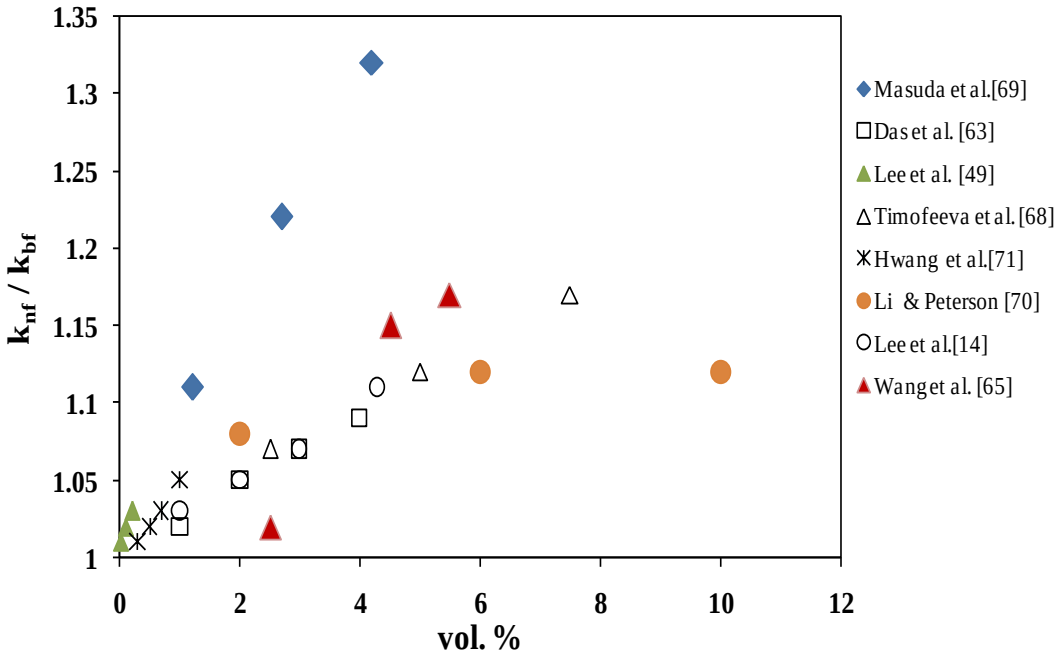

Figure 2.11 Effect of volume concentration of Al_2O_3 / DI water nanofluids on thermal conductivity ratio

2.5.1.5 Effect of base fluids

The type of base fluid used for the nanofluids preparation contributes in defining the thermophysical properties of nanofluids. As shown in Figure 2.12, it is observed that increase in the thermal conductivity of nanofluids is maximum for pump oil and minimum for the water based nanofluids as observed by Xie et al. [64] and Das et al.[63], respectively. This indicates sensitivity of base fluids on the thermal conductivity enhancement. The enhancement in the thermal conductivity of poorer heat transfer fluids such as water is more encouraging and beneficial from the practical application point of view.

In a study conducted by Wang et al. [97], Pump oil at 5 % volume alumina concentration shows an enhancement of 38 % in thermal conductivity as compared to that of 20 %

enhancement observed at 4 vol.% of alumina /Transformer oil. Whereas Das et al. [63] in their experimental study show an enhancement of 10.9 % at 4 vol. % concentration of alumina nanoparticles in water. Eastman et al. [63] used ethylene glycol as base fluid and obtained minimum and maximum value of 2 % and 30 % enhancement in thermal conductivity at 2.5 and 7 vol. % concentration.

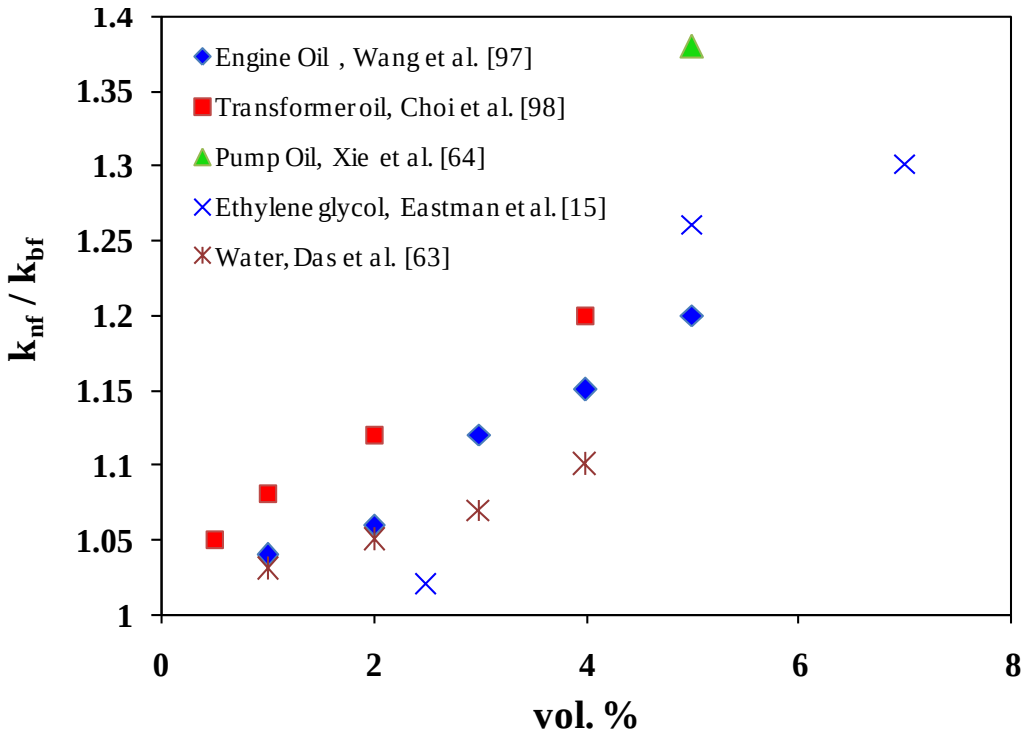

Figure 2.12 Effect of base fluids on the thermal conductivity ratio of Al_2O_3 based nanofluids

2.5.1.6 Effect of preparation method

Different preparation methods used for the preparation of nanofluids exhibit different thermal conductivity enhancement ratios as shown in Figure 2.13. Masuda et al. [69] used the high speed dispenser to obtain the highest values of thermal conductivity enhancement at all the selected volume concentrations as compared to other preparation methods. Xie et al. [64] used mixing ultrasonication technique to produce better results as compared to ultrasonic vibrator method.

Lee et al. [14] performed an experiment by dispersing Al_2O_3 nanoparticles of 38.4 nm size in water and the mixture is thoroughly shaken to ensure a uniform suspension in polyethylene container. The authors observed an enhancement of 10 % and 8 % when

loaded at 4.3 and 3 % vol. concentration. Same results were obtained by Das et al. [63] by using ultrasonic bath. The nanofluids which are prone to agglomeration and sedimentation may influence the thermal conductivity in the longer run and the studies need to be carried out in this regard.

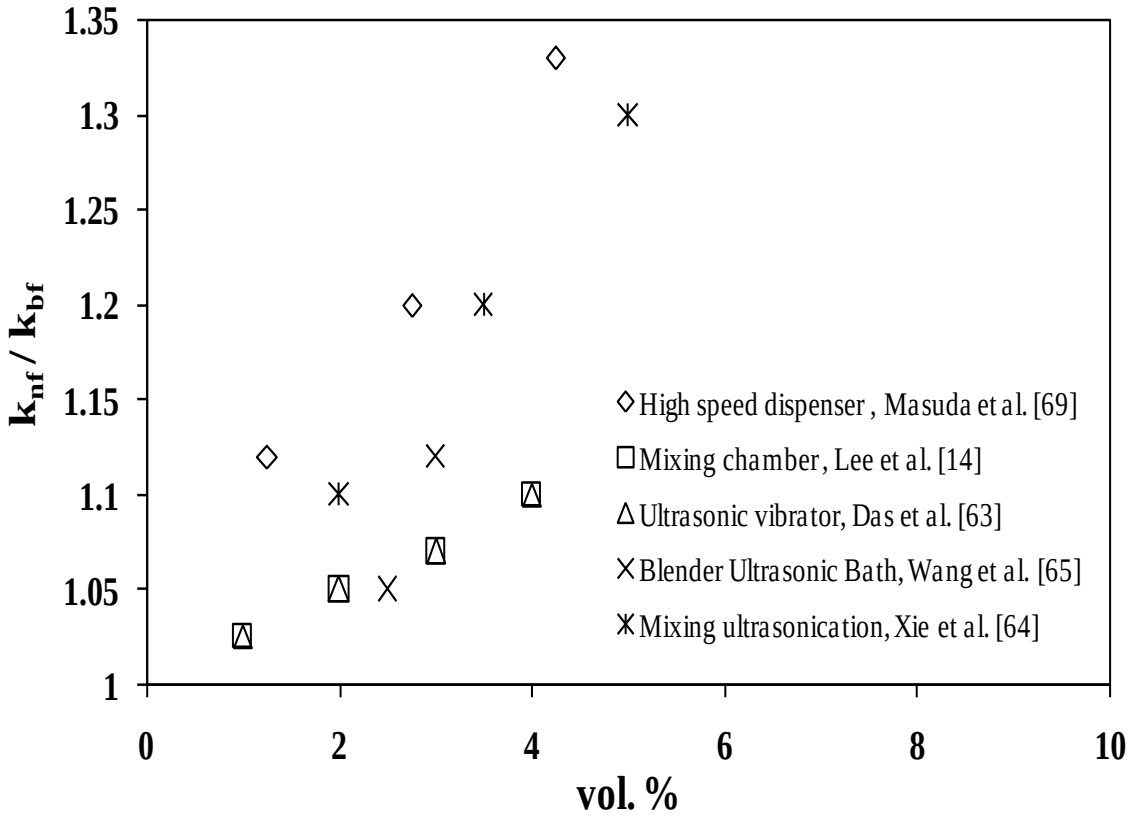

Figure 2.13 Effect of method of preparation on thermal conductivity ratio of Al_2O_3 based nanofluids

2.5.1.7 Effect of pH

The effect of pH values on the thermal conductivity of Al_2O_3 nanofluids as studied by Xie et al. [64] is graphically shown in Figure 2.14. Xie et al. obtained the thermal conductivity values using the Transient hot wire method. The Al_2O_3 nanoparticles with specific surface area of 5 to 124 m^2/g, have been tested at three different pH values of base fluid (4, 7 and 11.50). Interestingly, the thermal conductivity increases with the decrease in the base fluid pH value as shown in Figure 2.14.

From the figure below it is clear that the suspension of Al_2O_3 nanoparticles in acidic (pH < 7) water gives higher value of thermal conductivity rather than the basic (pH > 7) fluidic dispersion of nanoparticles.

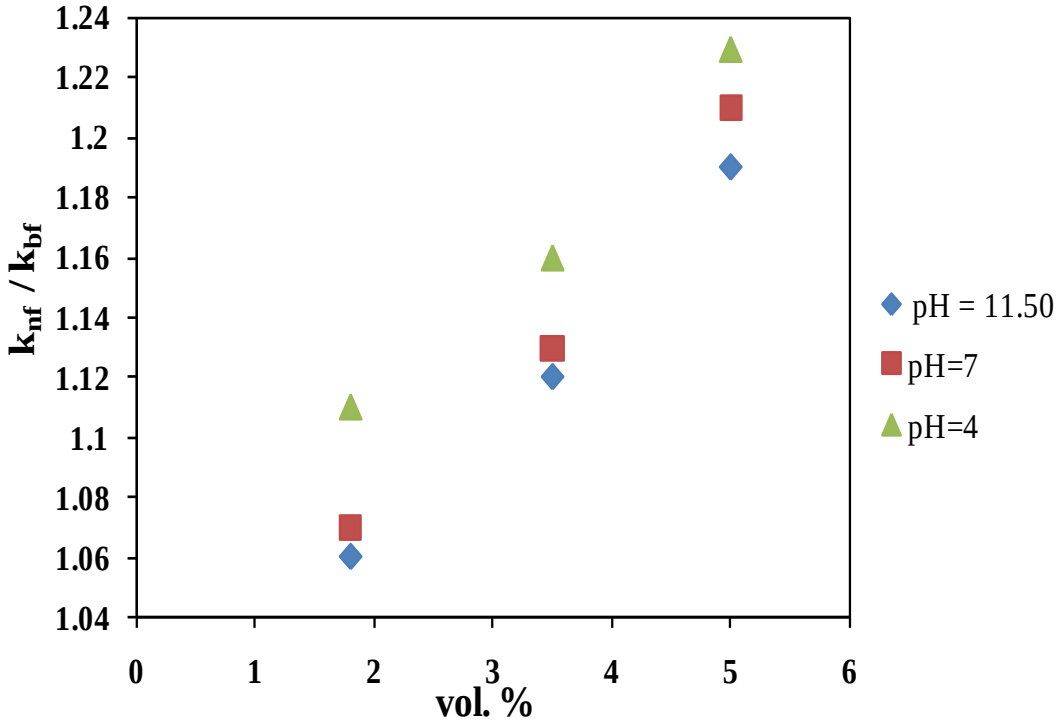

Figure 2.14 Effect of pH on the thermal conductivity ratio of Al_2O_3 / water nanofluids

2.5.1.8 Effect of surface active agents

The literature demonstrates advantages and disadvantages of using surfactants to enhance the stability of nanofluids. In an empirical investigation on the thermal conductivity of common surfactants conducted by Zhou et al. [54], it is concluded that the thermal conductivities of surfactant solutions reach a stable ratio after a certain concentration. It has been further found that at certain concentration, the thermal conductivity ratios of ionic surfactant solutions are higher than those of non- ionic surfactants. Xia et al. [73] in a study demonstrated the effect of two kinds of surfactants SDS (sodium Dodecyl sulphate) and PVP (polyvinyl pyrrolidone) on the thermal conductivity of Al_2O_3/ DI water nanofluids. The results so obtained indicated that the surfactant has negative role on the thermal conductivity of base fluid. Chen et al. [74] concluded that higher concentration of surfactant has a negative impact in improving the thermal conductivity of nanofluids. Yang et al. [75] investigated the stability of α-Al_2O_3 nanofluids using different mass fractions of surfactants (PAA, CTAB and SDBS) and found that the dispersion of Al_2O_3 suspensions first increased to an optimum level and then decreased with further increase of surfactant concentration.

2.6 Experimental results on viscosity of Al_2O_3/DI water nanofluids

In a study conducted by Das et al. [76], the viscosity of alumina-water nanofluids increases with the increase in the nanoparticle concentration indicating strong possibility that nanofluid may be non-Newtonian. In another study, a two-step method was used to produce Al_2O_3/ water nanofluids with low concentrations from 0.01 to 0.3 vol.% without the use of any surfactant [49] and viscosity is measured in the temperature range from 21 to 39°C. Experimental results showed that the effective viscosities of the dilute Al_2O_3/ water nanofluids significantly decrease with the increase in the temperature and slightly increase with increasing volume fraction. The result is similar in another experiment [77], wherein, the viscosity increased by 83.4% at a volume fraction of 0.05 (5 vol. %).

Murshed et al. [59] measured the viscosities of Al_2O_3 / water based nanofluids with nanoparticle size 80 nm. It was found that the viscosity increases by nearly 82% for the maximum volumetric concentration of 5% nanoparticles. A similar increment of 86 %in the viscosity of Al_2O_3 / distilled water based nanofluids with nanoparticle size of 28 nm was observed by Wang et al. [78] for the same volume fraction of 0.05. In another report published by Kole et al. [79], the use of alumina nanoparticles in engine coolant demonstrated a transitional shift from Newtonian to non-Newtonian behavior with increasing content of Al_2O_3in the engine coolant. The data also shows that the viscosity increases with an increase in concentration and decreases with an increase in temperature.

2.7 Thermal conductivity measuring techniques

Figure2.15 shows the thermal conductivity values of Al_2O_3 / water based nanofluid measured by different techniques. Fundamentally, Fourier's law of heat conduction has been used for the measurement of thermal conductivity. The trend shows that thermal conductivity increases with the increase in volume fraction irrespective of the technique employed.

The thermal conductivity data of Lee et al. [14] and Das et al. [63] for similar nanofluids shows similar results despite measured by different techniques. But the technique used by Oh et al. [80] shows higher values as compared to other researchers. The reason for this discrepancy during the measurement may be due to the sedimentation and

aggregation of nanoparticles, particle diameter, shape, size and method of nanofluid preparation.

The steady state parallel plate technique used by Wang et al. [65] shows a minimum enhancement of 1 % in the thermal conductivity of nanofluids when loaded with 2.5 % of nanoparticles. The results obtained beyond 3 % volume concentration are in agreement with the results obtained by Oh et al. [80]. It will be premature to say how these techniques will give results for a stable nanofluid but consistency in the results is observed for steady state parallel plate and transient hot wire techniques. Taking the time duration into consideration, the transient hot wire technique gives quick results as compared to steady state parallel plate method.

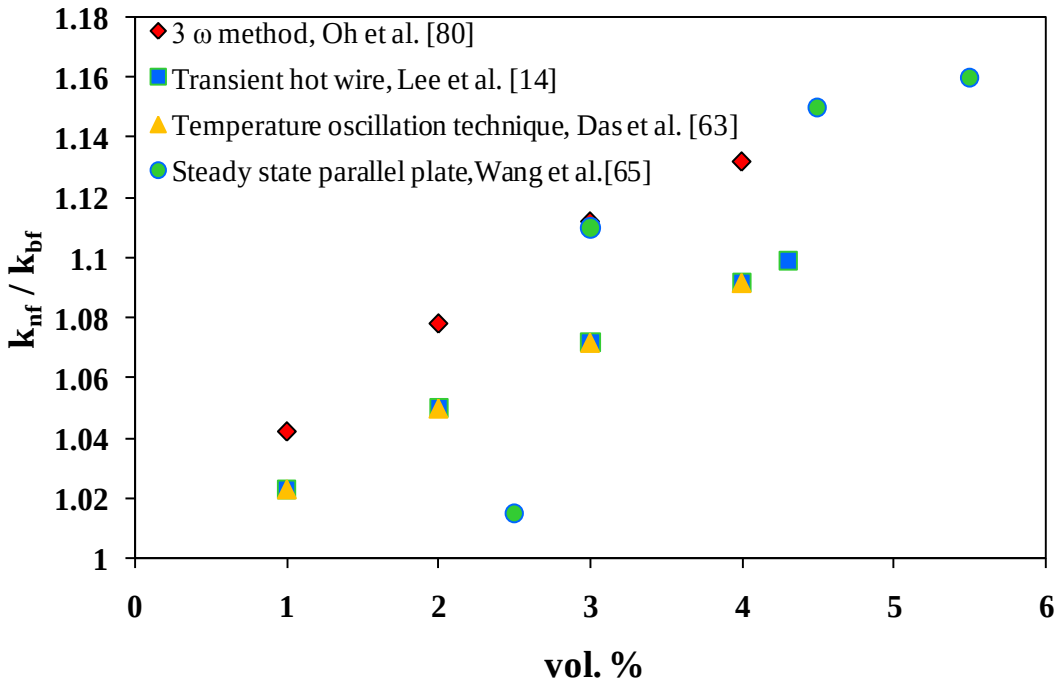

Figure 2.15 Thermal conductivity of Al_2O_3nanofluids measured by different techniques

2.8 Heat Pipe

Over the past decade extensive research work has been carried on the operating characteristics of heat pipes employing working fluids such as water, ammonia, alcohol etc. The introduction of nanofluids exhibiting superior heat transfer capabilities has open new opportunities in using nanofluids as working fluids in heat pipes. The data gathered from the literature review shows an improvement in the effective thermal conductivity of heat pipe with noticeable reduction in the thermal resistance.

An attempt has been made to review and summarize experimental and theoretical investigative reports on the use of nanofluids in heat pipes. As the literature is widely spread across numerous experimental studies using different types of metallic and oxide nanoparticles dispersed in different types of base fluids, the author has taken an exemption to focus only on relevant research work for the present work using water based nanofluids in modified screen mesh wick heat pipes.

2.8.1 Experimental investigations

The research groups working in the area of heat pipes have experimentally investigated the performance of heat pipe using different concentrations of nanofluids, heat inputs, charging ratios and orientations. The summary of experimental and theoretical studies as relevant to present work is given in Tables 2.3 and 2.4, respectively.

One of the elementary studies on the operating characteristics of heat pipes was carried out in 2005 by Wei et al. [81]. In this experimental study, the change in thermal resistance of heat pipe using silver nanofluids (10 nm nanoparticles size)in an axially grooved heat pipe was observed and compared with those of DI water. A reduction of 44 % in the thermal resistance of heat pipe has been reported as compared to DI water.

In 2008, Naphon et al. [82] conducted experiments on a copper pipe having a length of 600 mm and an external diameter of 15 mm. The effect of heat pipe tilt angle, charging ratio of working fluid at various concentrations of titanium / distilled water nanofluids were scrutinized. The outcome indicates the dependency and performance optimization of heat pipe on tilt angle, charging amount, volume concentration and the nature of working fluid.

Kang et al. [83] studied the effects of using different volume concentrations of silver nanofluids on an axially grooved heat pipe. A noticeable decrease of 50% and 80% in the thermal resistance of heat pipe was observed using 10 nm and 35 nm size of the nanoparticles, respectively.

Chen et al. [84] performed the experimental study on the heat pipe of length 200 mm and diameter 3 mm. Nano-sized silver particles of 35 nm average diameter were dispersed in water to prepare nanofluids. The heat pipe was tested in the power range of 20-40 W. It has been observed that the thermal resistance of heat pipe decreases with the use of

nanofluids as compared to base fluid. Furthermore, the thermal resistance of nanofluids shows inverse trend with increase in the concentration of silver/water nanofluids as shown in Figure 2.16.

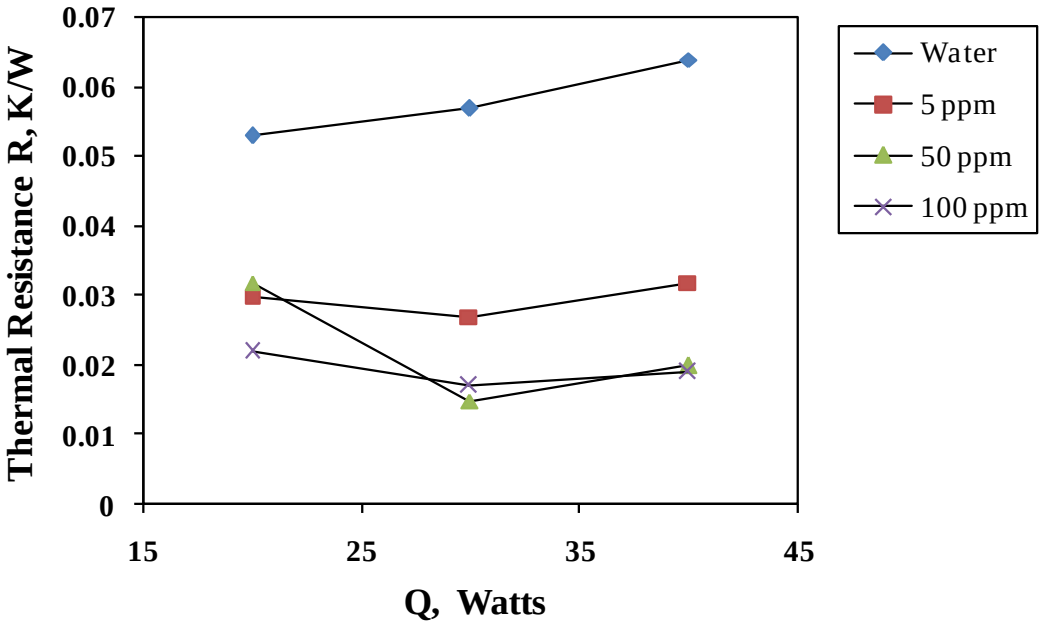

Figure 2.16 Variation of thermal resistance of heat pipe as a function of heat input and concentration [84]

In the same year, Mousa [85] too investigated the impact of using Al_2O_3/ Water nanofluids at different volume concentrations and charging ratios on the thermal resistance of heat pipe. The heat pipe was tested at different watt loads of heat input. The condenser section of heat pipe was cooled under natural convection and heat input to the evaporator section was provided by an electrical heater. Figure 2.17 shows the variation in the thermal resistance of the heat pipe with the increase in volume concentration of nanofluids and heat input. The study indicates an optimum value of filling ratio and volume concentration of nanofluids with respect to the heat input range for achieving the lowest value of thermal resistance.

In 2012, after an empirical study carried out by Hajian et al. [86], the impact of silver nanofluid was analyzed and compared to water as the base fluid in cylindrical shaped heat pipe.

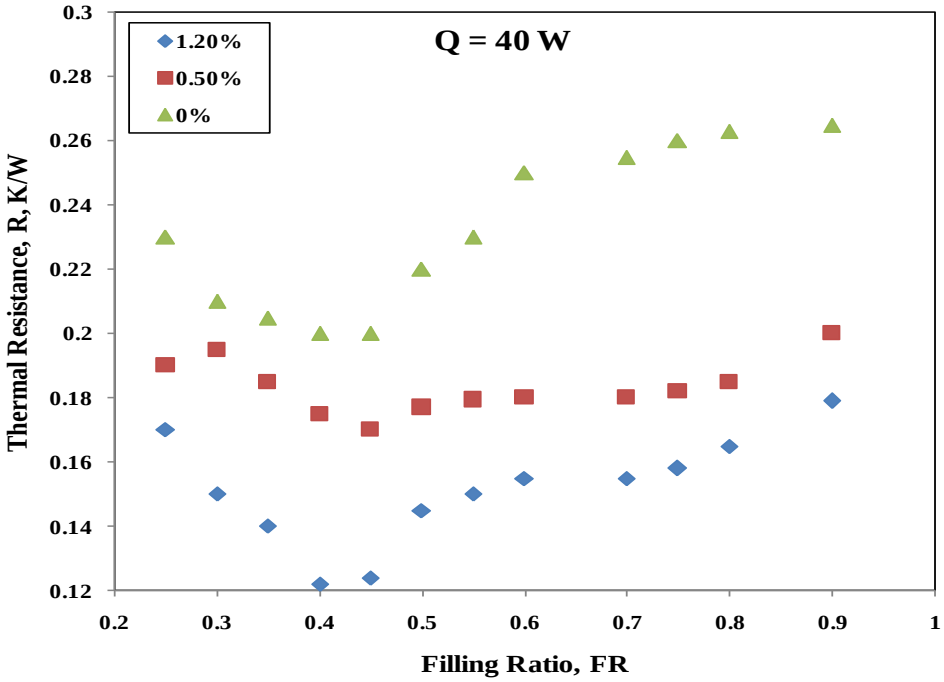

Figure 2.17 Variation of thermal resistance with filling ratio of different heat input rates [84]

Thermal resistance and response time for concentrations of 50, 200, and 600 ppm and heat rates ranging from 300 to 600 W, declined by 30% and 20% respectively. In the above experiments, what is of high significance is that raising the size and concentration of nanofluid improves thermal performance. In addition, utilizing nanoparticles with higher conductivity causes the thermal resistance to decrease from 30% for Al_2O_3 to 71% for silver nanofluid.

Tsai et al. [87] demonstrated the effect of size of spherical shaped gold nanoparticles dispersed in water on the operating characteristics of heat pipe. The TEM images of Figure 2.18 (a) show different sizes of gold nanoparticles with average diameters of A (21.3), B (43.7), C (8), D (9.3) and E (15.6) in nm. The heat pipe selected for the investigation was made of copper having length of 170 mm and diameter 6 mm. Using different nanoparticles sizes of gold, the thermal resistances of heat pipe vary from 0.17 to 0.21^{o}C/W as shown in Figure 2.18 (b). The results show strong dependency of the thermal resistance of heat pipe on the size of gold nanoparticles. The thermal resistances are found to decrease for the nanofluids A, B, C and D by 37%, 25%, 23% and 20%, respectively, as compared to DI water.

Do et al. [88] experimentally investigated the thermal performance of screen mesh wick heat pipe using Al_2O_3 water nanofluids as working fluids. The heat pipe of length 300

mm and diameter 4 mm is charged up to 255 % of the amount required to completely saturate the mesh wick. The thermal resistance decreases by 40 % when loaded with 3 vol. % concentration of Al_2O_3 water nanofluid as compared to DI water. The enhancement in the thermal performance results due to the formation of nano-coating on the screen mesh wick of the evaporator section of heat pipe as shown in 2.19.

Ghanbarpour et al. [89] performed an experimental study on screen mesh wick heat pipes using Al_2O_3/ DI water nanofluids as working fluids. The nanoparticles used in the study are in the range of 100 nm – 200 nm. The thermal performance of heat pipe is investigated at two different mass concentrations i.e 5 % and 10 % with the cyclic increase and decrease in heat input to the evaporator section of heat pipe.

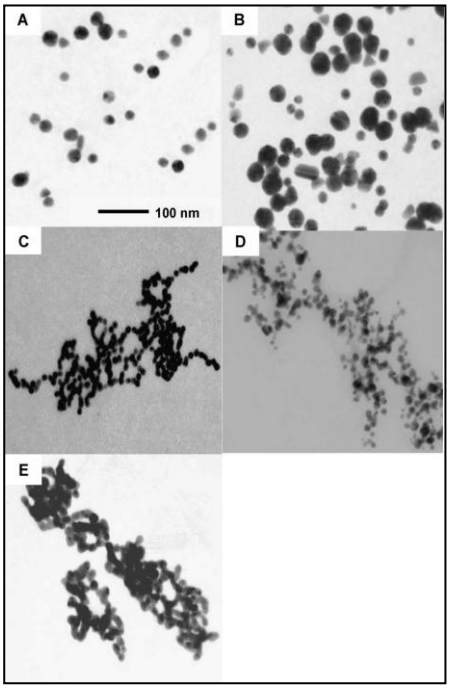

Figure 2.18 (a) TEM photographs of gold nanoparticles [87]

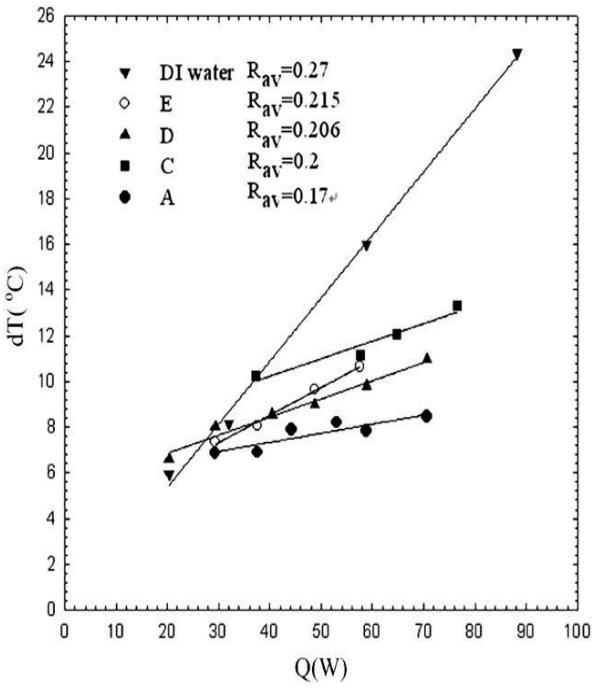

Figure 2.18 (b) Calculated values of thermal resistance of heat pipe [87]

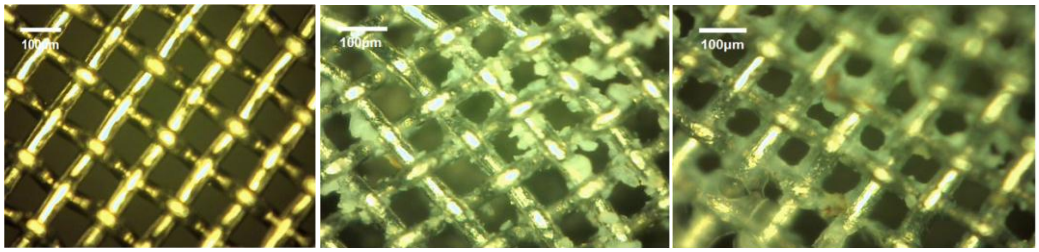

(a) At the beginning of experiment (b) At 1 vol. % after the experiment (c) At 3 vol.% after the experiment

Figure 2.19 Optical microscope images of mesh wick surface At the beginning of experiment (b) At 1 vol. % after the experiment (c) At 3 vol.% after the experiment [88]

It was observed that when the heat pipe was loaded with 5 wt. % Al_2O_3 nanofluids, the thermal resistance reduces between 6 % to 24 % and 20 % to 55 % during increasing and decreasing steps of the heat flux to the evaporator section, respectively. Whereas the thermal resistance of heat pipe increases between 187% to 206% for increasing and between 155% to 175% for decreasing steps in heat flux when loaded with 10 wt.% of Al_2O_3 nanofluids. So, better results were obtained at lower mass concentration i. e 5 wt % of Al_2O_3 / distilled water nanofluids. The SEM images of the wick structure before and after the tests are shown in Figure 2.20.

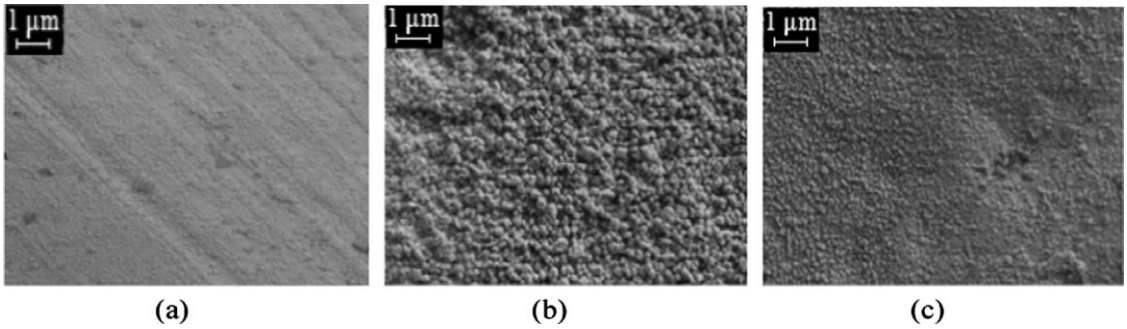

Figure 2.20 SEM images of the wick surface in the evaporator section (a) before the experiment (b) loaded with 5 wt.% Al_2O_3nanofluid and (c) loaded with 10 wt.% Al_2O_3 nanofluid [89]

Moraveji & Razvarz [90] investigated the efficiency of sintered circular heat pipe having 90^o degree bend as shown in Figure 2.21. The length and the diameter of heat pipe were 190 mm and 6 mm, respectively. Spherical aluminum oxide (Al_2O_3) nanoparticles of nominal diameter 35-45 nm are dispersed in de-ionised water to prepare nanofluids of 1 and 3% volume concentration. Similar trends in the thermal performance of heat pipe

were observed. The thermal resistance and the average temperature of heat pipe reduce with the charging of the nanofluids in heat pipe.

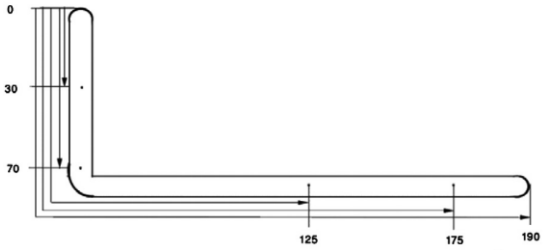

Figure 2.21 Heat pipe with 90^o bend [90]

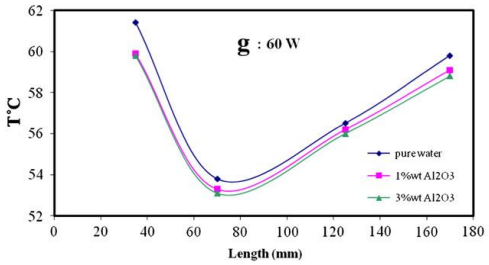

Figure 2.22 Wall temperature distribution along the length of heat pipe[90]

The striking observation was the lowest temperature at the curved zone of heat pipe as shown in Figure 2.22 and this temperature decreases from the evaporator to the bend and then increases. This sudden drop in temperature in the curved zone along the tube is due to vapor's impact and the lack of heat transfer at that point which is inside the heat pipe.

Putra et al. [91] conducted experiments on screen mesh wick heat pipe using 1 to 5 % volume concentration of different combinations of nanoparticles dispersed in base fluids (Al_2O_3 /water, Al_2O_3 / EG, TiO_2 / water, TiO_2 / EG and ZnO / EG).It has been reported that the heat pipe gives the best performance when loaded with 5% volume concentration of Al_2O_3 /water nanofluids as compared to their selected combinations of nanofluids. The formation of nano-coating of the nanoparticles results in the enhancement of heat pipe efficiency by promoting good capillary structure and increasing heat transfer area.

Kole and Dey [92] performed an experimental study using copper / distilled water nanofluids in heat pipe. The prepared nanofluids are fairly stable without the use of any surfactant. The thermal conductivity of Cu / distilled water shows an enhancement of 15% in the thermal conductivity value at 30°C when loaded to 0.5 wt. %. The thermal performance parameters of heat pipe such as average wall temperature of heat pipe, thermal resistance, and thermal conductivity are evaluated at three different orientations and the results are compared with that of DI water. The minimum average wall temperature of heat pipe has been reported at 90^o degree irrespective of the kind of working fluid used in the heat pipe. But the use of nanofluids as compared to DI water reduces the average wall temperature along the length of the heat pipe as shown in Figures 2.24 (a) and (b).

It was further observed that the thermal resistance of heat pipe attains high value at low watt heat input using the DI water and nanofluids and reduces to a minimum value with a further increase in the heat load. The thermal resistance of heat pipe at 90^{o} degree tilt angle shows a maximum reduction of 27 % loaded at 0.5 wt. % of Cu / distilled water. Once again the observation points to the deposition of nano-coating layer of the particles on the strands of the wick.

Asirvatham et al. [93] presented the study on the enhancement in the thermal efficiency of heat pipe using silver nanoparticles dispersed in DI water. The heat pipes used in the study are tested by gradually giving the heat input in steps in the range of 20 to 100 W, which is equivalent to the heat removal from power transistors used in the semiconductors industry.

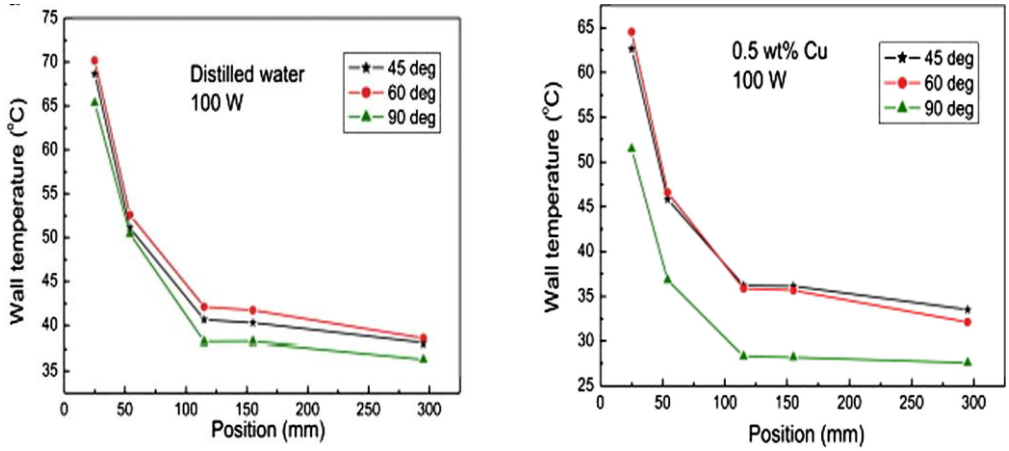

(a) **(b)**

Figure 2.23 Wall temperature distribution of heat pipe at 100 W input power containing (a) distilled water and (b) 0.5 wt % Cu / distilled water inclined at different angles [92]

The silver nanofluids with an average nanoparticle size of 58.35 nm in the volume concentration range of 0.003% to 0.009% have been used as working fluids in heat pipe. The vapor temperatures are measured at the core of the heat pipe directly. The thermal resistance reduced by 76.2 % when loaded at 0.009 vol. % concentration of silver nanoparticles. Furthermore, an increase in the evaporation heat transfer coefficient of 52.7 % has been observed for the same concentration. The use of nanofluids in heat pipe shows an enhancement in the operating range of heat pipe by 21% as compared with that of DI water.

Liu and Shu [94] investigated the heat transfer characteristics using CuO /water nanofluids in cylindrical mesh wick heat pipe. The length and diameter of the heat pipe was kept at 350 mm and 10 mm respectively. Inside the heat pipe, there are two layers of mesh screen wick along the length of the heat pipe. It was found that the nanoparticle mass concentration influences the heat transfer coefficients of the evaporator and condenser region of heat pipe. Also there exists an optimal mass concentration of 1.0 % tested at different operating temperatures. Figure 2.24 shows that the total heat resistance of the heat pipe using nanofluids is significantly smaller than that without nanoparticles.

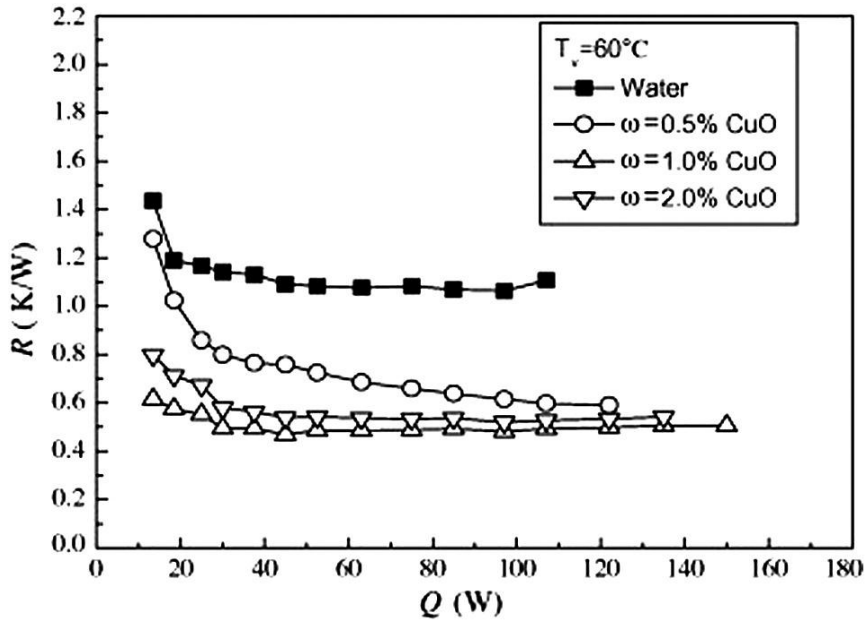

Figure 2.24 Heat resistance as a function of heat input and nanofluids concentration

Hung et al. [95] tested the heat pipe filled with three different concentration levels of Al_2O_3/water nanofluids (0.5, 1.0, and 3.0 wt. %). The straight heat pipes were made of copper tubing having different lengths of 0.3 m, 0.45 m, and 0.6 m with diameter 9.52 mm. This study presents a discussion on the effects of the charged volume ratio of the working fluid, tilt angle, heating power (20 W, 30 W, and 40 W), and weight fraction of nanoparticles on the overall thermal conductivity of the heat pipe. Experimental results show that at a heating power of 40 W, the optimal thermal performance for Al_2O_3/water nanofluid heat pipes measuring 0.3 m, 0.45 m, and 0.6 m is 22.7%, 56.3%, and 35.1%, respectively, better than that of pipes using distilled water as the working fluid.

2.8.2 Theoretical investigations

Various theoretical investigations has been done by the researchers but only the relevant studies are discussed as applicable to Al_2O_3 water based nanofluids in heat pipes.

Do and Jang [96] numerically investigated the performance of axially grooved heat pipe using Al_2O_3 water nanofluids as working fluid. Using the Young-Laplace equation for the phase change process, one dimensional conduction equation has been solved considering axial wall temperature of heat pipe, phase change rates during the evaporation and condensation process, thermo physical properties of Al_2O_3 water nanofluids and the formation of the thin porous coating.

There exists a feasibility of increasing the thermal performance of heat pipe up to 100 % using Al_2O_3water nanofluids at concentration levels less than 1.0 %.The formation of this coating on the mesh plays a vital role in the enhancement of thermal performance.

Shafahi et al. [97] theoretically applied two dimensional approaches for calculating the thermal performance of cylindrical shaped heat pipe charged with CuO, Al_2O_3, and TiO_2nanoparticles in DI water. The use of nanofluids reduces the thermal resistance and average wall temperature of heat pipe as compared to base fluids.

Furthermore, the maximum heat carrying capacity of heat pipe resulting due to use of nanofluids and geometrical features of the wick have been numerically investigated. It is concluded that there exists a maximum thermal performance of heat pipe at optimum mass concentration.

2.9 Summary

The literature studies indicate inconsistency in the thermal conductivity values of nanofluids influenced by particle size, shape, preparation method, morphology, volume concentration, pH and stability procedure. With few exceptions, the literature studies highlight the use of nanofluids in heat transfer applications due to their enhanced thermophysical properties.

Specific to alumina / water nanofluids, wide variation in the thermal conductivity ratios at the same temperature and volume concentration has been reported and this needs to be

experimentally explored for better understanding of results, validation and comparative statistics.

As per the referred journals studied in the literature, the use of nanofluids in heat pipes justifies its applicability by enhancing the operating characteristics of heat pipe. But the inconsistencies found in the performance parameters resulted due to particle loading, charging ratio, heat pipe tilt angle has challenged the present work for its validation at each step.

Most of the studies are concentrated on the regular profile of cylindrical shaped heat pipe brazed with circular end caps. Very few studies are available on the changed profile of heat pipe incorporating the velocity fluctuations along the travel of vapor flow. The geometric features of heat pipe are altered to accommodate the practical application. Most importantly, with limited studies available on the operational limitations of heat pipe using nanofluids, the author fails to find any study indicating the temporal performance of heat pipe.

2.10 Objectives

The objectives of the study are to prepare stable nanofluids and to investigate its solid state characteristics and thermophysical properties at selected volume concentrations and temperatures. The thermal conductivity being the dominating and an important thermal property of nanofluids is experimentally investigated using the transient hot wire method.

The surfactant free nanofluids with enhanced thermophysical properties are used as working fluids in heat pipes. In the present research work, the geometrical feature of the heat pipe has been altered as per the application by crimping the ends and providing minute circumferential surface depressions on the surface of heat pipe. The operating characteristics of heat pipe are investigated at different volume concentrations of alumina / DI water nanofluids and the heat pipe is tested in the power range of 12 W to 72 W to cover the temperature range of electronic gadgets.

Uniform heat flux to the evaporator section of heat pipe is provided by the construction of specially built up heating chamber. The heat pipe test rig has been designed and

constructed to accommodate the flow meters, RTD's and measuring instruments used for the evaluation of thermal performance of heat pipe.

The operating characteristics of heat pipe are sensitive to its orientation and the performance of the heat pipe is compared at favorable tilt angles in range 0 to $90^{o.}$ Another suitable gap in the literature studies has been found on the temporal performance or consistency in performance of heat pipe with the use of nanofluids. It is expected that the use of the nanofluids in heat pipe is prone to agglomeration and sedimentation with time leading to inconsistency in its performance. An attempt in this direction has been made by conducting a temporal study on the performance of heat pipe. This feature gives the practical utility of using heat pipe with nanofluids as working fluids.

2.11 Scope

In the present work, the commercially available alumina nanoparticles with an average size of40 - 45 nm are dispersed in the de-ionised water to be used as working fluid in the heat pipe. The spherically shaped alumina nanoparticles possess phase stability, high hardness, and good dimensional stability. With due consideration to mesh aperture and layers inside the heat pipe, the prepared Al_2O_3 / DI water nanofluids having volume concentrations in the range 0.005 to 1 vol. % prepared by two step method are used in heat pipe. The wall surface temperature and the thermal resistance of heat pipe at different volume concentrations and heat inputs (12 W to 72 W) are investigated at favorable tilt angles from 0^o to 90^o. The nanofluids prone to sedimentation and agglomeration with the passage of time can affect the operating characteristics of heat pipe. Keeping in view the practical application of heat pipe, a temporal study on the performance parameters of heat pipe has been conducted in the designed time frame of 0 to 9 months from the date of manufacturing.

Table 2.1 Nanofluids preparation methods and their observations

Authors	Method	Nanofluid/size	Observation(s)
Eastman et al. [15]	One step method	Cu / Ethylene glycol<10 nm	Particle size can be controlled and nanofluids are stable without the use of any surfactant
Lo et al. [18]	One step method	Cu,CuO,Cu_2Odispersed in different dielectric liquid medium	The process is compatible with low vapor pressure fluids, minimum cluster formation
Lee [14]	One step method & Two step method	Al_2O_3,CuO/ 2 –200 nm	There is tendency to form clusters
Murshed et al. [59]	Two step method	TiO_2/ Water (15 nm)	The surfactants Oleic acid and cetyl tri methyl ammonium bromide are used to ensure stable dispersion
Beck et al. [67]	Two step method	Al_2O_3/ Ethylene Glycol	Sufficient surface charge on the nanoparticles maintains the uniform dispersion
Hung et al. [95]	Two step method	Al_2O_3 / Water (surfactant - chitosan)	Less than 5% difference in the concentration levels was seen after two weeks

Table 2.2 Summary of stability process adoption for Al_2O_3/ DI water nanofluids

Nanoparticles	Base/Host Fluid	Concentration	Stability Process	Duration	Sedimentation	Investigator
Al_2O_3(80 nm) Al_2O_3 (150 nm)	DI water	1 vol. %	Ultrasonication	N/A	N/A	[40]
Al_2O_3(40 - 50nm)	Distilled water	1 vol.%	Ultrasonication	0-30 min	Reduction in particle size	[45]
Al_2O_3 (20 nm) Al_2O_3 (50 nm) Al_2O_3 (100 nm)	DI water	0.1-0.5 vol.%	Ultrasonication	N/A	N/A	[63]
Al_2O_3 (38.4 nm)	Distilled water	1- 4 vol.%	Ultrasonication	11 hours	After 12 hours	[63]
Al_2O_3 (11 nm) Al_2O_3 (20 nm) Al_2O_3 (40 nm)	DI water	0.5 - 10 vol. %	Ultrasonication	5-20 hours	40 nm particle suspensions shows more stability	[68]
Al_2O_3 (36 nm)	DI water	0.5 – 6 vol. %	Ultrasonication	1.5 hrs	N/A	[70]
Al_2O_3 (28 nm)	DI water	3 - 6 vol. %	Ultrasonication	-----	----------	[78]
Al_2O_3 (30 ± 5nm)	Distilled water	1.0 vol. % 3.0 vol. %	Ultrasonication	N/A	Separation line occurs after 20 days	[88]
Al_2O_3 (35-45 nm)	DI water	1.0 vol. % 3.0 vol. %	Ultrasonication	90 minutes	45 days	[90]

Table 2.3 Compilation of experimental studies using nanofluids in heat pipes

Experimental studies			
Research people	**Geometric details of heat pipe**	**Working fluid**	**Impact**
Naphon et al. [82]	Straight copper tube, Length = 600 mm, Diameter = 15 mm	TiO_2 / alcohol (21nm), TiO_2 / DI water	+
Chen et al. [84]	Flat mesh wick heat pipe, Diameter = 3 mm, Length = 200 mm	Ag / water	+
Mousa M. G. [85]	Cylindrical shaped heat pipe	Al_2O_3/ water (40 nm)	+
Tsai et al. [87]	Cylindrical heat pipe, Length = 170 mm, Diameter = 6 mm	Au-water (21.3, 43.7, 8, 9.3, 15.6 nm)	+
Do et al. [88]	Screen mesh wick Length = 300 mm, Diameter = 4 mm	Al_2O_3 / water (30 ±5 nm)	+
Ghanbarpour et al.[89]	Cylindrical copper heat pipe, Length= 200 mm, Diameter = 6.35 mm	Al_2O_3/distilled water	+
Moraveji & Razvarz [90]	Straight copper tube L = 190 mm, Diameter = 8 mm	Al_2O_3–pure water	+
Putra et al. [91]	Copper tube, Length= 200 mm, Diameter = 8 mm	Al_2O_3/ water, Al_2O_3 / EG, TiO_2/water, TiO_2/ EG, ZnO/EG	Al_2O_3/water shows +
Dey et al. [92]	Screen mesh wick heat pipe Length= 300 mm, Diameter = 10 mm	Cu / water (approx.40 nm)	+
Asirvatham et al. [93]	Copper tube, Length = 180 mm Diameter =10 mm	Silver-Deionised water	+
Liu and Shu [94]	Copper tube, Length= 350 mm Diameter =10 mm	CuO-water	---------
Hung et al. [95]	Copper tube, Length= 300,450 & 600 mm, Diameter = 9.52 mm	Al_2O_3/water	+
Suresh et al. [99]	Copper tube, Length = 1000 mm, Diameter = 12 mm	Al_2O_3 / water (15 nm)	+
Solomon et al. [100]	Copper tube, Length= 400 mm, Diameter = 19.5 mm	Cu / water (80-90 nm)	+
Saleh et al. [101]	Copper tube, Length = 200 mm, Diameter = 8 mm	ZnO / EG(18,23 nm)	+
Utomo et al. [102]	Stainless steel tube	Al_2O_3/ water, TiO_2/water (50-60 nm, 20- 30 nm)	+
Kumar et al. [103]	Straight copper tube Length = 600 mm, Diameter= 20 mm	Cu –water (approx.40nm)	+
+ Positive effect on heat pipe performance- Negative effect on heat pipe performance			

Table 2.4 Compilation of theoretical studies on using nanofluids in heat pipes

Theoretical studies		
Researcher	**Nanofluids**	**Suggestions**
Do et al. [96]	Al_2O_3/ water	• The use of nanofluids in heat pipe enhances the performance by 100%. • The thermal resistance of heat pipe decreases with the increase in the size of nanoparticles.
Shafahi et al. [97]	TiO_2, Al_2O_3, CuO / water	There exists an optimum mass concentration of nanofluids for the maximum efficiency.

CHAPTER 3

DESIGN CONSIDERATION, FABRICATION AND EXPERIMENTAL SETUP OF HEAT PIPE

3.1 Introduction

The performance of heat pipe and its operational limitations are dependent on wick structure, heat pipe geometric dimensions, shape, tilt angle and most importantly the thermophysical properties of working fluid. Careful consideration of the heat transport limitations can optimize the performance of heat pipe and provide an accurate representation of its performance within operational limitations.

The Al_2O_3/ DI water nanofluids prepared by direct mixing of the alumina nanoparticles in water are used as working fluids in modified screen mesh wick heat pipe. The performance of the heat pipe has been tested at different volume concentrations of nanofluids and power inputs. The nanofluids are prone to agglomeration and sedimentation with respect to time. With the result, the study is extended to evaluate the temporal performance of modified heat pipe in designed time frame of 0 to 9 months.

3.2 Design Considerations

3.2.1 Working Fluid

The type of the working fluid in heat pipe depends on its thermophysical properties in the selected temperature range. Based on the operating temperature range of electronics ($\leq 70^{o}C$), water has better heat transport capability and it is a chemically non-toxic and economically viable option as compared to other working fluids.

In the present work, Al_2O_3 nanoparticles of 45 nm average size are suspended in de-ionised water in the concentration range of 0.005 to 1 vol. % to be used as working fluid. The heat pipe operating characteristics are tested at three different watt loads of heat input i.e. 12 W, 32 W, 72 W to cover the operating temperature range of 30– 100 ^{o}C as applicable to electronics cooling. The nanofluids exhibiting enhanced thermophysical properties have shown promising results when used as working fluids in heat pipes. The research is still in the nascent stage due to disproportionate results quoted by various researchers.

3.2.2 Heat pipe material

The production of non-condensable gases (NCG), corrosion and material transport in the heat pipe are the possible problems arising due to incompatible heat pipe material and the working fluid. Based on the life tests conducted, Copper envelope with water as working fluid are the most commonly used heat pipe material and working fluid for the electronics cooling.

The present work is dedicated to the application of heat pipe for the electronics cooling application. The modified heat pipe is made of copper charged with Al_2O_3/ DI water nanofluids as working fluids. But there will be generation of non-condensable gas at elevated temperatures when using the oxide form of aluminum (Al_2O_3) in working fluid. The elevated temperature is beyond the scope of this study, whereas the compatibility of copper with DI water is already tested and documented.

3.2.3 Heat pipe structural considerations

Unlike flat heat pipe or other configured heat pipes, the cylindrical shaped heat pipes are not associated with structural problems. Cylindrical heat pipes are considered natural pressure vessels due to their shape, and can withstand large pressure differences as well as the resulting compressive or tensile forces on their walls. Since heat pipes can exist at pressures lower than atmospheric pressure when not in use, and can exceed atmospheric pressure at elevated, in-use temperatures, the cylindrical design has clear advantages, whereas large surface area to volume ratio of flat heat pipes is detrimental to its structural integrity. Giving due consideration to these selected features, cylindrical shape of the heat pipe is considered for the investigation at different concentrations of Al_2O_3/ DI water nanofluids.

3.2.4 Forming or shaping effect

A heat pipe is known to transport the heat from intricate parts through its flexible tubing's. This flexibility in heat pipe design helps in designing separate heat source and heat sink. The sudden change in the profile of heat pipe during the forming process may hinder its performance as the flattening and sharp curves may be obstructions to the fluid flow. With nanoparticles loaded in distilled water, it has become further challenging to design the heat pipe with changed geometric configuration.

3.2.5 Effects of length and pipe diameter

The flow rate of vapor inside the heat pipe depends upon the pressure differential developed across the evaporator and condenser section of heat pipe. The speed at which the vapor flows in the axial direction through the vapor core and the liquid return through the annular mesh wick depends on the geometrical features (length and diameter) of heat pipe which are to be considered during the designing phase. The heat pipes with larger cross-sectional area possess the higher heat transfer carrying capability. The length of heat pipe has a negative impact when working in opposition to gravity as the capillary action required for the liquid to be returned back to evaporator gets affected due to long length of the heat pipe. Under adverse tilt angles, it is recommended to use shorter heat pipes as they transfer more heat than the longer heat pipes.

Considering due practical applicability of heat pipe utilization, the length and diameter of the modified heat pipe have been kept as 200 mm and 10 mm, respectively. The heat pipe is made of copper and the thickness is kept at 1 mm. The evaporator, adiabatic and condenser sections of heat pipe are60, 40 and 100 mm in length, respectively.

In the present work, small surface depressions of up to 2 mm along the length of the cylindrical shaped heat pipe are made to accommodate the velocity variations and the ends are crimped as per application and to disregard any contamination effect generating out of brazing of end caps.

3.2.6 Wick Structures

At adverse tilt of heat pipe, the condensed fluid from the condenser section returns back to the evaporator section through the annular placed layers of mesh wick sliding along the inner walls of heat pipes to support the capillary action. The wick structures are exposed to axial and radial heat flow conditions.

In the present work, the use of axially grooved and sintered powder metal as wick structures is ruled out due to the extensive use of Al_2O_3 / DI water nanofluids with an average nanoparticle size of 40-45 nm. Furthermore the modifications in heat pipe restrict our study to the use of screen mesh wick inside the heat pipe. With the assumption of nanoparticle deposition on the wick strands resulting in clogging of the condensate flow path, a three

layered square patterned wire screen mesh of 200 strands per inch is employed for the capillary action.

The screen mesh wick is made of phosphor bronze for its non-corrosive and stiffness properties. The scheme of the mesh wick used in the present work has been shown in the Table 3.1.

Table 3.1 Scheme of the mesh wick used in the heat pipes

Weave pattern Plain wrap wire with Square pattern	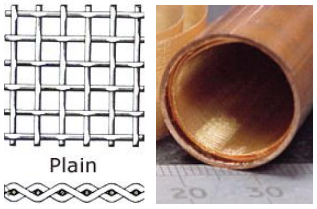
Material	Phosphor Bronze
Thermal Conductivity @ 23 ^{o}C (Wm^{-1}K^{-1})	50
Melting Point ^{o}C	900 -1050
Density g cm^{-3}	8.9
Number of multiple layers of similar screen mesh	3
Wire diameter (mm)	0.0406
Aspect Ratio (AR)	1
Aperture size per linear inch (mm)	17.28
Mesh count per unit inch	199
Percent Open area (POA)	46.41 %
Volumetric Porosity of mesh wick, ε_w	0.7363
Wick Crimping factor	1.05

3.2.7 Heating chamber

In the literature studies, extensive use of electric heater in controlling the heat input to the evaporator section of heat pipe has been made. In the present work, heating chamber has been designed for the uniform heat flux from the axial and radial directions. The heat supplied to the evaporator section is controlled through the circulating hot water. A suitable working temperature range (< 70^{o}C) of electronics equipment has been selected for the investigation of modified heat pipe using the stable Al_2O_3 / DI water nanofluids as working fluids.

3.2.8 Inventory of working fluid

The working fluid in the heat pipe must be charged to a limit so that the axial vapor space must be filled with the base fluid vapors and the wick must be saturated with the liquid phase of nanofluids. An optimum filling of the heat pipe will enhance its performance and avoid the blockage of the condenser during the overfilling condition. The calculation of required quantity of nanofluid can be determined by the following equation:-

$$m = A_v L_T \rho_{v+} A_w L_T \varepsilon_w \rho_l \quad (3.1)$$

3.3 Analytical Calculations

Volume concentration, φ x 100

$$\varphi \times 100 = \frac{\left[\frac{w}{\rho}\right]_{Al_2O_3}}{\left[\frac{w}{\rho}\right]_{Al_2O_3} + \left[\frac{w}{\rho}\right]_{base\ fluid}} \quad (3.2)$$

Density of nanofluids

$$\rho_{nf} = (1 - \varphi)\rho_{bf} + \varphi\rho_{np} \quad (3.3)$$

3.4 Analytical model

The various thermal resistances to the heat flow path from the evaporator to the condenser section of heat pipe are shown in Figure 3.1. A thermal resistance network approach has been discussed to ascertain the radial and axial heat flow interactions.

In the radial direction, the heat input to the evaporator section of the heat pipe is through the interface of the heat source and external heat pipe wall, the wall of heat pipe, liquid-wick interface at the evaporator and the condenser section, and at the external condenser section of the heat pipe and heat sink. Whereas, in the axial direction of heat pipe, the thermal resistances occur in the vapor core along the length. The thermal resistance of vapor flow through the vapor core of heat pipe from evaporator to condenser section is very small compared to the resistances offered by external surface of evaporator and condenser.

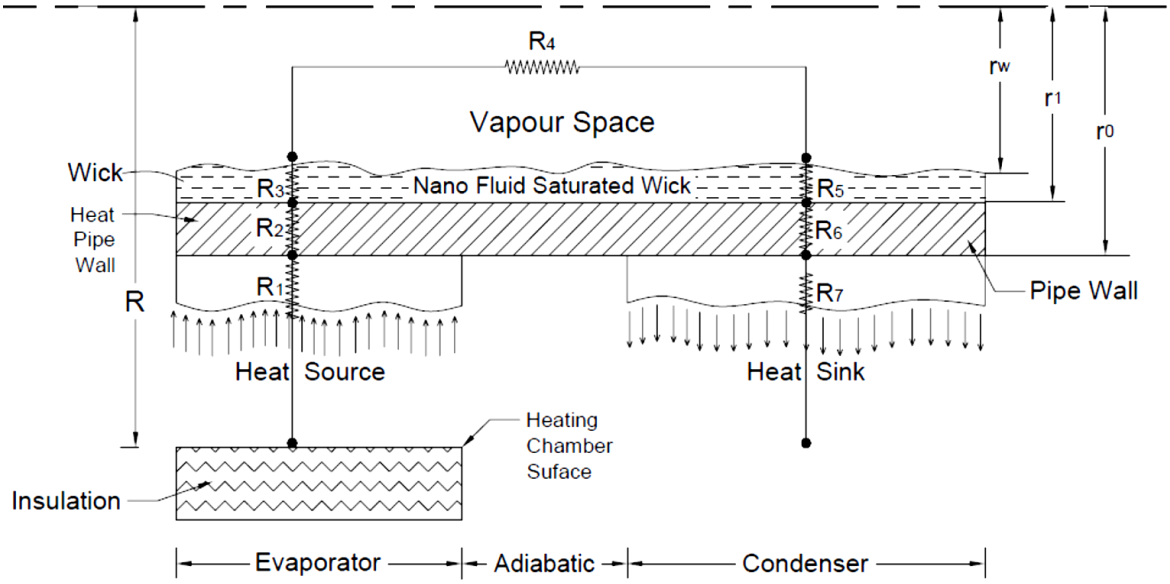

Figure 3.1 Thermal resistance network of heat pipe (View 1)

Table 3.2 Thermal resistances of heat pipe [109]

Resistance	**Description**	**Equation**
R_2	Evaporator wall resistance	$\frac{r_o t_{pi}}{2L_e k_{pi}}$
R_3	Evaporator wick resistance	$\frac{r_o^2 t_w}{2L_e r_i k_{e,e}}$
	Effective thermal conductivity of liquid saturated wick at evaporator	$\frac{k_l[k_l + k_w - (1-\varepsilon)(k_l - k_w)]}{[k_l + k_w + (1-\varepsilon)(k_l - k_w)]}$
R_4	Vapor duct resistance	$\frac{\pi r_o^2 F_v \left(\frac{L_e}{6} + L_a + \frac{L_c}{6}\right) T_{v,e}}{J\lambda\rho_v} r^2$
R_5	Condenser wick resistance	$\frac{r_o^2 t_w}{2L_c r_i k_{e,c}}$
R_6	Condenser wall resistance	$\frac{r_o t_p}{2L_c k_p}$

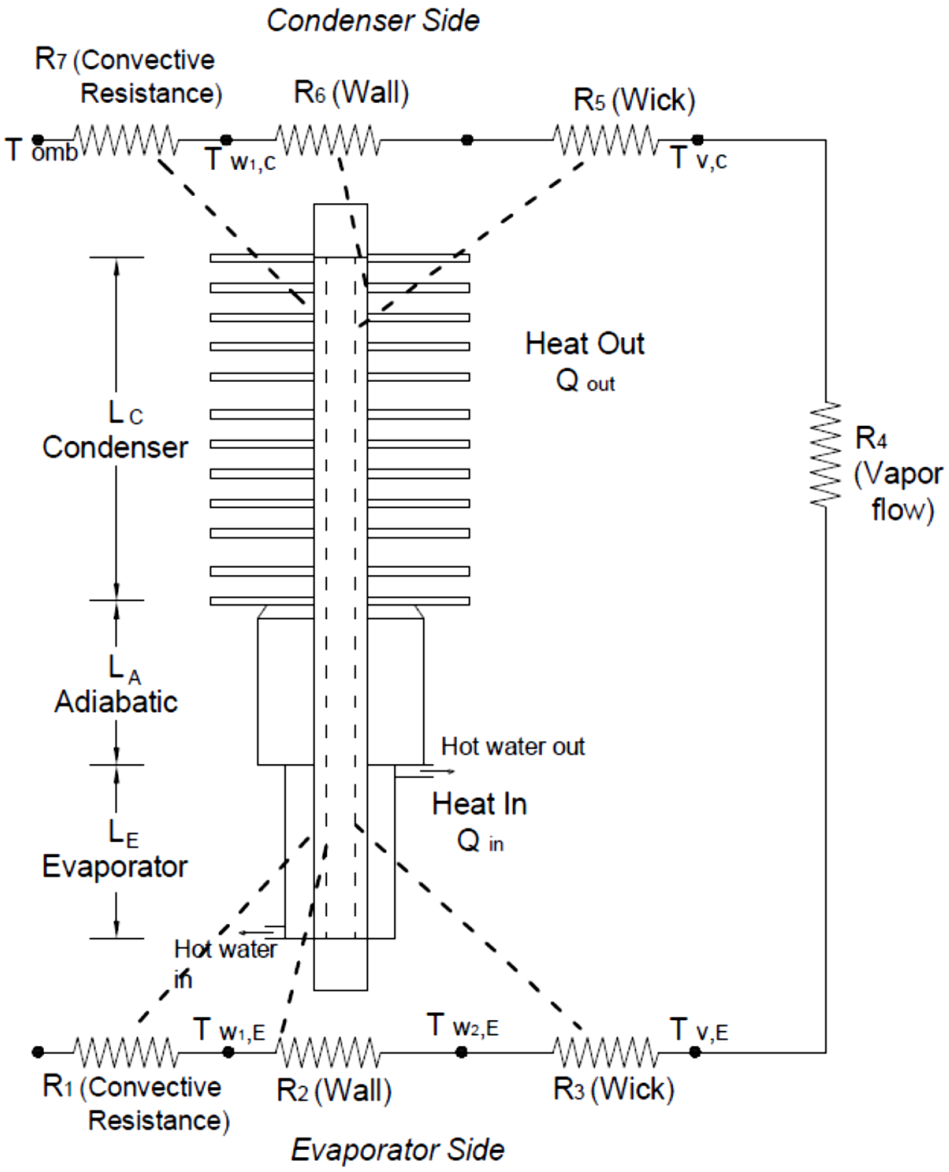

Figure 3.2 Thermal resistance network of heat pipe (View 2)

3.5 Heat Pipe Operational Limitations

The maximum heat transfer capability of heat pipe depends on its operational limitations. The various operational limitations of heat pipe are capillary limit, boiling limit, entrainment limit, sonic limit, and viscous limit. The relevant equations for obtaining the heat pipe operational limits are referred from Peterson [103].

3.5.1 Capillary Limit

The maximum capillary pressure, $\Delta P_{ca,\,max}$ developed in the evaporator section of heat pipe must exceed the pressure losses along the vapor and liquid flow paths

$$\Delta P_{ca,\,max} \geq \Delta P_l + \Delta P_v + \Delta P_{ph,e} + \Delta P_{ph,c} + \Delta P_g \tag{3.4}$$

Where ΔP_l and ΔP_v are the inertial and viscous pressure drop in liquid and the vapor phase of flow of working fluid, $\Delta P_{ph,e}$, $\Delta P_{ph,c}$ are the pressure drop due to phase transition in evaporator and condenser section and ΔP_g is the pressure drop due to gravitational force in the condensate flow.

$$\Delta P_{ca,\,max} = 2\sigma \cos\theta / r_{ca} \tag{3.5}$$

Where r_{ca} is the effective capillary radius, $\cos\theta$ is the wetting angle, σ is the surface tension of the working fluid.

$$\Delta P_l = [\mu_l / (K\, A_w \rho_l\, \lambda)]\, L_{eff}\, Q \tag{3.6}$$

$$\Delta P_v = [(f_v\, Re_v)\, \mu_v) / (2\, (r_{h,v})^2\, A_v \rho_v\, \lambda)] \tag{3.7}$$

$$\Delta P_g = \rho_l\, g\, d_v \cos\psi \tag{3.8}$$

Where, $\cos\psi$ is the tilt angle of heat pipe.

The capillary limit of heat pipe is stated by its maximum heat load capability and given as

$$Q_{ca,\,max} = 2\left(\frac{\rho_l\, \lambda\, \sigma}{\mu_l}\right)\left(\frac{K}{r_{eff}}\right)\left(\frac{A_w}{L_{eff}}\right)\cos\theta \tag{3.9}$$

Where K, A_w, r_{eff} are the wick permeability, cross-sectional area and capillary radius of wick. L_{eff} is the effective length of the liquid flow path, and θ is the apparent contact angle at the evaporating meniscus interlines.

3.5.2 Boiling Limit

The boiling limit $Q_{b,\,max}$ of heat pipe is given as

$$Q_{b,max} = 2\pi \frac{L_{eff}\; k_{eff}\; T_v}{A_v\; \lambda\; \rho_v\, In\left(\frac{r_i}{r_v}\right)}\left[\frac{2\sigma}{r_n} - \Delta P_{\;ca,max}\right] \tag{3.10}$$

Where r_i, r_v, r_n are the inner radius, vapor core radius and nucleation radius respectively. The effective length of heat pipe, $L_{eff} = 0.5L_e + L_a + 0.5L_c$ and k_{eff} is the effective thermal conductivity of the liquid–wick combination calculated as

$$k_{eff} = \frac{\left(k_l\left(k_l + k_w - (1-\varepsilon)(k_l - k_w)\right)\right)}{k_l + k_w + (1-\varepsilon)(k_l - k_w)} \tag{3.11}$$

k_l is the thermal conductivity of liquid and k_w is the wick thermal conductivity, ε is the wick porosity calculated as

$$\varepsilon = 1 - \left(\frac{\pi S N d_{wi}}{4}\right) \tag{3.12}$$

d_{wi} is the diameter of the wick wire, and N is the screen mesh number, S is the wick crimping factor (1.05), $\Delta p_{ca,max}$ is the maximum capillary pressure discussed above, r_n is the nucleation site radius.

3.5.3 Sonic Limit

The sonic limit is calculated based on the following equation

$$Q_{S,max} = A_v \rho_v \lambda \left[\left(\frac{\gamma_v R_v T_v}{2(\gamma_v + 1)}\right)\right]^{1/2} \tag{3.13}$$

Where γ_v = specific heat ratio of vapor, $R_v = 8.314 \times 10^3/18 = 462$ J/(kg K), M is molecular mass of water vapor.

3.5.4 Viscous limit

The viscous limit $Q_{v,max}$ is calculated based on the following equation

$$Q_{v,max} = d_v^2 \lambda A_v \left(\frac{P_v \rho_v}{4(f_v Re_v) L_e \mu_v}\right) \tag{3.14}$$

Where Re_v = local axial Reynolds number in the vapor

3.5.5 Entrainment limit

The entrainment limit $Q_{en,max}$ is calculated based on the following equation

$$Q_{en,max} = A_v \lambda \left[\frac{\sigma \rho_v}{2 r_{h,s}} \right]^{1/2} \quad (3.15)$$

Where A_v is the cross-sectional area of the vapor core = $\pi d_v^2 / 4$ and $r_{h,s}$ is the wick surface pore hydraulic radius given by:

$$r_{h,s} = \frac{1}{2N} - \frac{d_{wi}}{2}$$

3.6 EXPERIMENTAL DETAILS

3.6.1 Thermal conductivity measurement of Al_2O_3 nanofluids and data validation

Various techniques have been developed and discussed in the literature to find the thermal conductivity of nanofluids. In the present work, a transient hot wire (THW) technique (Nagasaka & Nagashima [105]) has been adopted because recent advances in electronic techniques have helped to establish this method as one of the most accurate ways to determine fluid thermal conductivity and it also eliminates the effect of natural convection as compared to steady state apparatus.

In this method, a thin metallic wire of platinum is used as temperature sensor and is also act as a line heat source. The wire is surrounded by the liquid whose thermal conductivity is to be measured. The wire is then heated by sending current through it. Higher the thermal conductivity of the surrounding liquid, lower will be the temperature rise of the wire. This principle is used to measure thermal conductivity of the liquid. The experiment lasts for a maximum of 2-5 seconds and hence this is a very fast method. The natural convection does not take place due to very small time interval. In conjunction with an advanced data acquisition system, the method gives very accurate value of thermal conductivity.

The schematic diagram of laboratory level setup consists of measurement cell and the electrical circuit as shown in Figure 3.3. A pure platinum wire of diameter 100 μm and length 15 cm (aspect ratio 1500) having high electrical resistivity (1.06×10^{-7} unit at 20^oC) and high temperature coefficient of resistance ($0.003925/^oC$) is employed to act as line heat source and temperature sensor. Platinum is used for the hot wire because of its resistance/temperature relationship is well known over a wide temperature range. The

platinum wire was coated with a thin coating of PPR (positive Photo Resistive) which acts as electrical insulator. The vertically positioned platinum wire is immersed in the fluid whose thermal conductivity is to be measured.

The fluid is placed in borosilicate glass tube of inner diameter 20 mm and thickness of 1mm.The platinum wire dissipating heat in the radial direction acts as one arm of the Wheatstone bridge circuit. The applied voltage is optimally chosen so that the wire gets heated slowly and reaches an asymptotic temperature.

The circuit is attached to the data acquisition system. With the observed slope obtained between the temperatures of the heat source at time t_1 and $t_2$taken asT_1 and T_2 respectively, the thermal conductivity of the liquid is calculated as

$$k = \frac{q}{4\pi (T_2 - T_1)} \ln \left(\frac{t_2}{t_1} \right) \qquad (3.16)$$

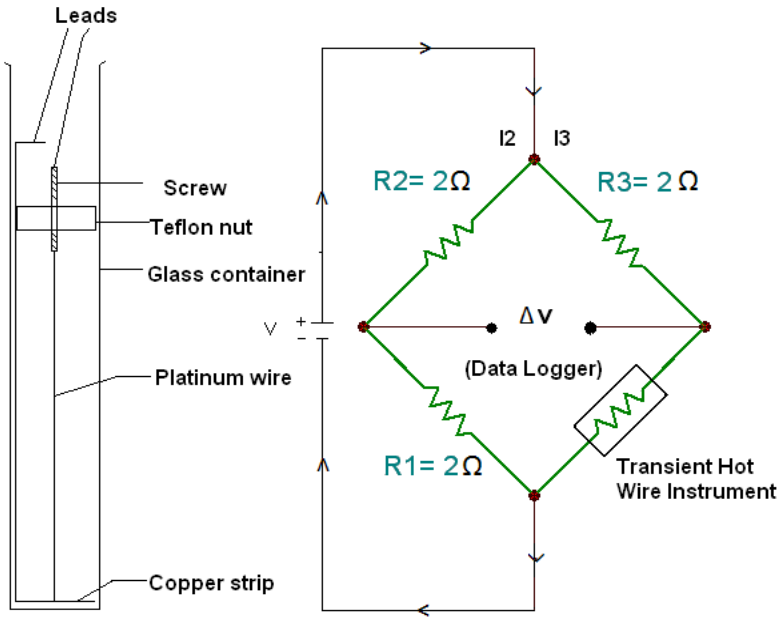

Figure 3.3 Measurement cell of transient hot wire equipment

The uncertainties in the resistance of platinum wire, voltage applied across the bridges and length of the wire are incorporated to calculate the uncertainty in the thermal conductivity values and are found to be ± 1.6%. The thermal conductivity of de-ionised water was

measured in the selected temperature range of 20°C to 70°C. At 30°C, the value of thermal conductivity of water is measured to be 0.615 W/ (m.K) which increased to 0.65 W/(m.K) at 60°C. The comparison of experimental data with the literature values are graphically plotted and shown in Figure 3.4 (VDI Wärmeatlas [106]).

From the obtained values, a standard deviation of 0.5 % is observed whereas the maximum deviation was found to be less than 1.4 %, which is quite acceptable and less than the maximum uncertainty value calculated by theoretical uncertainty analysis (1.5 %).The equipment is found to be working with high accuracy and repeatability over the selected range of thermal conductivity values. Using this technique, the thermal conductivity of Al_2O_3/DI water nanofluids at 0.005, 0.05, 0.5 and 1.0 vol.% concentration are obtained at room temperature and in the working temperature range of heat pipe from 20°C - 70°C which are discussed in detail in the next chapter.

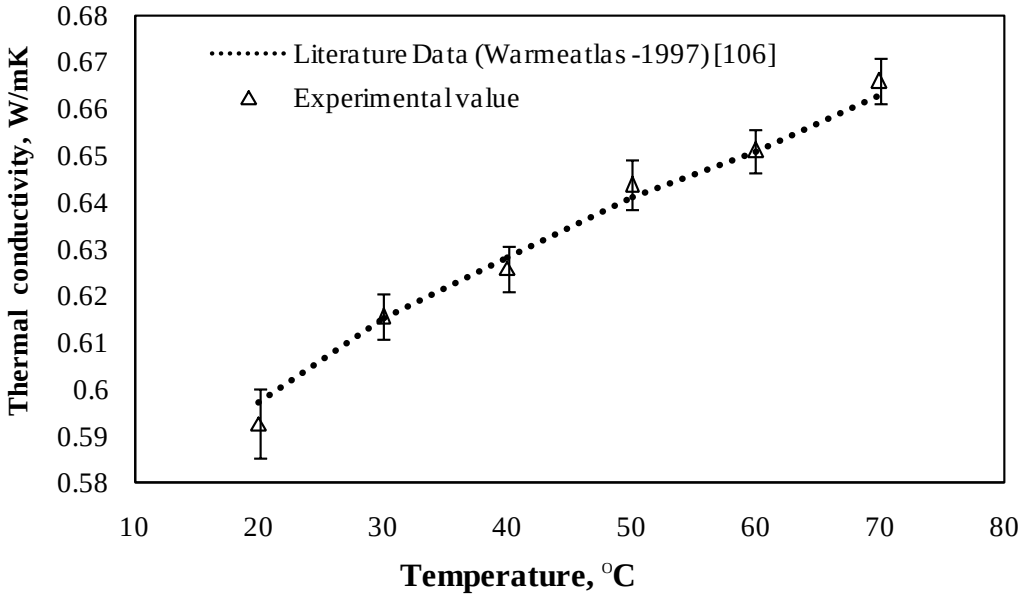

Figure 3.4 Comparison of thermal conductivity values of DI water using THW technique from literature value [106]

3.6.2 Heat pipe experimental setup

The schematic diagram of the experimental set up is shown in Figure 3.7. The experimental setup consists of thermostatically controlled heating system, the heat pipe test section, data acquisition system, tilt mechanism and the rotameter console.

3.6.2.1 Fabrication of screen mesh wick heat pipe

The heat pipes tested in the experimental work are made of copper having outer diameter, inner diameter and length as 10, 8 and 200 mm, respectively. Each heat pipe is inserted with three layers of square patterned wire screen mesh of 200 strands per inch. The screen mesh wick is made of phosphor bronze with wire diameter of 0.0406 mm. The heat pipe is evacuated using a rotary vacuum pump and the pipe is filled with the working fluid using a specially designed heat pipe filling rig at M/s Golden Star, Pune. The dissolved gases in the heat pipe are removed and the minimum vacuum pressure during the pumping process is kept at 0.009 mbar.

The geometrical features of the heat pipe are changed and the ends are crimped from sides to act as conduction lengths as shown in the Figure 3.5 and Figure 3.6. The crimping of heat pipe edges helps in neglecting the effects of freezing and thawing on the concealed joints when the temperature of the heat pipe falls below the freezing temperature of working fluid. In addition to it, minute circumferential surface depressions up to 2.5 mm are made along the length of the heat pipe to overcome the reduced vapor velocity.

The heat pipes are charged up to 40% of the evaporator section volume (8.33 % of the total volume of the heat pipe) with DI water and with four different volume concentrations viz. 0.0005, 0.005, 0.05 and 1 vol. % of Al_2O_3/DI water nanofluids. No surfactant is added in the working fluid as the stability of alumina nanoparticles dispersed in de-ionized water has shown promising results without indicating any separation line in the sedimentation test (Mousa [85], Hung et al. [95] and Moraveji et al. [90]). Also the DI water being slightly acidic (pH< 7) due to formation of carbonic acid shows better quality of the dispersion of alumina nanoparticles in DI water.

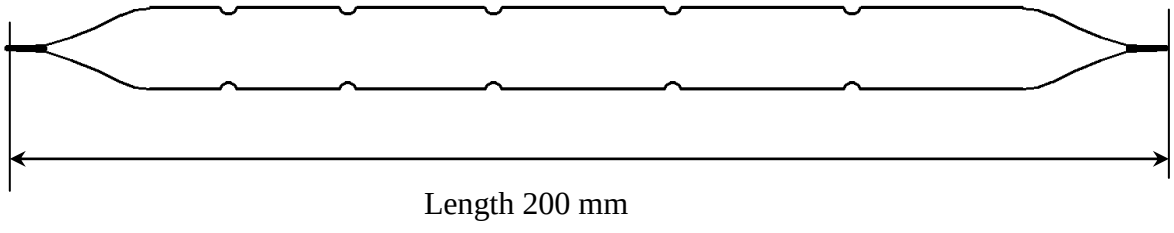

Figure 3.5 Schematic diagram of modified heat pipe

The suspensions, even without any dispersant, dispersed well because of their positive surface charge as reported in the literature. There will be generation of non-condensable gas (NCG) in using the oxide form of aluminum (Al_2O_3) at the elevated temperatures (Reay et al. [107]). The elevated temperatures are beyond the scope of this study.

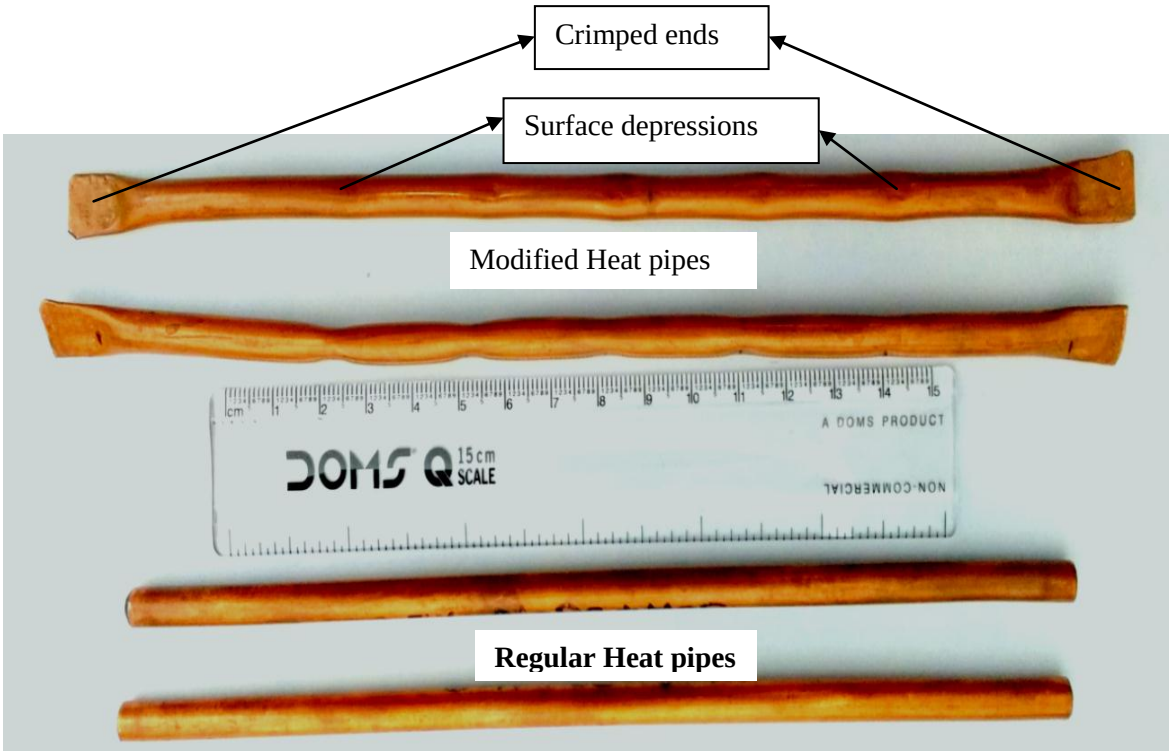

Figure 3.6 Picture of modified and regular heat pipe used in the present study

3.6.2.2 Experimental setup and instrumentation

The thermal performance of heat pipe is tested in a laboratory level test rig as shown in the schematic diagram in Figure 3.7. The evaporator, adiabatic and condenser sections of the heat pipe are 60, 40 and 100 mm in length, respectively. The evaporator section of heat pipe is inserted into cylindrical shaped heating chamber constructed around it. The heat input to the heating chamber is through circulating hot water. The flow rate and temperature of the circulating water are controlled by rotameter and thermostatic bath, respectively. The heating chamber is insulated using layers of glass wool to minimize the heat loss. The condenser section of 100 mm axial length is cooled under natural convection by fitting

annular circular fins. The measurement scheme and the thermocouple layout are shown in Figure 3.8.

The evaporator, adiabatic and the condenser sections of heat pipe contain two RTD's each. The photograph of the heat pipe experimental setup is shown in Figure 3.9 (a). To know the performance of heat pipe at various inclinations, provision of tilting mechanism is made and shown in Figure 3.9 (b). The flow rate and the temperature of the circulating water in heating chamber are controlled by rotameter and temperature controlled thermostatic bath.

The rotameter used in the experimental work is calibrated by volumetric method at National Physical Laboratory, New Delhi. The accuracy of the rotameter is found to be± 3% of FSD (calibration method confirms to ISA R.P 16.6).

The temperature of the circulating water is recorded using Pt-100 RTDs which are calibrated using Hart Scientific sensor; Precision Thermometer ASL Model F-150-D and dry block calibrator of Isotech (Europa 520) for the specified range. The read out uncertainty of the data logger is ± 0.37°C.To reduce the thermal contact resistance, thermal paste is applied to all the contacting surfaces of heat pipe.

3.6.2.3 Experimental Procedure

The operating characteristics of heat pipe are investigated after keeping it statically in the horizontal position for 10 days from the date of manufacturing. This exercise will incorporate any sedimentation effect at the initial stage under the prevailing ambient conditions inside the heat pipe. A total of four heat pipes are manufactured using DI water, 0.005, 0.005, 0.05 and 1 vol. % of Al_2O_3 – DI water nanofluids as working fluids. Each heat pipe is tested for three heat load inputs i.e.12 W, 32 W and 72 W to cover the safe operating temperature range of electronic equipments (< 70^oC). Constant voltage supply for the pump and steady state conditions up to a temperature variation of 0.1^oC for 5 min is ensured while taking the readings.

The heat input to the evaporator section is controlled with the flow rate and inlet temperature of the circulating water. The temperature of the circulating water is maintained by

thermostat. With the control of these parameters, the thermal performance of four heat pipes is evaluated at 12 W, 32 W and 72 W heat input.

Once the steady state is reached, the temperature distributions along the evaporator, adiabatic and condenser sections of heat pipe are plotted and observed. The heat input to the evaporator section is given in the incremental steps from 12 W to 32 W and then from 32 W to 72 W. At times, an attempt has been taken to study the temperature distribution randomly at 32 W and 72 W directly. The values so obtained are within the uncertainty range of RTD's and data logger.

Difficulty has been encountered in maintaining the required heat input with the control of two variables but unlike in the literature review, an attempt has been taken to study the performance of heat pipe under uniform axial and circumferential heat flux. The condenser is cooled under the natural convection conditions. Due to directional sensitivity of heat pipe, the same procedure is adopted to study the temperature distribution at different tilt angles i.e. 0^o, 30^o, 45^o, 60^o& 90^o.

Very few studies in the literature have evaluated the temporal performance of heat pipe using nanofluids. The present study is extended to compare the performance of heat pipe after 0, 3, 6 and 9 months of intermittent operation This study will be helpful in understanding the impact of sedimentation of nanoparticles inside the heat pipe.

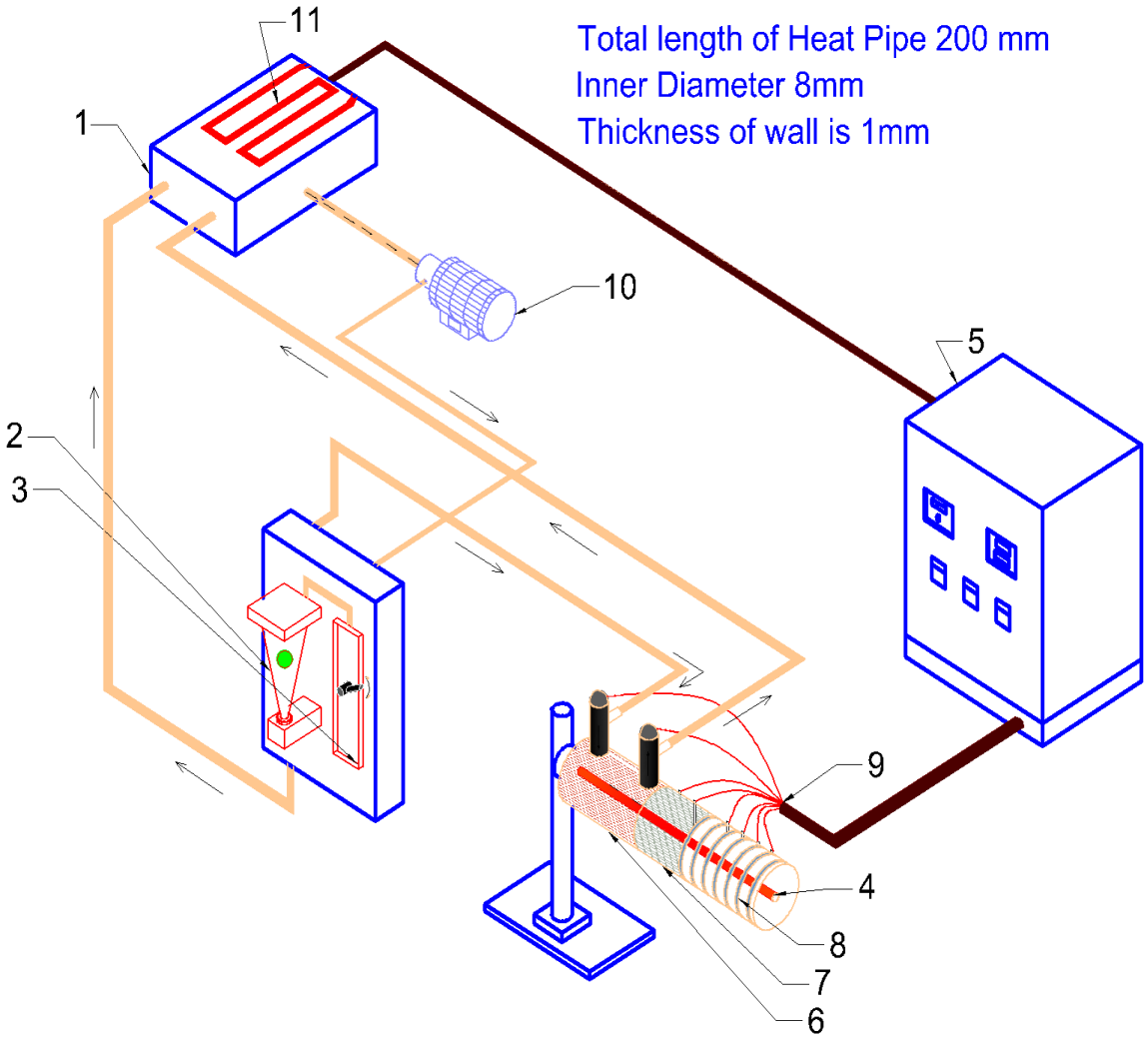

Label No	Description
1	Temperature control bath
2	Rota meter
3	Bypass valve
4	Heat pipe
5	Data acquisition and display
6	Evaporator
7	Adiabatic section
8	Condenser section with fins
9	Thermocouples
10	Water circulation pump
11	Water heater
12	Insulation

Figure 3.7 Schematic diagram of the experimental apparatus

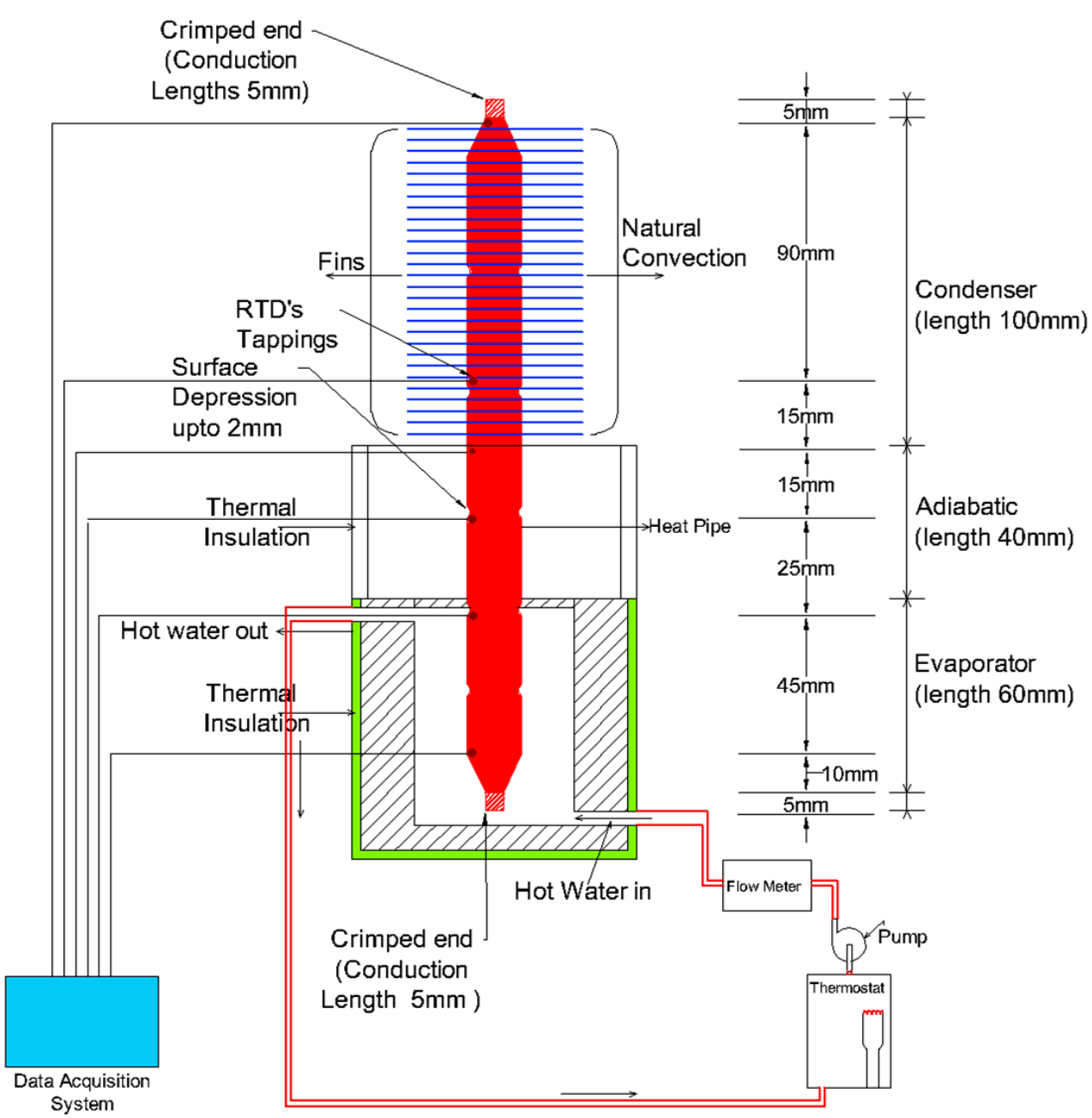

Figure 3.8 Measurement scheme and thermocouple layout along the length of heat pipe

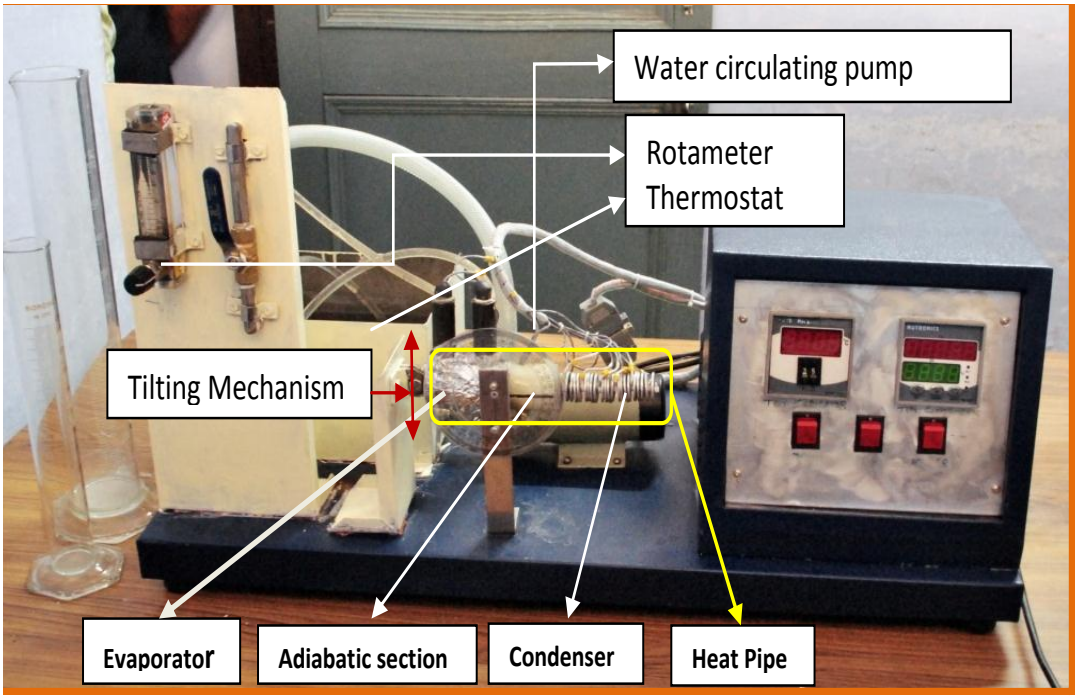

Figure 3.9(a) Photograph of the experimental setup

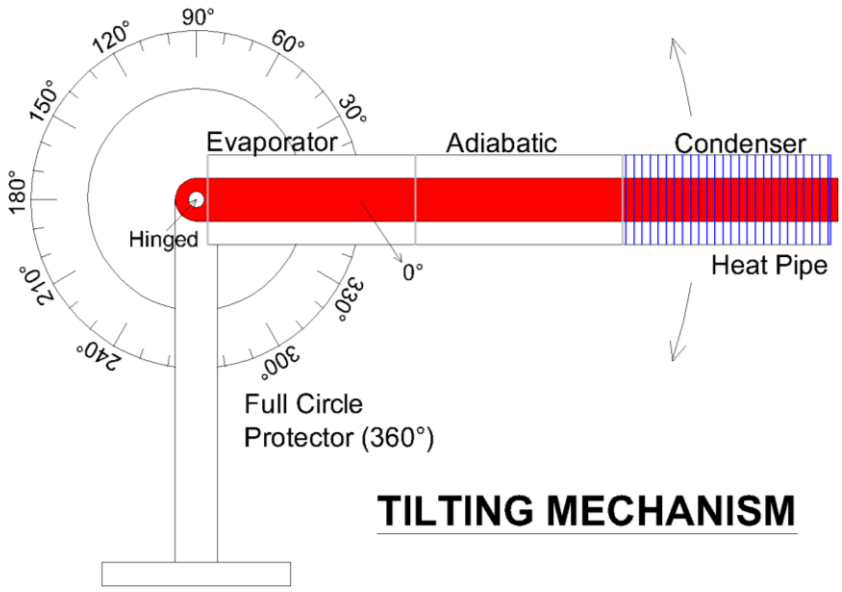

Figure 3.9(b) Schematic diagram of tilting mechanism

3.7 Data Reduction and Uncertainty in the measurements

To investigate the operating characteristics of heat pipe, the heat input to the evaporator section, temperature distribution along the length of heat pipe and the thermal resistance at varying heat loads of 12 W, 32 W and 72 W using DI water and different concentrations i.e. 0.0005, 0.005, 0.05 and 1 vol. % of nanofluids are calculated. The heat input to the evaporator section is calculated by

$$Q_{in} = m\, C_p\, (T_{out} - T_{in}) \quad (3.16)$$

The overall thermal resistance (R) of the heat pipe is calculated as

$$R = \frac{T_{avg,e} - T_{avg,c}}{Q_{in}} \quad (3.17)$$

Where $T_{avg,e}$, $T_{avg,c}$ and Q_{in} average evaporator temperature, average condenser temperature and heat input respectively.

3.7.1 Uncertainty and validation in the measurement of thermal conductivity using transient hot wire method

The step by step calculation for the uncertainty associated with the transient hot wire method used for measurement of the thermal conductivity of nanofluid is described below:

The thermal conductivity of liquid is given by

$$k = \frac{1}{4\pi} q \times \text{slope} \quad (3.18)$$

Where slope is given as

$$\text{slope} = \frac{\text{In}\left(\frac{t_2}{t_1}\right)}{(T_2 - T_1)} \quad (3.19)$$

The average value of the measured entities and the associated uncertainties are given below

Resistance	**Value**	**Uncertainty**
$R_1 + R_2$	4.009Ω	0.001 Ω
R_2	1.998Ω	
R_3	1.993 Ω	
$R_{34\text{-}w} = R_3 + R_4 - R_w$	2.1797 Ω	
R_0 Resistance of platinum wire at 0^oC	1.7333 Ω	
Voltage applied across the bridge	2.4412 V	0.002
Initial voltage difference across the bridge, ΔV	58.3 mV	1 μV
Length of the wire	13.85 cm	0.1 mm

To calculate the uncertainty associated with k, the uncertainty in 'q' and 'slope' are to be calculated as

$$q = \frac{I_{wi}^2 R_{wi,mean}}{L} \tag{3.20}$$

I_{wi} is the instantaneous current flowing through the wire and $R_{wi,mean}$ mean is the average resistance of the wire over the period of interest. The uncertainty associated with 'q' depends on I_{wi} , L, $R_{wi,mean}$ and is calculated as

$$R_{wi} = \frac{VR_3}{I_2 R_2 - \Delta V} - R_{34-wi} \tag{3.21}$$

R_{wi} is the instantaneous resistance of the wire and its uncertainty is dependent on I_2 as given by

$$I_2 = \frac{V}{R_1 + R_2} = \frac{2.4412}{4.009} = 0.6089 \text{ Amp}$$

Uncertainty in I_2 is calculated as

$$\frac{dI_2}{I_2} = \left[\left(\frac{dV}{V}\right)^2 + \left(\frac{d_{R1+R2}}{R_1 + R_2}\right)^2\right]^{1/2}$$

$$\frac{dI_2}{I_2}=\left[\left(\frac{0.002}{2.441}\right)^2+\left(\frac{0.001}{4.009}\right)^2\right]^{1/2}$$

$$=8.5644 \text{ x } 10^{-4}$$

$$dI_2= 8.5644 \text{ x } 10^{-4} \text{ x } 0.6089 = 5.2152 \text{ x } 10^{-4} \text{ A}$$

With R_{wi} = 2.0205 Ω, and uncertainty in value is

$$\frac{dR_{wi}}{R_{wi}}=\left[\left(\frac{dV}{v}\right)^2+\left(\frac{dR_3}{R_3}\right)^2+\left(\frac{dI_2}{I_2}\right)^2+\left(\frac{dR_2}{R_2}\right)^2+\left(\frac{d\Delta V}{\Delta V}\right)^2+\left(\frac{dR_{34\text{-}wi}}{R_{34\text{-}wi}}\right)^2\right]^{1/2}$$

$$\frac{dR_{wi}}{R_{wi}}=\left[\left(\frac{0.002}{2.4412}\right)^2+\left(\frac{0.001}{1.993}\right)^2+\left(\frac{5.2148 \text{ x}10^{-4}}{0.60893}\right)^2+\left(\frac{0.001}{1.998}\right)^2+\left(\frac{1 \text{ x } 10^{-6}}{58.3 \text{ x } 10^{-3}}\right)^2+\left(\frac{0.001}{2.1797}\right)^2\right]^{1/2}$$

$$\frac{dR_{wi}}{R_{wi}}=\left[6.7120 \text{ x } 10^{-7}+ 2.5175 \text{ x } 10^{-7}+7.339 \text{ x } 10^{-7}+ 2.505 \text{ x } 10^{-7}+2.9421 \text{ x } 10^{-22}+2.1047 \text{ x } 10^{-7}\right]^{1/2}$$

$$\frac{dR_{wi}}{R_{wi}}=\left[6.7120 \text{ x } 10^{-7}+ 2.5175 \text{ x } 10^{-7}+7.339 \text{ x } 10^{-7}+ 2.505 \text{ x } 10^{-7}+2.9421 \text{ x } 10^{-22}+2.1047 \text{ x } 10^{-7}\right]^{1/2}$$

$$\frac{dR_{wi}}{R_{wi}}=\left[2.1172 \text{ x } 10^{-6}\right]^{1/2}$$

$$\frac{dR_{wi}}{R_{wi}} = 1.4550 \text{ x } 10^{-3}$$

From the experimental data, the value of R_{wi} is 2.035 Ω and its uncertainty is

$$dR_{wi}= \pm 2.1172 \text{ x } 10^{-3} \text{ Ω}$$

The uncertainty in I_{wi} is estimated as

$$I_{wi} = \frac{V}{R_{wi,mean} + R_{34\text{-}wi}} = \frac{2.4412}{2.035+2.1797} = 0.5792 \text{ A}$$

Uncertainty in I_{wi} is

$$\frac{dI_{wi}}{I_{wi}}=\left[\left(\frac{dV}{V}\right)^2+\left(\frac{dR_{wi,mean}}{R_{wi,mean}}\right)^2+\left(\frac{dR_{34\text{-}wi}}{R_{34\text{-}wi}}\right)^2\right]^{1/2} = 1.059\, x\, 10^{-3}$$

$$dI_{wi}=\pm 6.13807 \text{ x } 10^{-4} \text{A}$$

For q = 4.9293 W/m, the uncertainty value comes out to be

$$\frac{dq}{q}=\left[\left(\frac{dI_{wi}}{I_{wi}}\right)^2+\left(\frac{d\,R_{wi,mean}}{R_{wi,mean}}\right)^2+\left(\frac{dL}{L}\right)^2\right]^{1/2}$$

$$\frac{dq}{q}=\left[\left(\frac{6.1307\ x10^{-4}}{0.5732}\right)^2+\left(\frac{2.1172\ x\ 10^{-3}}{2.035}\right)^2+\left(\frac{0.1}{138.5}\right)^2\right]^{1/2}$$

$$\frac{dq}{q}=\left[2.2106\ x\ 10^{-6}\right]^{1/2}$$

$$dq = \pm 7.3290\ x\ 10^{-3}\ W/m$$

To find the uncertainty in 'slope', we have to calculate the uncertainty in temperature difference (T_2-T_1).The temperature of the wire at any time is given as

$$T\ =\left[\frac{R_{wi}}{R_o}-1\right]\frac{1}{\alpha}$$

At time t_1 = 0.369 s, temperature of the wire T_1 = 44.57^{o}C and at time t_2 = 2.387 s. temperature of the wire, T_2 = 45.677^{o}C.

Considering the input voltages and the resistances to be constant over the experiment range, then the uncertainty associated in temperature difference measurement is

$$\frac{dT}{T}=\left[\left(\frac{dR_{wi}}{R_{wi}}\right)^2+\left(\frac{dR_o}{R_o}\right)^2\right]^{\frac{1}{2}}$$

$dT = 44.57[(1.4550\ x10^{-3})^2 + (5.769\ x10^{-4})^2]^{1/2} =\ 0.06976^oC$

The error in the temperature measurement is insignificantly small.

Calculating the slope from the equation, slope = 1.6866.Considering a manual error of 0.025 in the measurement of slope, the thermal conductivity of water is k = 0.9916 W/(m.K) and the total uncertainty associated with the thermal conductivity value is obtained as follows

$$\frac{dk}{k}=\pm\sqrt{\left(\frac{dq}{q}\right)^2+\left(\frac{dk}{k}\right)^2}$$

$$dk=\pm\sqrt{2.2141\ x\ 10^{-6}+2.1971\ x\ 10^{-4}}$$

$$dk = \pm 0.009855\ W/(m.K)$$

$$k = 0.6616 \pm 0.009855\ W/(m.K)$$

Using transient hot wire method, the total uncertainty in the thermal conductivity value comes to be less than 1.5 % of the mean value.

3.7.2 Uncertainty in the measurement of thermal resistance of heat pipe

Based on the accuracies of the used instruments, the uncertainties of the measured quantities are evaluated. Various instruments used for the measurements in the present research work are calibrated from nationalized laboratories and the uncertainty associated in the calculations of various parameters is given below:

Uncertainty in rotameter readings

$$\frac{d\dot{V}}{\dot{V}} = \left[\left(\frac{dV}{V}\right)^2 + \left(\frac{dt}{t}\right)^2\right]^{1/2} \tag{3.22}$$

The rotameter used for the mass flow rate measurement is calibrated by volumetric method at National Physical Laboratory and its accuracy is ±3% of FSD.

Uncertainty in evaporator section

The uncertainty in the evaporator section is due to the mass flow rate of water, specific heat of water, inlet and outlet temperature of water from the evaporator. The read out uncertainty of the data logger is ± 0.37^{o}C. Neglecting the uncertainty due to specific heat, $dC_p/C_p = 0$, the uncertainty in the evaporator section is

$$\frac{dQ}{Q} = \left[\left(\frac{d\dot{m}}{\dot{m}}\right)^2 + \left(\frac{dC_p}{C_p}\right)^2 + \left(\frac{dT_{in}}{T_{in}}\right)^2 + \left(\frac{dT_{out}}{T_{out}}\right)^2\right]^{1/2} = 1.62\ \% \tag{3.23}$$

Uncertainty in thermal resistance of heat pipe

The uncertainty in thermal resistance depends on the applied heat input and the temperature difference between the condenser and evaporator ends is

$$\frac{dR}{R} = \left[\left(\frac{dQ}{Q}\right)^2 + \left(\frac{d(\Delta T)}{\Delta T}\right)^2\right]^{1/2} = 5.6\ \% \tag{3.24}$$

The uncertainty is calculated taking the maximum value in each case and is found to be within 6 %.

CHAPTER 4

CHARACTERIZATION OF Al_2O_3/ DI WATER NANOFLUIDS

4.1 Solid state characterization

The Al_2O_3 nanoparticles used in the present experimental work are procured from a leading supplier of nanoparticles i.e Alfa-Aesar from USA. Although some information was provided by the supplier but a reconfirmation test has been performed on the solid state characteristics of Al_2O_3 nanoparticles using X-ray powder diffraction technique. The X-ray diffraction measurements have been conducted and are shown in Figure 4.1 (a).

PANalytical X'Pert Pro MPD instrument available in the leading nationalized laboratory of IIT Ropar has been used to record the X-ray diffraction patterns. The obtained XRD pattern of Al_2O_3 nanoparticles confirm to the typical recorded spectra documented with JCPDS data bearing ICDD-card No. 00-046-1131 [104].

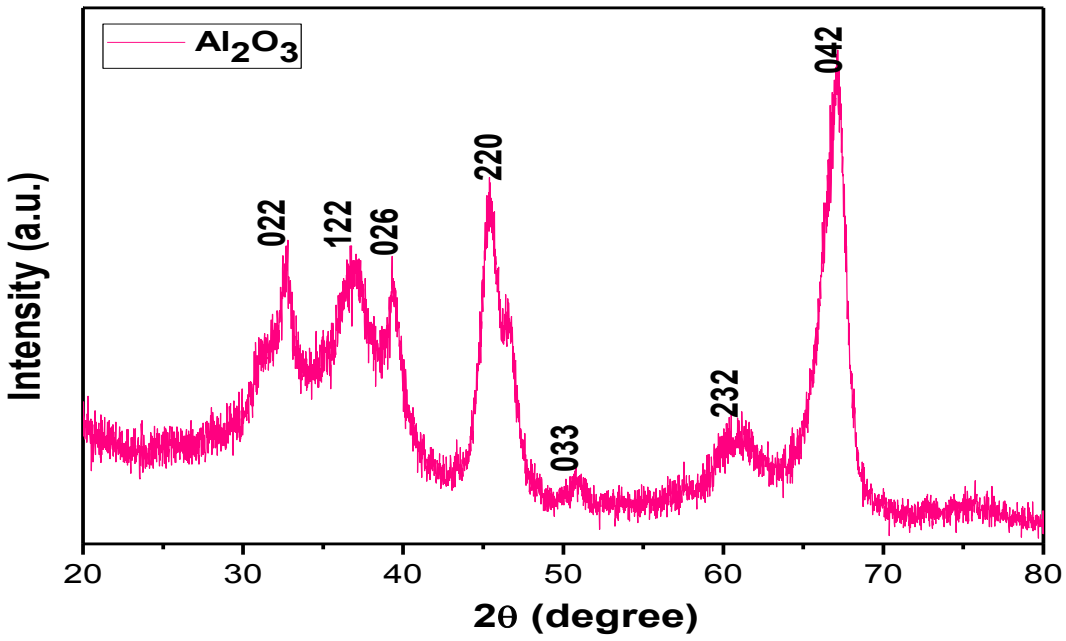

Figure 4.1(a) X-ray diffraction (XRD) patterns of Al_2O_3 nanoparticles (ICDD 00-046-1131)

From the XRD pattern, seven peaks were observed at approximately 2θ = 32.65, 36.87, 39.40, 45.32, 50.41, 60.12 and 67.04 which correspond to the Braggs reflection plane of (022), (122), (026), (220), (033), (232) and (042) respectively. No other peaks related to any

other impurity have been found. The average crystallite size is calculated by well-known Debye-Scherrer formula as shown below:

$$D_{vol} = 1.2\delta / B \cos\theta \quad (4.1)$$

Where δ is the X - ray source wavelength equal to 1.5406 Å, B denotes the peak width, θ is the angle of the same peak (bragg angle) and D_{vol} represents the volume weighted crystallite diameter of the equivalent spherical particles. For the evaluation of the crystallite size the width of the most intense X-ray diffraction peak has been taken into consideration. The average crystal size of alumina particles used in the present research work is found to be in the range 9-15 nm. The details are tabulated below in the Table 4.1.

The crystal size of alumina nanoparticles estimated from PXRD peak broadening are 3 to 5 times smaller than the nominal particle size determined by the supplier from surface area measurements. The discrepancy is subjected to agglomeration of crystallites in the pure solid form. The literature emphasizes the impact of agglomerated state on the thermal conductivity of nanofluids. The agglomerated state has a strong dependency on time and the present research work is extended to understand the temporal behavior of nanofluids on the performance of heat pipe. The literature also divides by citing the benefits of using the extended elliptical, dendritic, fractal aggregates of nanoparticles over the spherical shapes in increasing the enhancement of thermal conductivity of nanofluids.

Table 4.1 Properties of Al_2O_3 nanoparticles used in this study

Al_2O_3 Nanoparticles	**Description**
Color	White powder
Density	3880 kg/m^3
Thermal conductivity	27-38 W/(m.K)
Particle size	40–45 nm
Purity (%)	≥99.9
Specific surface area	≥100m^2/m^3

Using two step method, the Al_2O_3nanoparticles are dispersed in DI water without the use of any surfactant. The prepared nanofluids are oscillated for 6 hrs at 40 kHz frequency using Branson 3510 ultrasonic homogenizer to attain a stable suspension (Lee et al. [49]).

The prepared Al_2O_3/ DI water nanofluid is characterized using Transmission Electron Microscope (FEI TF-20; FEI, Hillsboro, Oregon at 200 kV)). The morphology of Al_2O_3/ DI water nanofluids is shown in Figure 4.1(b) below. The micrograph shows that the Al_2O_3nanoparticles are 10 to 100 nm in size with spherical shape. The average size of the nanoparticle is found to be in the narrow range of 40-45 nm as shown in the DLS report in Fig. 4.1 (b).

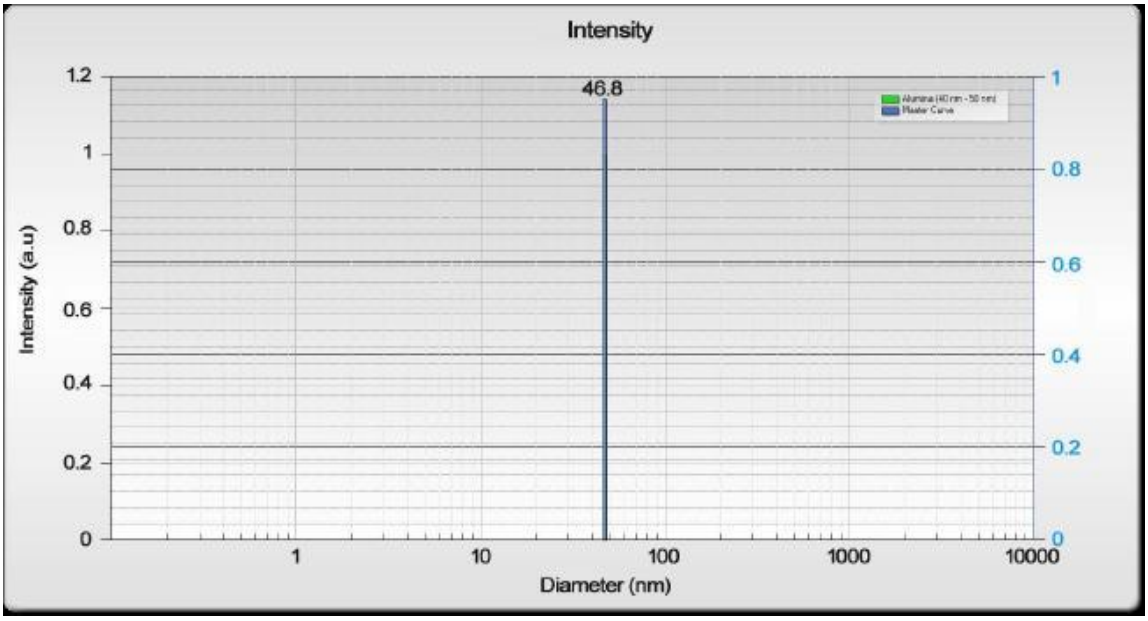

Figure 4.1(b) Scattering intensity versus nanoparticle diameter for Al_2O_3 nanoparticles from dynamic light scattering measurements

Close examination at high magnification may reveal truncated polyhedral shapes. However, few agglomerated Al_2O_3 nanoparticles are observed. No attempt has been made to further break the agglomerated nanoparticles.

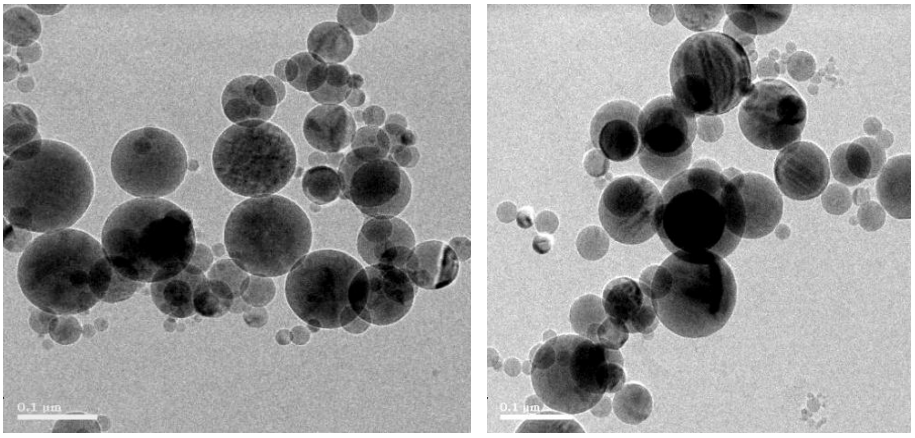

Figure 4.1(c) TEM on 100 nm scale showing the particle size and morphology of the agglomerated Al_2O_3 used in this study

4.2 Thermal conductivity enhancement of Al_2O_3 / DI water nanofluids

The thermal conductivity of nanofluids for the selected concentration range is measured at room temperature and no attempt was made to maintain the temperature of the nanofluids at constant temperature because of the fluctuations of the room temperature in the laboratory are very small. The reduced conductivity counted as the ratio of nanofluid thermal conductivity to that of the base fluid thermal conductivity (k_{nf} / k_{bf}) shows an increase with the increase in concentration of alumina nanoparticles in DI water as shown in Figure 4.2.

The results obtained by using the THW method are compared with the literature values at room temperature within the selected volume concentration range. The literature values are plotted irrespective to any shape and size consideration of Al_2O_3 nanoparticles. The results so obtained in the present work do not show any anomalous enhancement in the thermal conductivity values but indicate minor variation among the literature values. This variation may be attributed due to different preparation method adoption for nanofluids preparation, size and shape of nanoparticles, ultrasonication duration, stability technique and uncertainty associated with the measurement of thermal conductivity.

The thermal conductivity of Al_2O_3 / DI water nanofluid increases with increase in the nanoparticle concentration as depicted in the literature studies and the same trend has been observed in the present work.

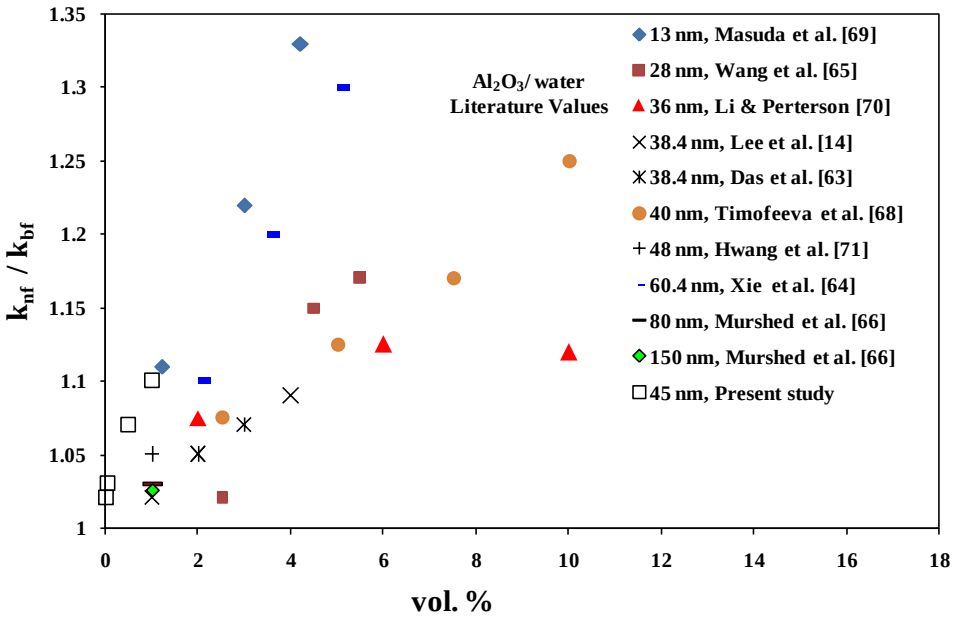

Figure 4.2 Comparison with the literature values

At room temperature, a maximum enhancement of 10% has been achieved at 1 vol. % concentration ofAl_2O_3/ DI water nanofluids. This value is equivalent to that achieved by Xie et al. [64] with 2 vol.% concentration. Much variation has been seen in the thermal conductivity values which may be due to the reasons cited above. Also the size of the nanoparticles gives a dubious picture on its relationship with the enhancement of thermal conductivity.

The rise in temperature increases the thermal conductivity of nanofluids as reported in literature. So an attempt has been made in the present study to investigate the effect of temperature on the thermal conductivity of Al_2O_3 / DI water nanofluids in the selected temperature range of 20 – 70^{o}C. Sufficient numbers of reading sets have been taken and the calculated mean values are graphically plotted as shown in Figure 4.3.

From the plotted values, it was observed that with the suspension of spherical shaped Al_2O_3 nanoparticles in DI water, an enhancement in thermal conductivity is observed with rise in temperature.

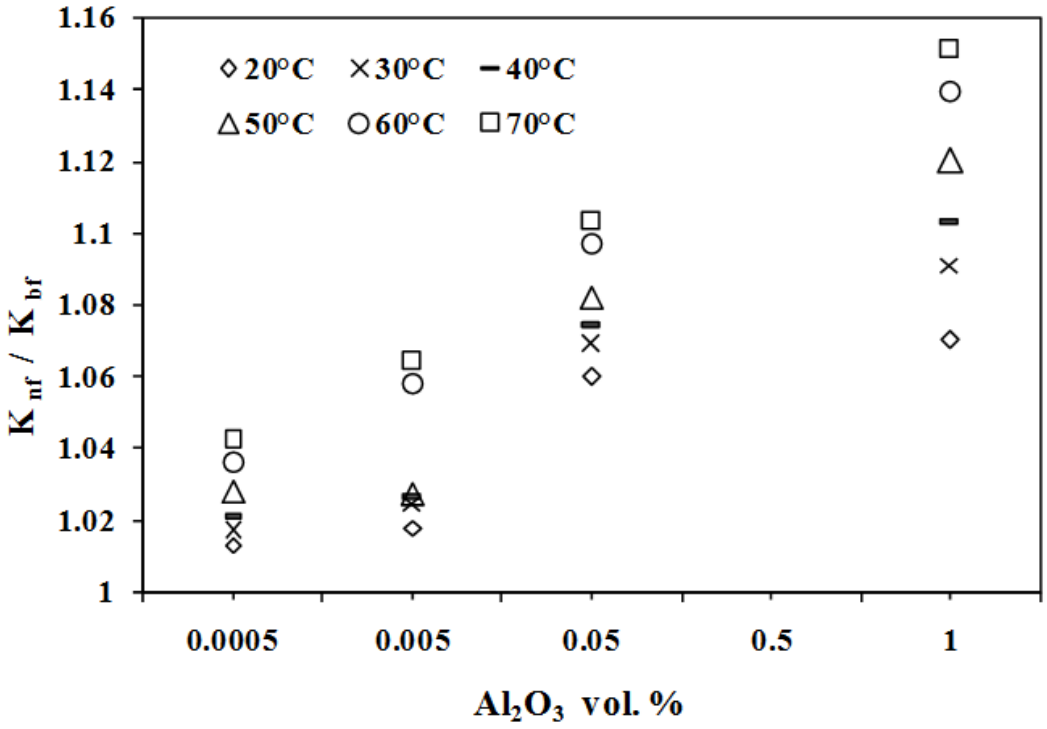

Figure 4.3 Thermal conductivity ratio of Al_2O_3 / DI water nanofluids as a function of volume concentration and temperature

As shown in Figure 4.3, an enhancement of 1 to 5 %, 2 to 7 %, 6 to 11 % and 7 to 15 % has been observed in the thermal conductivity values of nanofluids as compared to DI water when loaded at 0.0005, 0.005, 0.05 and 1 volume % of Al_2O_3/ DI water nanofluids, respectively in the selected temperature range of 20 to 70^{o}C.

The thermal conductivity enhancement factor varies linearly with the increase in temperature at higher volume concentration of 1 % as compared to other selected range of investigation. The probable mechanism behind the enhancement in the thermal conductivity with the rise in temperature is either because of intensive Brownian motion or aggregation of Al_2O_3 nanoparticles.

The thermal conductivity enhancement taking into account the Brownian motion of particles can therefore be expressed by Kumar et al. [112] as

$$\frac{k_{eff}}{k_m} - 1 = c.\bar{u}_p \frac{\varepsilon r_m}{k_m(1-\varepsilon)r_p} \tag{4.2}$$

Where $\bar{u}_p$the average particle velocity, c is is a constant. The k_{eff} is effective thermal conductivity, $k_m$is thermal conductivity of medium, $r_m and\ r_p are$ the spherical radii of suspended medium and nanoparticle ,ε is the volume fraction of the nanoparticles. The mean velocity of the nanoparticle has been calculated using the Stokes-Einstein's formula,

$$\bar{u}_p = \frac{2\,k_p T}{\pi \eta d_p^2} \tag{4.3}$$

it is evident from the above expression that the particle velocity ($\bar{u}_p$) depends upon the factor T/η, where η is the dynamic viscosity of the fluid medium and T is the temperature. Since viscosity of the medium such as water decreases significantly with temperature, particle velocity increases. This explains the strong dependence of thermal conductivity enhancement with temperature and Brownian motion.

The enhanced thermal conductivity values of Al_2O_3/ DI water nanofluids with the rise in temperature (20 to 70^{o}C) are plotted and compared with the documented values from the literature as depicted in Figure 4.4. The literature values clearly demonstrates an enhancement in the thermal conductivity with the rise in the temperature except the values quoted by Masuda et al. [69]which indicate the reverse trend of decrease in the thermal conductivity with the rise in the temperature while testing at 1.25 and 2.75 vol. % concentration.

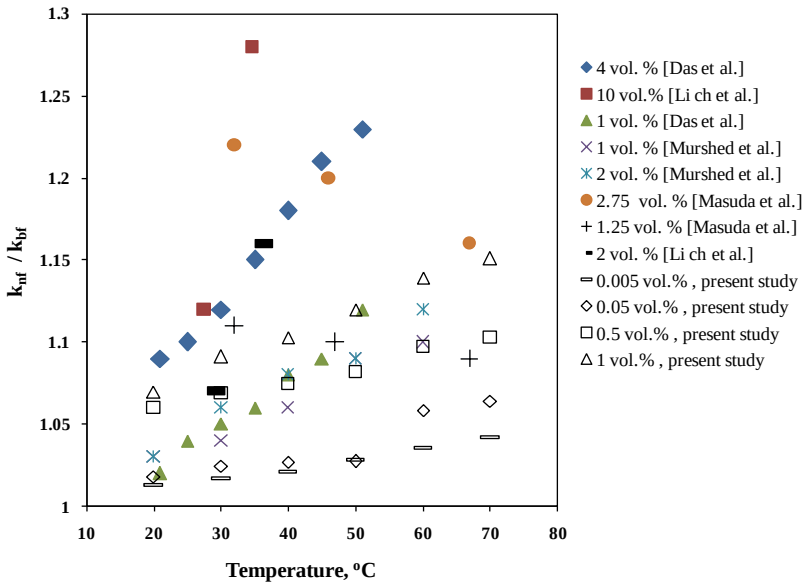

Figure 4.4 Data comparison of thermal conductivity ratio of Al_2O_3/DI water nanofluids at different temperatures

The present study agrees to the widely accepted findings of various research groups worldwide strongly indicating enhancement in thermal conductivity with the increase in temperature and volume concentration of nanofluids. As compared to base fluid, the present study obtained a maximum enhancement of 15 % in the thermal conductivity of Al_2O_3/ DI water nanofluids when loaded at 1 vol. % and tested at 70^oC temperature.

CHAPTER 5

AUGMENTED PERFORMANCE AND OPERATIONAL LIMITATIONS OF MODIFIED HEAT PIPE USING NANOFLUIDS

5.1 Introduction

The prepared Al_2O_3 / DI nanofluids without the use of any surfactants are employed as working fluids in the modified heat pipe. The operating characteristics of heat pipe are evaluated at 0^o, 30^o, 45^o, 60^o, 90^o tilt angles and at three heat inputs viz. 12 W, 32 W and 72 W, loaded with increasing concentrations of Al_2O_3/ DI water nanofluids in the range 0.005 to 1 vol. %. The heat input to the heat pipe covers the workable operating range (< 70^oC) of the electronic equipment for practical understanding. The wall surface temperature along the length of heat pipe at selected heat inputs is plotted and the pattern is observed for analysis. The operational limitations of heat pipe (capillary, entrainment, sonic, boiling, viscous) are calculated based upon the thermophysical properties of nanofluids. The performance of heat pipe has been investigated within the operational limitations and the results are discussed in detail.

The nanofluids are prone to agglomeration resulting in sedimentation with the passage of time. The stability of suspended particles in dispersed fluid plays a key role in justifying its e importance in applications. It has become important to conduct the time based performance of fabricated heat pipe using Al_2O_3/ DI water nanofluids. So the operating characteristics of heat pipe are investigated, analyzed and discussed after0, 3, 9, 12 months from the date of manufacture. This temporal study will unfold its usefulness in the practical applications in the longer run.

5.2 Augmented performance of modified heat pipe using surfactant free Al_2O_3 / DI water nanofluids

Within one month from the date of manufacturing of heat pipe, an investigation on the thermal performance of modified heat pipe at 12 W, 32 W and 72 W load of heat input has been performed. The surface wall temperature of the evaporator, adiabatic and condenser section of heat pipe at different concentrations of Al_2O_3/DI water nanofluids are shown from Figure 5.1 (a) to (c).It has been found that the average temperature along the length of heat

pipe decreases with increase in the nanofluid concentration. The heat pipe duly modified to accommodate the velocity fluctuations and the brazing contamination shows similar trends in the temperature profiles recorded at 0.005, 0.05, 0.5and 1 vol. % concentrations of nanofluids. The results are in agreement with literature values quoted for the cylindrical shaped heat pipe with end caps (Wei et al. [81], Kang et al. [83], Mousa [85], Kole & Dey [92], Asirvatham et al. [93], Hung et al. [95], Do & Jang [96], Shafahi et al. [97]).

It has been observed that at the same heat input, the wall surface temperature of modified heat pipe decreases with increase in the volume concentration of filled Al_2O_3/ DI water nanofluids. From Figure5.1 (a), it has been observed that at low heat input of 12 W, the surface wall temperature of heat pipe does not show any significant drop using DI water and at small concentration of 0.005 vol. % Al_2O_3 / DI water nanofluids. This implies that the use of nanofluids at low watt of 12 W and at low concentrations of 0.005 vol. % does not show any quantified drop in temperature and hence thermal performance of heat pipe.

It has been further observed from Figure 5.1 (a) that with an increase in volume concentration from 0.005 to 0.5 and at low heat input of 12 W, the wall surface temperature drops significantly. Further increase in the concentration from 0.5 to 1 vol. % appears to arrest further drop in the average temperature of heat pipe.

At 32 W load of heat input, same trend has been observed as at 12 W load heat input but it shows improvement in the temperature drop at low concentration of 0.005 vol. %. Furthermore, the temperature drops with increase in the concentration levels from 0.005 to 1 vol. % as shown in Figure 5.1 (b).

At 72 W of heat input, the average temperature of the evaporator, adiabatic and condenser sections of heat pipe decreases with increase in the volume concentration of nanofluids. A significant drop in the heat pipe surface temperature is clearly seen from DI to 0.5 vol. % concentration. As compared to 12 W, similar arresting trends for the temperature drop has been visualized in the range 0.005 to 0.5 vol. % concentrations. The changed configuration of heat pipe at zero orientation with crimped ends and surface depressions appears to attain

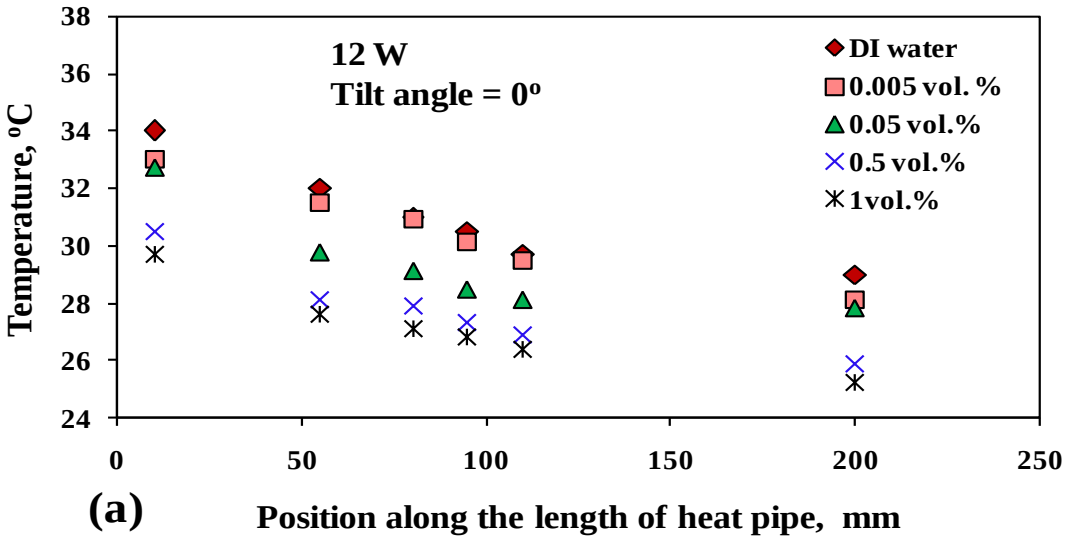

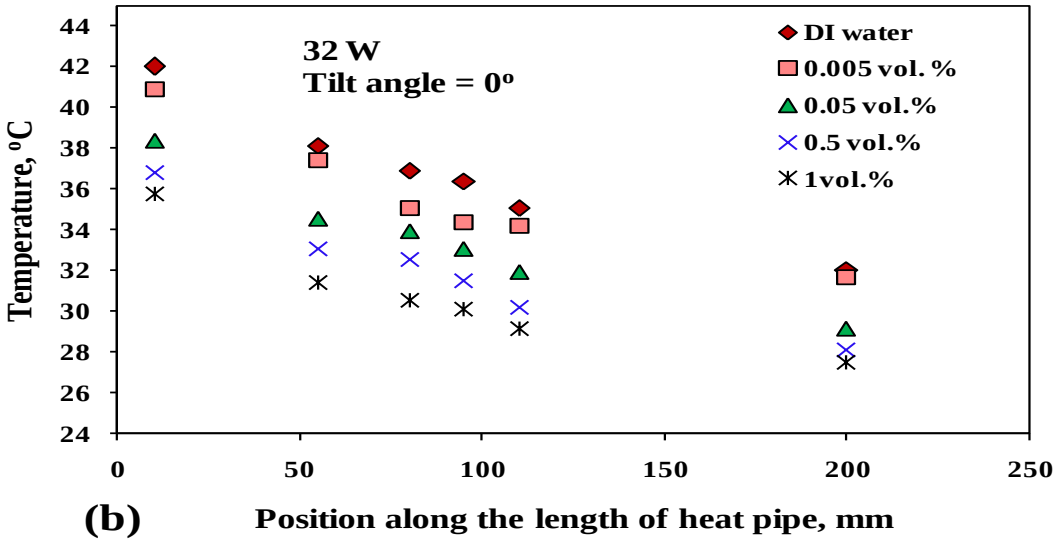

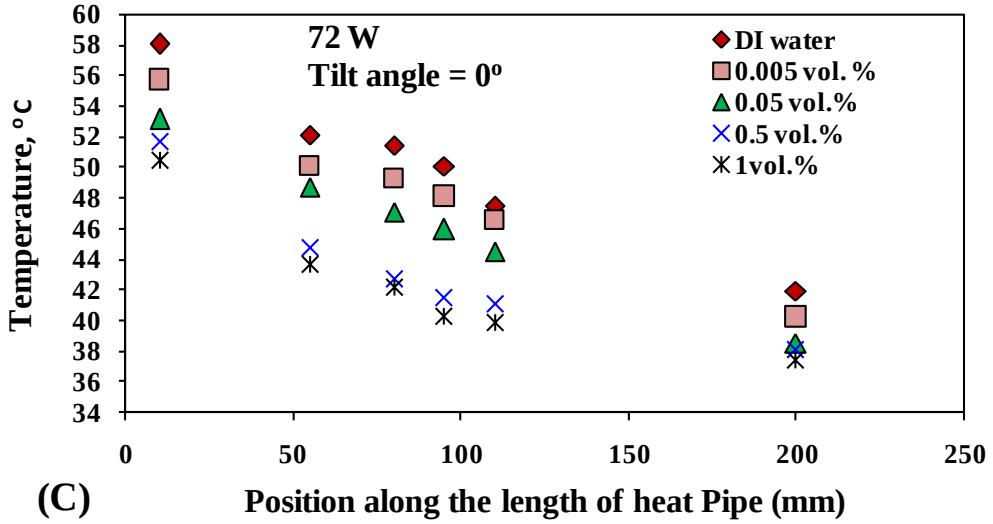

Figure 5.1 **Wall temperature distributions along the length of the heat pipe, a) 12 W, b) 32W, c) 72 W**

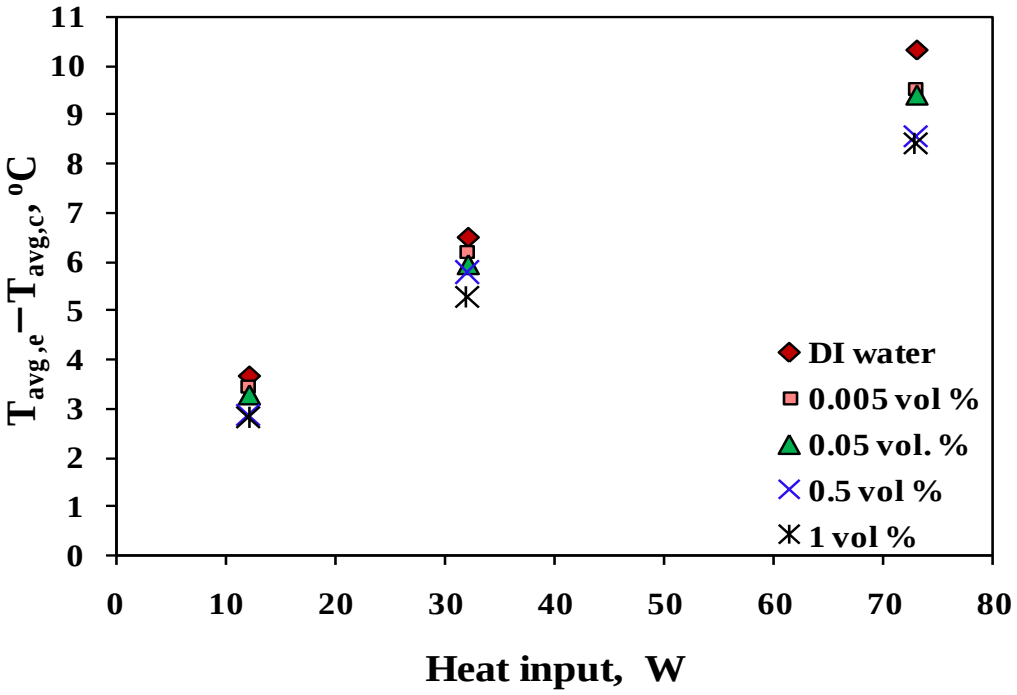

Figure 5.2 Variation of ($T_{avg.\ e} - T_{avg.\ c}$) as a function of heat input for DI water and nanofluids

the saturation value in the range 0.5 to 1.0 vol. % with the increase in heat input from 12W 32 W and from 32 W to 72 W. The obtained values indicate consistency in the performance of heat pipe in the concentration range of 0.5 to 1 vol. % at 72 W heat input.

From Figure 5.2, it has been observed that irrespective of the heat input the average temperature difference between the evaporator section and the condenser section of heat pipe decreases with increase in the concentration of nanoparticles in the base fluid. Using the Al_2O_3/ DI water nanofluids, the heat pipe indicates better results at high heat input of 72 W when loaded with 0.5 vol. % of nanofluid.

Figure 5.3 shows the variation of effective thermal resistances of heat pipes with the increase in heat input from 12 W to 72 W. The thermal resistance values are obtained by

$$R = \frac{T_{avg.E} - T_{avg.C}}{Q_{in}} \qquad (5.1)$$

It has been observed that the at low watt load of heat input, the thermal resistance of heat pipe is high for all the selected working fluids. This is due to high surface tension of working fluid at low heat input of 12 W which indicates the recorded wall surface temperature of 34^{o}C [Figure 5.1 (a)]. With increase in the working fluid temperature, the decrease in the surface tension does play a role in decreasing the thermal resistance of heat pipe.

Using the nanofluids in the concentration range of 0.005 to 1 vol. %, the thermal resistance of modified heat pipe reduces with the increase in the concentration of nanofluids. Higher variations in the values of thermal resistances have been observed at 12 W load heat input as among the selected concentrations. With the increase in the heat input from 12 W to 32 W and 32 W to 72 W, the thermal resistances values shows consolidation with minimum variation in its values.

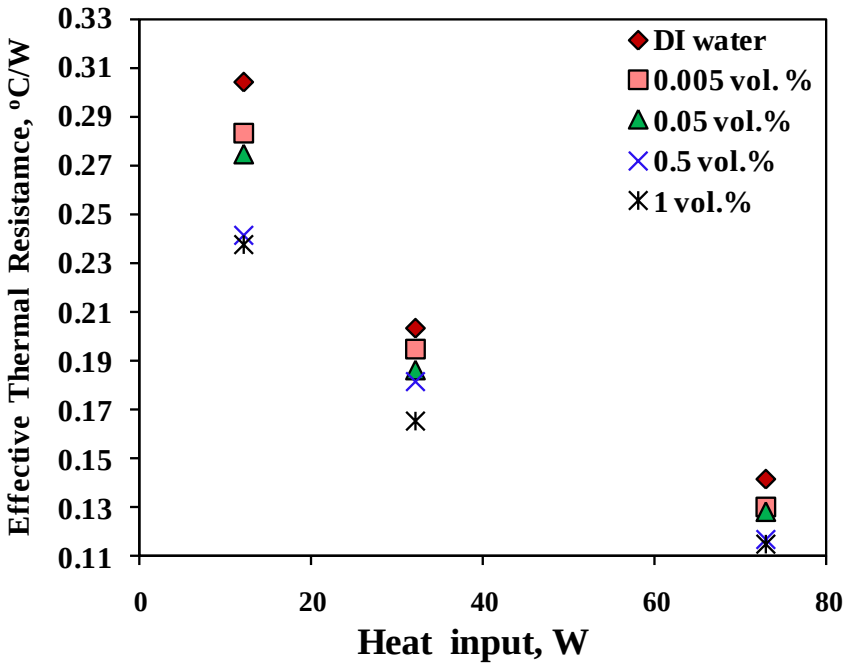

Figure 5.3 Variation of effective thermal resistance as a function of heat input

The decrease in the thermal resistance due to Al_2O_3/ DI water nanofluids is due to its thermophysical properties primarily thermal conductivity. The other convective transport phenomenon such as thermophoresis, particle drag and shear induced migration of nanoparticles are also contributory in reducing the thermal resistance of heat pipe. This is

demonstrated in convective heat transfer studies of nanofluids [108]. The enhancement resulted due convective heat transfer was quoted much higher compared to the thermal conductivity alone

The results obtained in testing the modified heat pipe are compared with similar studies using the Al_2O_3/DI nanofluids (Mousa [85], Do & Jang [88], Moraveji & Razvarz [90])and the results are plotted graphically in Figure 5.4.

An interesting finding has been observed that the thermal resistance of modified heat pipe tends to consolidate with increase in the heat input (12 W to 72 W) and the nanofluids concentration. It appears as if saturation in thermal resistance of heat pipe has been attained.

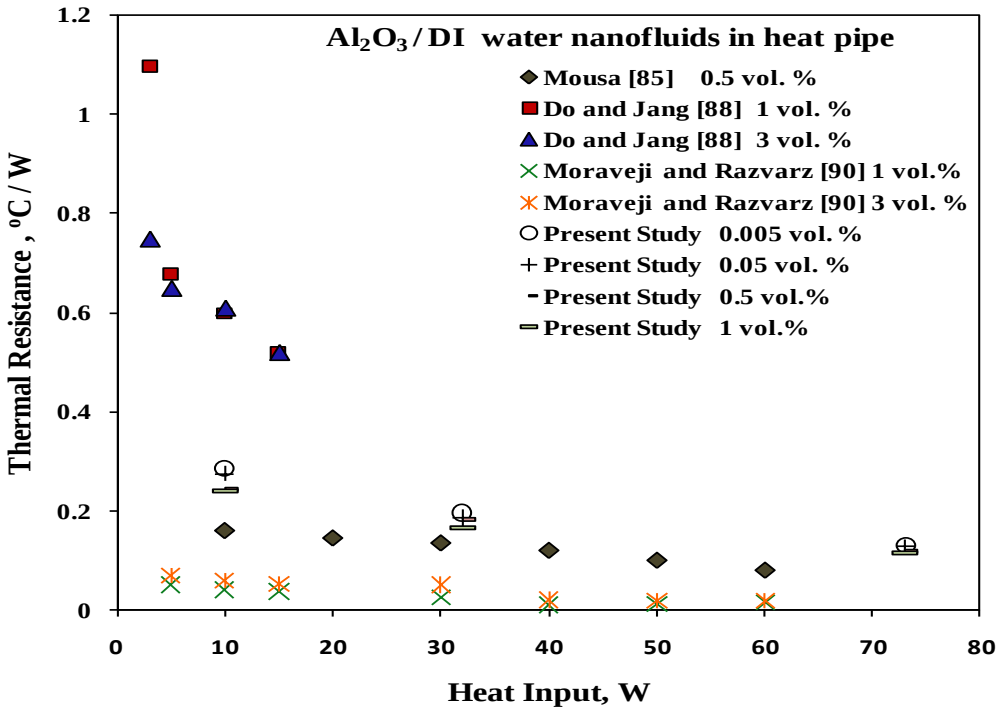

Figure 5.4 Comparative study of heat pipe thermal resistance with heat input using Al_2O_3 / DI water nanofluids

As compared to mere thermal conductivity enhancement in the nanofluids, the rapid and dominating effect of convective heat transfer coefficient resulted in its rapid vaporization. This has resulted in the sedimentation of the spherical shaped nanoparticles on the strands of the wick structure in the evaporator section of heat pipe. This biased and random distribution

of alumina nanoparticles concentration inside the heat pipe nullifies its impact at high heat load (Anoop et al. [108], Naphon et al. [82]).

Figure 5.5 shows the relative resistances obtained using nanofluids as compared to de-ionised water in modified heat pipes and the values so obtained are graphically shown in Figure 5.5. The maximum reduction in the thermal resistance of heat pipe has been obtained at low heat input of 12 W when loaded with 1 vol.% of Al_2O_3/DI water nanofluid.

With further increase in the heat input to 72 W, the saturation temperature prevailing at corresponding saturation pressure has resulted in the gradual shift of the nucleate boiling to transition boiling after attaining the critical heat flux and has resulted in lower relative resistances. This change is expected out of modified features of heat pipe enabling uniform heat flux to the evaporator section from the axial and radial directions. A maximum relative reduction of 22 % in thermal resistance has been observed at 12 W heat input loaded with 1 vol. % of Al_2O_3/DI water nanofluids.

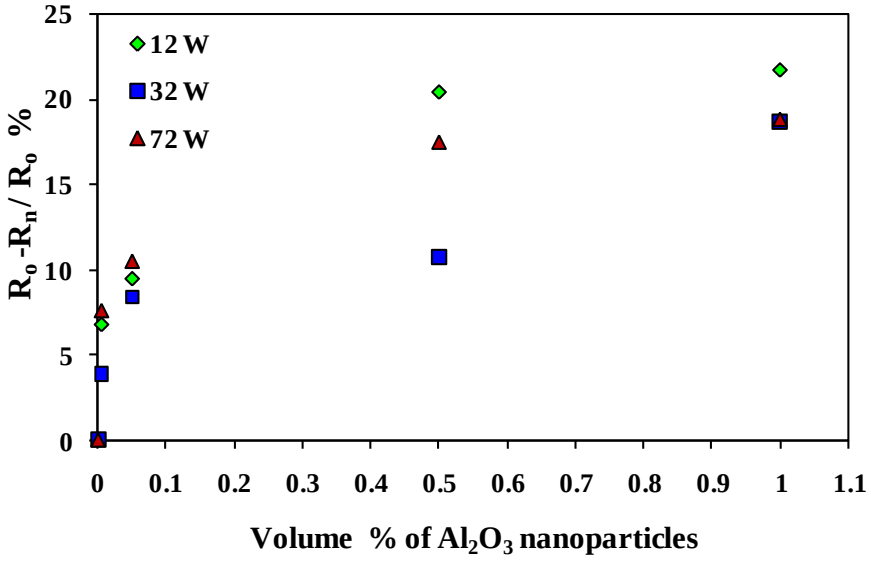

Figure 5.5 Thermal resistance reduction of heat pipe as compared to DI water

As shown in Figure 5.6, the effective thermal conductivity of heat pipe is calculated by the following equation

$$k_{eff} = \frac{Q_{in} L_{eff}}{A_c (T_{avg\,E} - T_{avg.C})} \qquad (5.2)$$

L_{eff} is the effective length of the heat pipe given as 0.5 L_e + L_a + 0.5 L_c

As shown in Figure 5.6, the effective thermal conductivity of heat pipe increases with increase in the concentration of nanofluids. Interpretation of the data has resulted in the attainment of maximum effective thermal conductivity of 13328 W/(m.K) which is 1.23 times the value obtained using DI water as working fluid in modified heat pipe.

At high heat flux rates of 40000 W/m^2, a marginal improvement in the thermal conductivity of heat pipe has been observed when the concentration of nanofluids increases from 0.5 to 1 vol. %.This again points to the saturation value attained in the concentration levels of nanofluids used as working fluid in heat pipe.

Comparing with the literature studies, the thermal performance of heat pipe as a function of volume concentration, temperature, orientation, thermal resistance and the thermal conductivity are in agreement with the literature findings but the obtained values varies due to the heat pipe modification, filling ratio of working fluid, mesh parameters and variable amount of uncertainty associated with the experimental procedures.

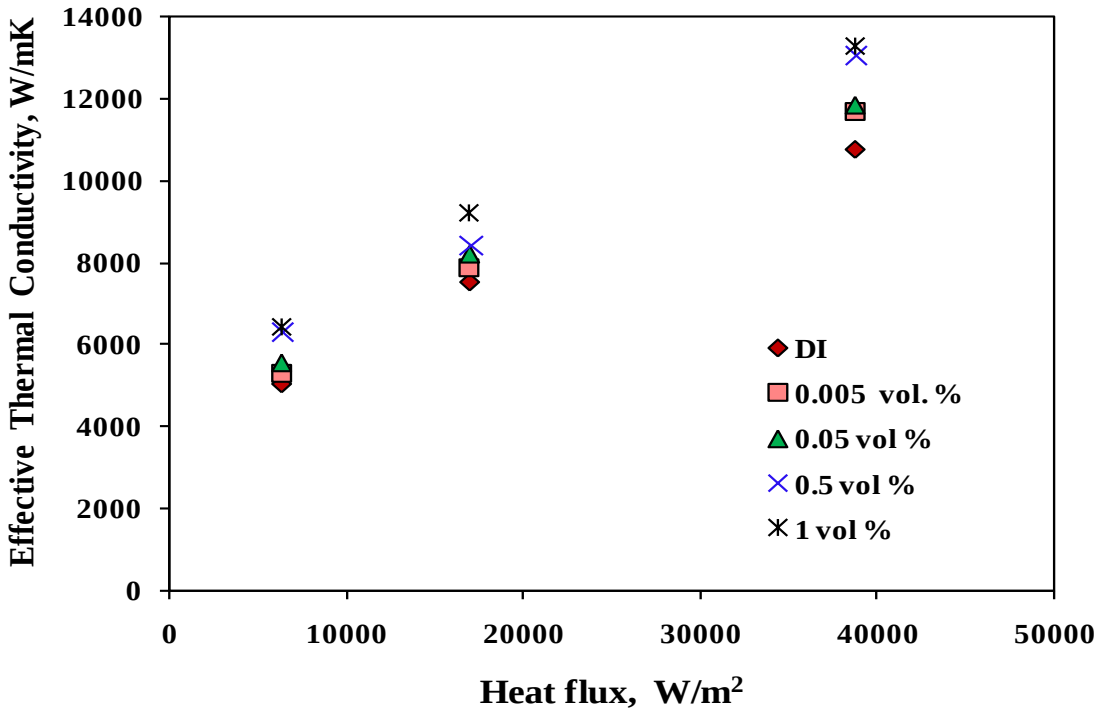

Figure 5.6 Enhancement in effective thermal conductivity with heat flux

5.3 Operational limitations of heat pipe

The mean operating temperature of heat pipe at tested heat inputs in the range 12 W to 72 W and concentration range of 0.005 to 1 vol. % of Al_2O_3/ DI water nanofluids are tabulated in Table 5.1.

Table 5.1 Heat pipe mean operating temperatures

Q, Watts	Mean operating temperature, ^oC					
	water	0.005 vol.%	0.05 vol.%	0.5 vol.%	1 vol.%	Mean Temperature, ^oC
12	31.03	30.51	29.33	27.76	27.13	29.15
32	36.75	35.61	33.48	32.03	30.73	33.72
72	50.16	48.3	46.3	43.28	42.28	46.06

The operational limitations of heat pipe are calculated based on the thermophysical properties of nanofluids and are shown in Appendix A. The performance of heat pipe is evaluated within the operational limits obtained and are discussed in detail in this section.

5.3.1 Entrainment Limit

In entrainment limit, heat transport capacity as function of mean operating temperature is shown in Figure 5.7. The logarithmic plot shows enhancement in the heat transport capacity of heat pipe with the increase in the volume concentration of the alumina nanoparticles in DI water. The entrainment limit is a function of vapor density, surface tension and latent heat of working fluid. From the observed thermophysical properties of Al_2O_3/ DI water in Appendix A, the increase in the concentration of nanofluids has resulted in the increase in surface tension and latent heat of vaporization of nanofluids.

The enhancement in the dependent parameters with a change in the operating temperature and volume concentration of nanofluids has resulted in the enhancement of the entrainment limit value.

The dispersion of nanoparticles in base fluid enhances the adhesive property of nanofluid travelling through the strands of the wick. With the result, the high velocity of vapors due to high operating temperatures fail to entrain or tear the liquid film from the wick surface while travelling through the core of the heat pipe back to the condenser section

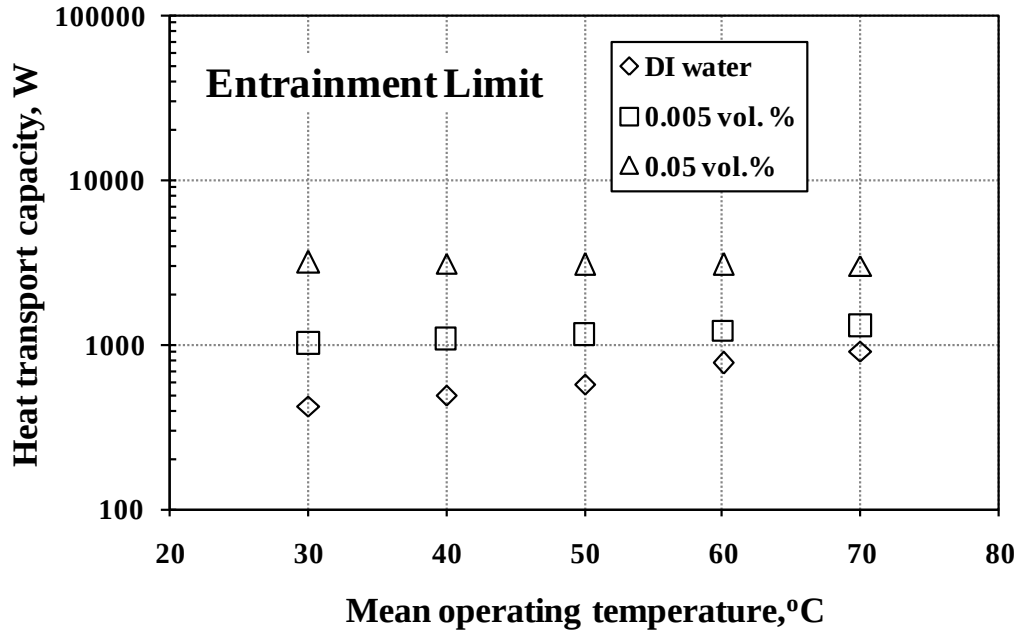

Figure 5.7 Entrainment limit of heat pipe using Al_2O_3/DI water nanofluids

Also at a higher concentration of nanofluid, the entrainment limit capacity tends to attain a constant value with increase in the temperature. In the present study, the heat pipe operating within the range of 12 W to 72 W of heat input does not indicate any constraint for its entrainment limit.

5.3.2 Sonic Limit

In sonic limit, the heat carrying capacity as a function of mean operating temperature is graphically plotted in Figure5.8. The velocity of the vapor formed in the evaporator section may reach the sonic and supersonic limit while travelling through the vapor core of the heat pipe. The magnitude of velocity depends on the condensation rate of the vapors in the condenser section of heat pipe .In the present research work, the annular fin fitted condenser section of heat pipe is cooled under the constant ambient conditions prevailing during the natural convection, thus ruling out the possibility of unexpected rise in the heat rejection rate during the testing of heat pipe.

It has been observed from the Figure 5.8 that while using nanofluids the sonic limit increases with the increase in mean operating temperature of heat pipe. This positive impact of using nanofluids in heat pipe will be helpful in practical scenario of unconstrained heat

rejection rates prevalent due to uncontrolled ambient conditions. The values obtained in the present case indicate safe operational sonic limits of heat pipe.

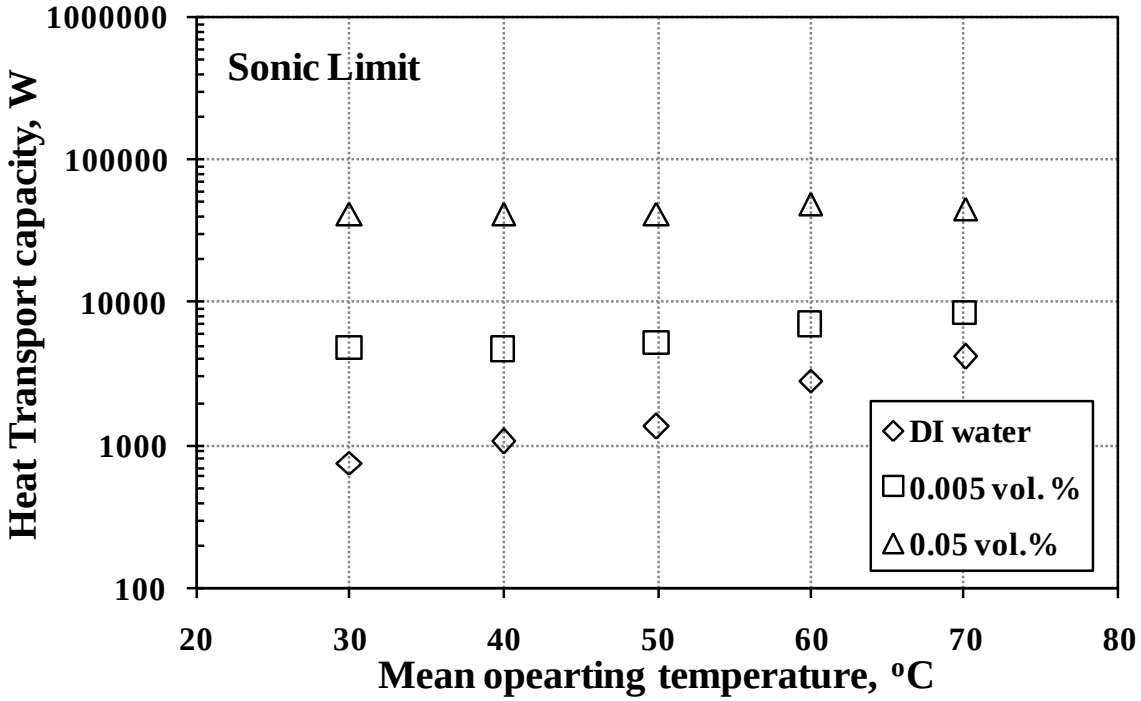

Figure 5.8 Sonic limit of heat pipe using Al_2O_3/DI water nanofluids

5.3.3 Viscous Limit

The viscous limit shows its dominance during the startup operations due to low temperature and vapor pressure of the working fluid. Insufficient pressure gradient across the length of the heat pipe is overpowered by the viscous forces of the working fluid, thus resulting in poor circulation flow of the working fluid. The viscous limit as function of mean operating temperature of heat pipe is graphically shown in Figure 5.9.

As compared to earlier described limits, the viscous limit too increases with increase in the concentration of nanofluid evaluated at 0.005 and 0.05 vol. %.This enhancement in the viscous limit of working fluid will remove the constraint of working with long heat pipes when the working fluid is near to melting temperature (of frozen startup condition) due to low saturation pressure prevailing in the heat pipe.

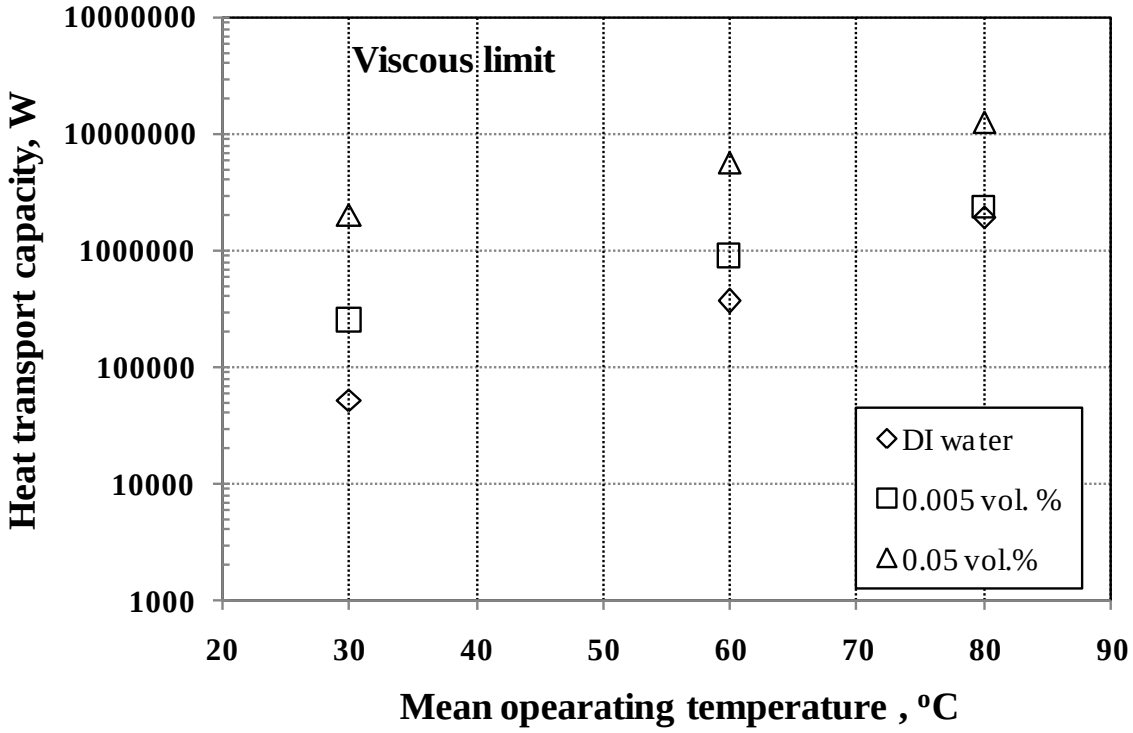

Figure 5.9 Viscous limit of heat pipe using Al_2O_3 / DI water nanofluids

5.3.4 Boiling Limit

Boling limit is one of the most important aspects of operational limitations of heat pipe. The values obtained from the thermophysical properties of nanofluids are plotted in Figure 5.10.It is worth mentioning that the use of nanofluids in heat pipe improves the boiling limit. It increases with the increase in concentration of nanofluids and decreases with the increase in operating mean temperature.

At 70^{o}C, an enhancement of 12.2 % and 38.4 % in boiling limit has been observed for 0.005 and 0.05 vol.% concentration, respectively as compared to de-ionized water. The increase in the boiling limit of heat pipe by using the nanofluids improves the thermal conductivity of combined liquid- wick structure.

This is possible due to the formation of nano-coating layer of alumina nanoparticles on the strands of the wick facilitating the formation of additional nucleation sites and hot spots resulting in increasing the effective heat transfer.

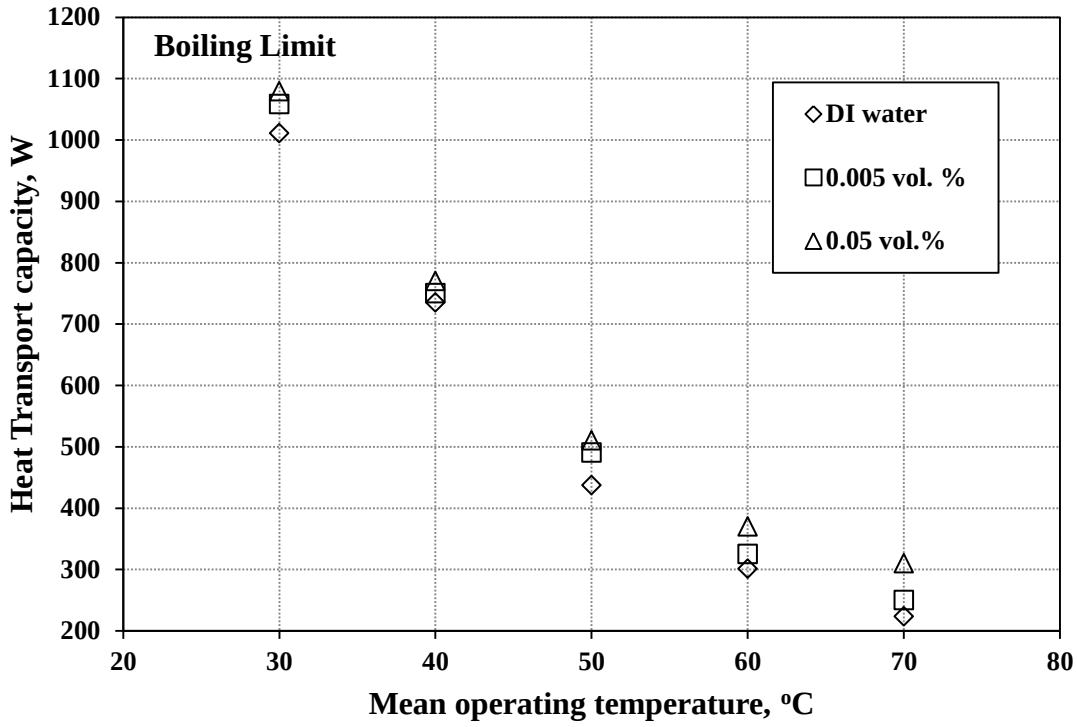

Figure 5.10 Boiling limit of heat pipe using Al_2O_3/DI water nanofluids

5.3.5 Capillary Limit

Unlike the other calculated limits of heat pipe, the capillary limit decreases with the increase in the volume concentration of nanoparticles in base fluid but increases with the increase in mean operating temperature of heat pipe. The deposition of nanoparticles on the mesh wick creates small pores resulting in increase in the capillary pressure.

This increase in the capillary pressure head tends to be overpowered by the increase in the liquid and vapor frictional coefficient. The capillary limit is found to be decreased by 4.6 % and 9.4 % for 0.005 and 0.05 vol. % concentration, respectively as compared to DI water at 30^{o}C mean operating temperature.

But with the increase in the mean operating temperature from 30^{o}C to 70^{o}C, the capillary limit is decreased by 1.9 % and 1.1 % for 0.005 and 0.05 vol. % concentrations, respectively as compared to DI water.

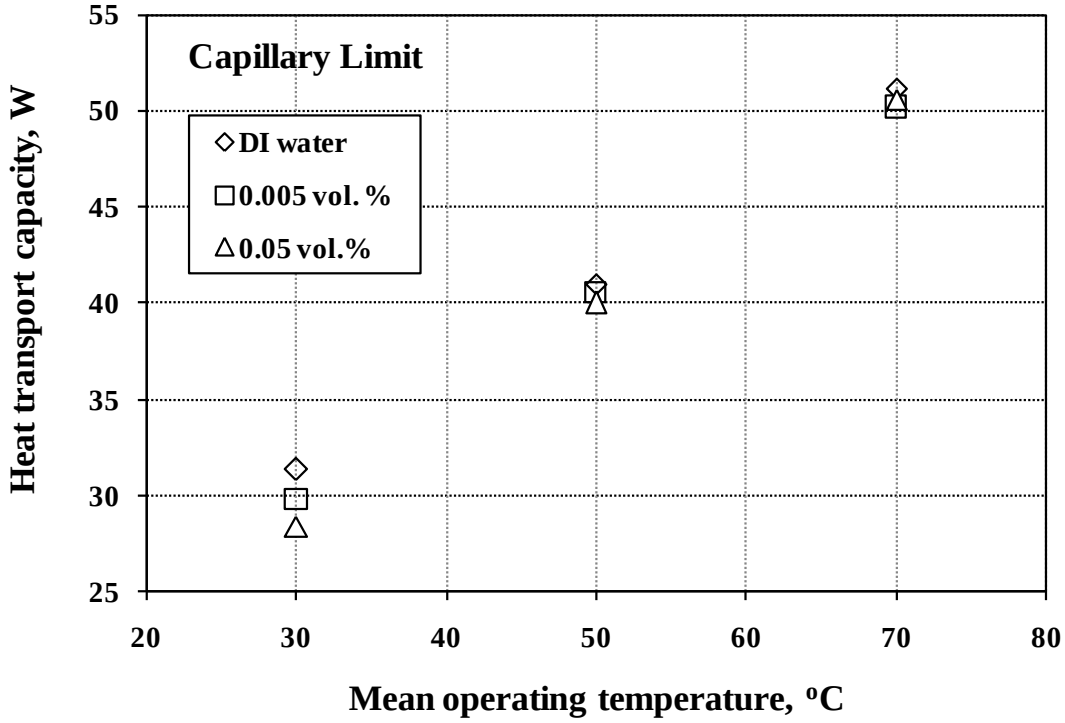

Figure 5.11 Capillary limit of heat pipe using Al_2O_3/DI water nanofluids

5.4 Thermal performance of modified heat pipe at tilted angles

The heat pipe is sensitive to its orientation or tilt angle. The average wall temperature of the modified heat pipe using the DI water and nanofluids increases with the increase in heat input from 12 W to 72 W irrespective of any tilt angle selected in the range 0^o to 90^o. The heat pipe using DI water and selected volumes of concentrations has been tested at favorable tilt angles of 30^o, 45^o, 60^o, 90^o as shown in Figure 5.12 to 5.14.

Figure 5.12 (a –c) shows the wall temperature distribution of heat pipe at 12 W, 32 W &72 W heat input and at different tilt angles using DI water. As compared to zero tilt angle, the wall temperature of heat pipe shows the reverse trend with the increase in tilt angle in the range 0^o to 30^o. Further increase in the tilt angle from $30^o$to 90^o raises the average wall temperature of heat pipe. This gives an optimum performance of heat pipe using DI water as working fluid at 30^ofavorable tilt angle and simultaneously validating the findings of Kumar et al. [109] which concludes the optimum performance of heat pipe using DI water at approximately 25^o tilt angle. The change may be attributed due to geometric dimensions, ambient environment conditions, uncertainty and associated experimental error.

The wall temperature of heat pipe at 0.005 and 0.05 vol. % concentrations of Al_2O_3 / DI water nanofluids are shown in Figures 5.13 and 5.14, respectively. The optimum tilt angle shifts to 45^{o}irrespective of the quantum of heat input (12 W to 72 W) at both the selected concentrations of 0.005 and 0.05 vol. %. The optimum angle obtained at the selected concentrations shows strong dependency of the volume concentration on the wall temperature distribution.

The wall temperature of modified heat pipe increases with increase in tilt angle beyond 45^o.This is attributed to the quick return of the condensate from the evaporator to condenser section thus influencing the vapor production rate. Also the tilt angle beyond 45^o results in the reduction of heat exchanging time in the condenser section leading to poor heat dissipation efficiency.

The thermal performance of heat pipe using Al_2O_3 / DI water nanofluids at this optimized angle of 45^{o}is in agreement with the findings of Hung et al. [110] and Kumaresan et al.[111] as shown in Figure 5.12 (a) and 5.12 (b).

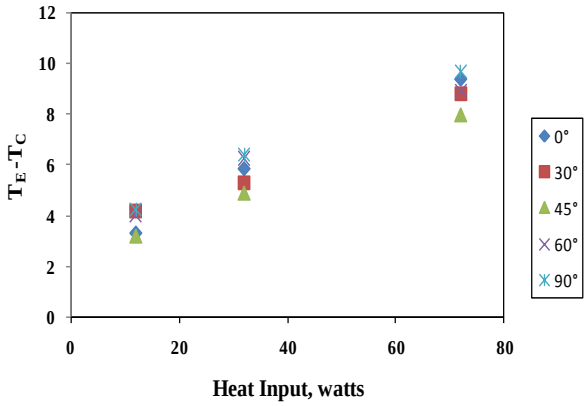

Fig. 5.12 (a) Temperature difference between the evaporator and condenser section at different tilt angles for 1 vol.% of Al_2O_3/ DI water nanofluid (Present Study).

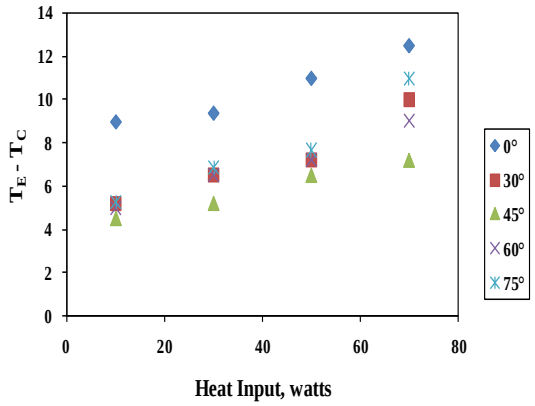

Fig.5.12(b) Temperature difference between the evaporator and condenser section at different tilt angles for 1 wt. % of CuO nanofluid [Ref. 111].

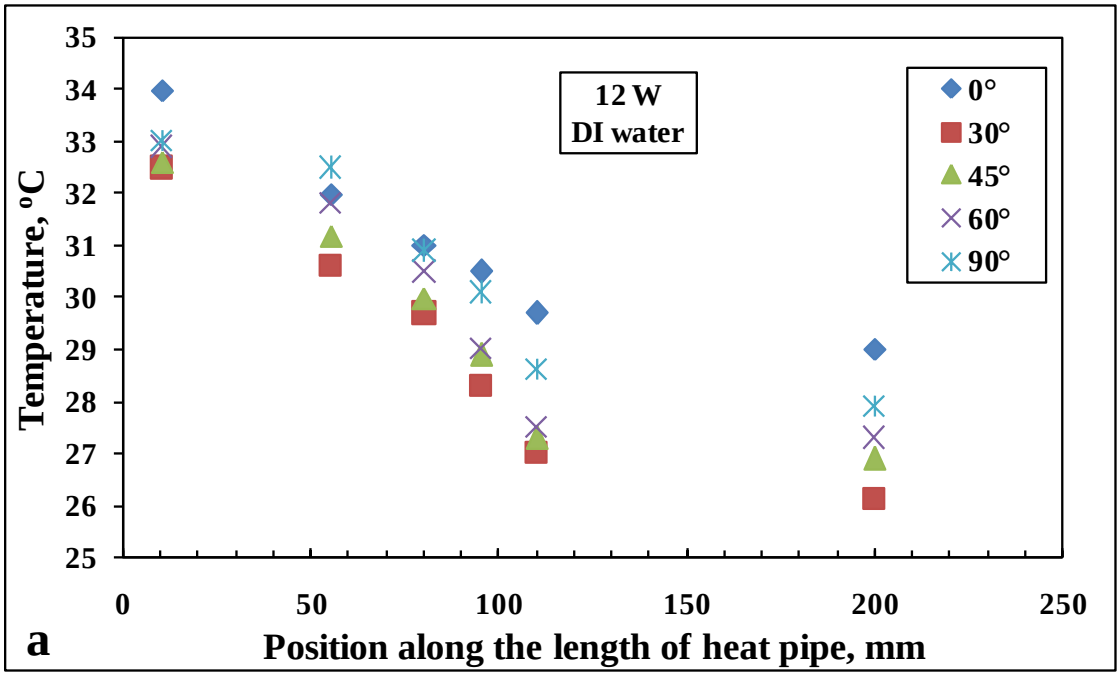
12 W
DI water
0°
30°
45°
60°
90°
Temperature, °C
35
34
33
32
31
30
29
28
27
26
25
0
50
100
150
200
250
a
Position along the length of heat pipe, mm

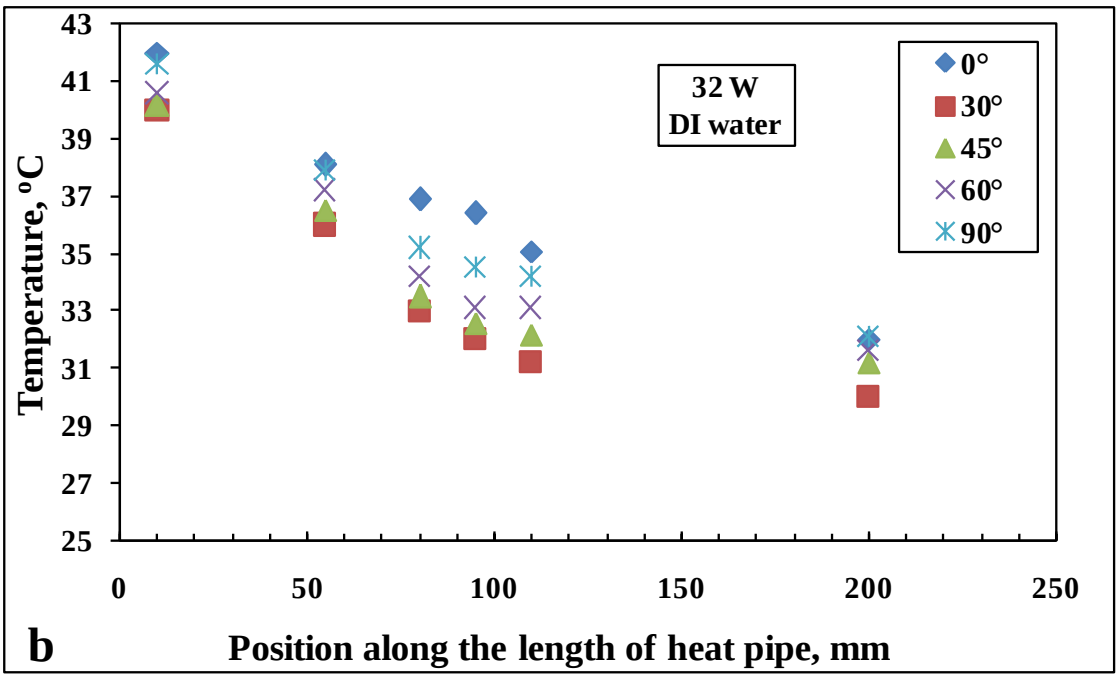
32 W
DI water
0°
30°
45°
60°
90°
Temperature, °C
43
41
39
37
35
33
31
29
27
25
0
50
100
150
200
250
b
Position along the length of heat pipe, mm

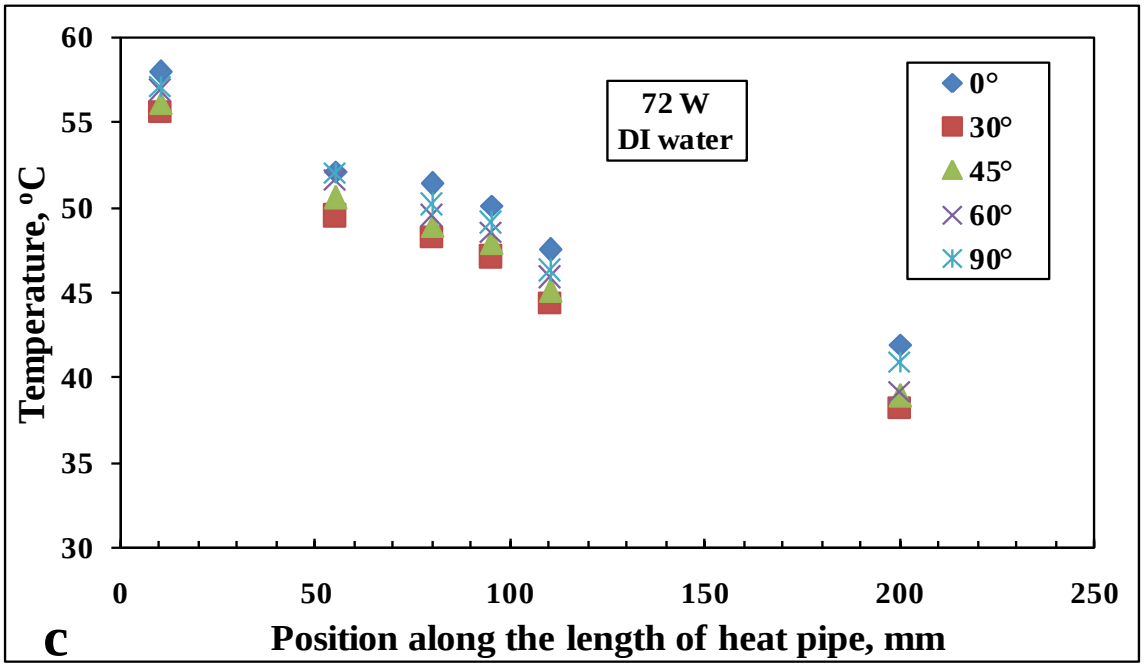

Figure 5.13 **Wall temperature distributions along the length of heat pipe using DI water at different favorable tilt angles (a) 12 W, (b) 32 W (c) 72 W**

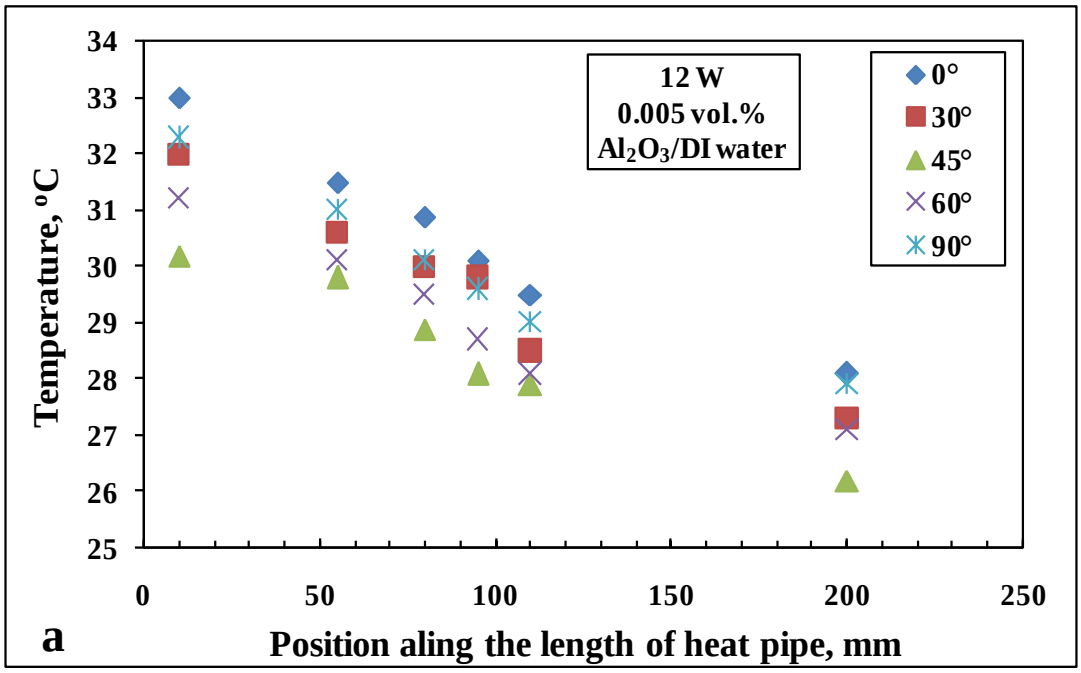

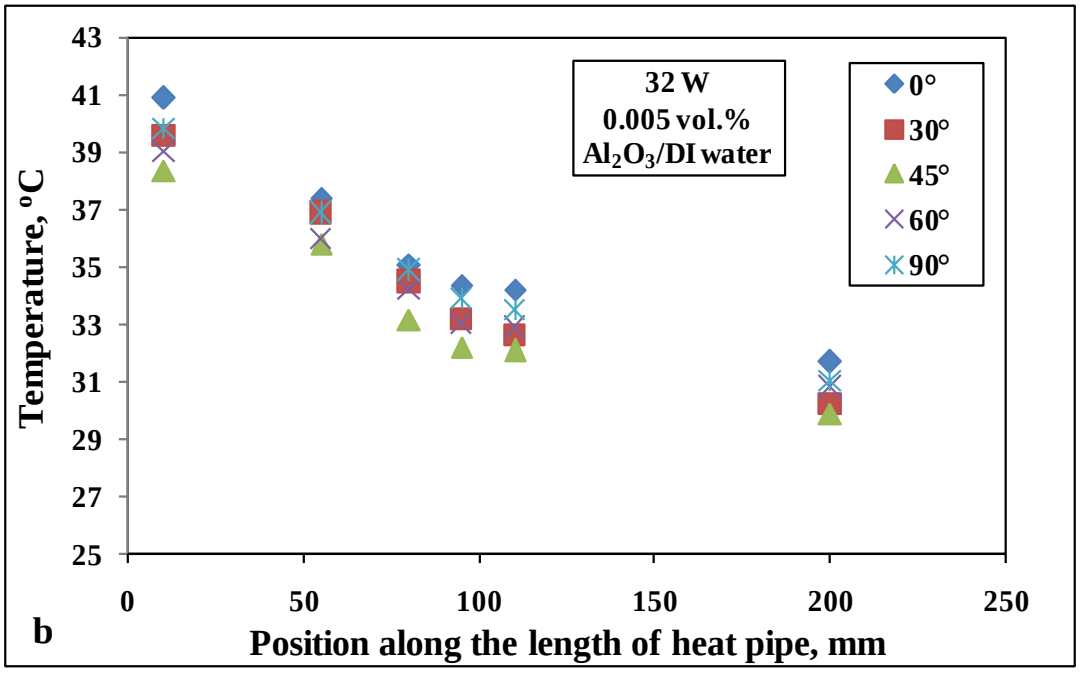

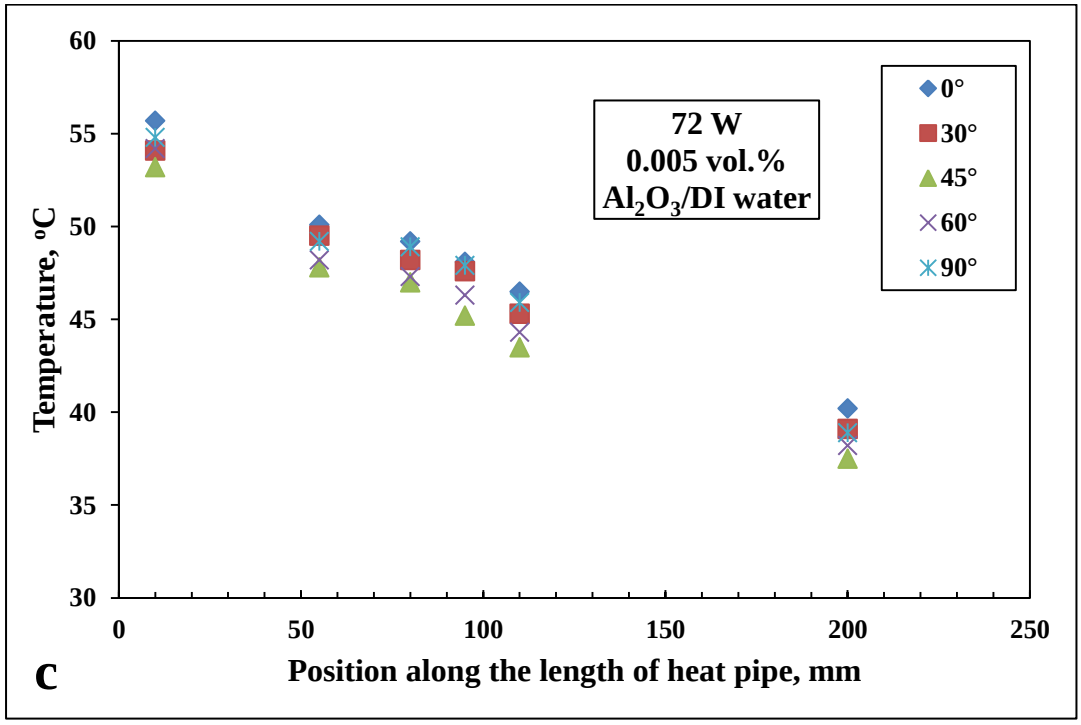

Figure 5.14 Wall temperature distribution along the length of heat pipe using0.005 vol.% Al_2O_3/DI water at different favorable tilt angles (a) 12 W, (b) 32 W (c) 72 W

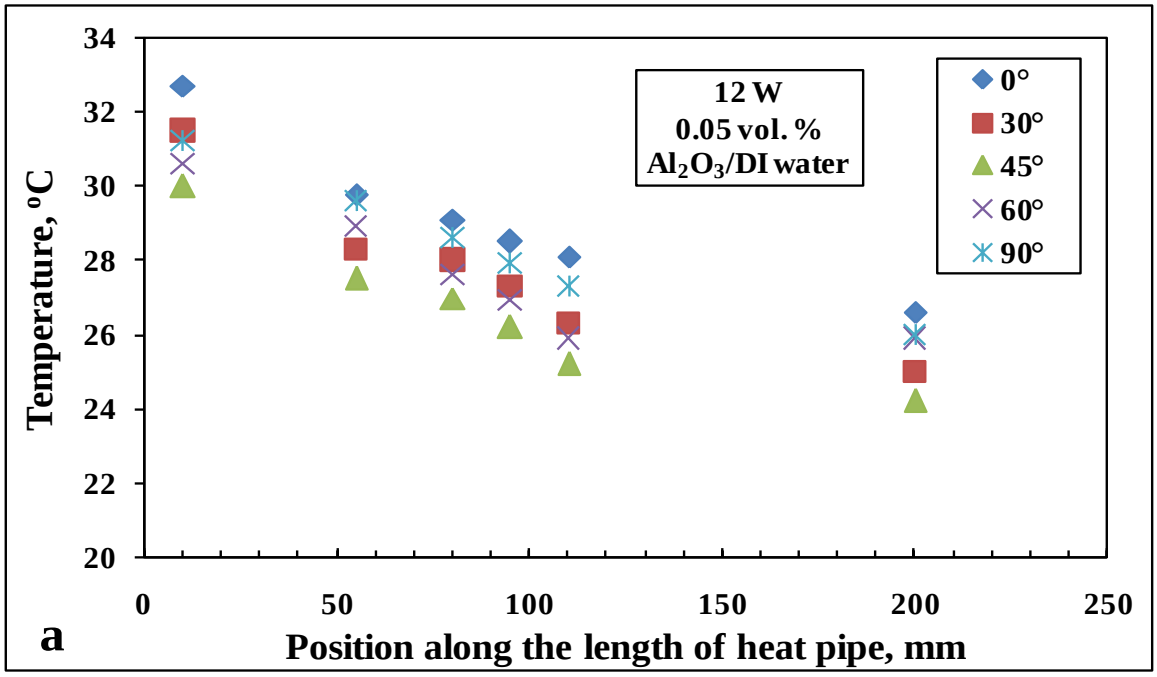
12 W
0.05 vol. %
Al2O3/DI water
0°
30°
45°
60°
90°
Temperature, °C
Position along the length of heat pipe, mm
a

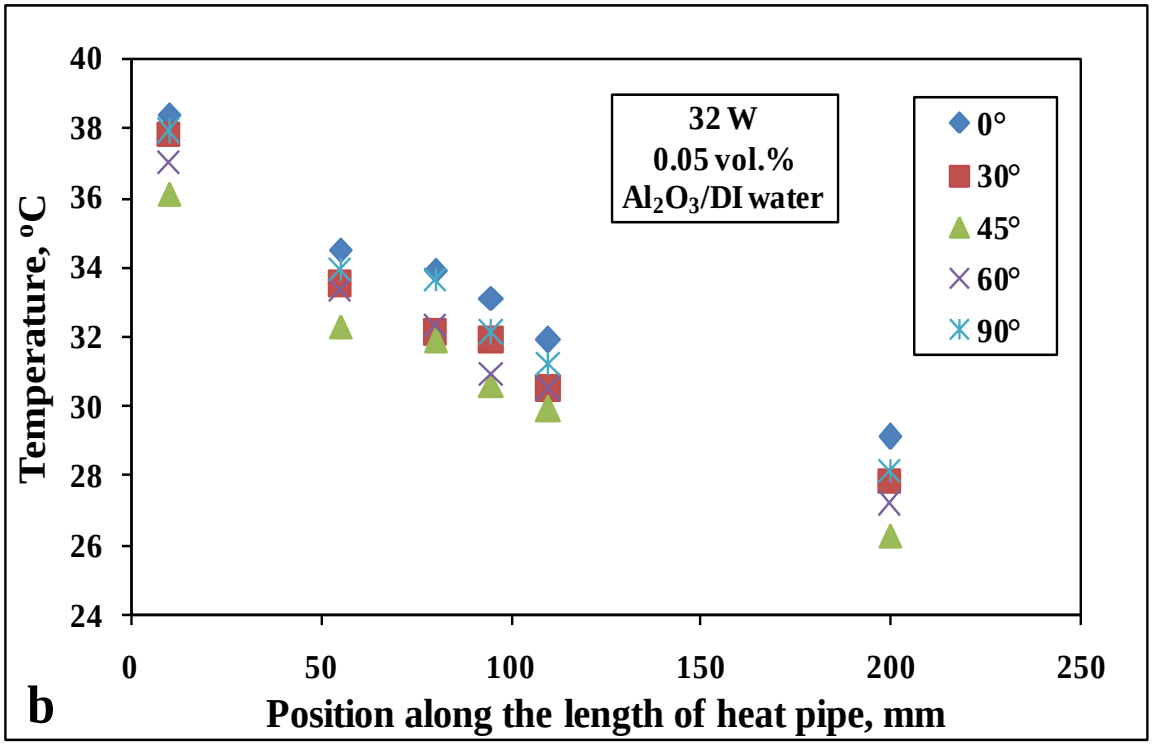
32 W
0.05 vol.%
Al2O3/DI water
0°
30°
45°
60°
90°
Temperature, °C
Position along the length of heat pipe, mm
b

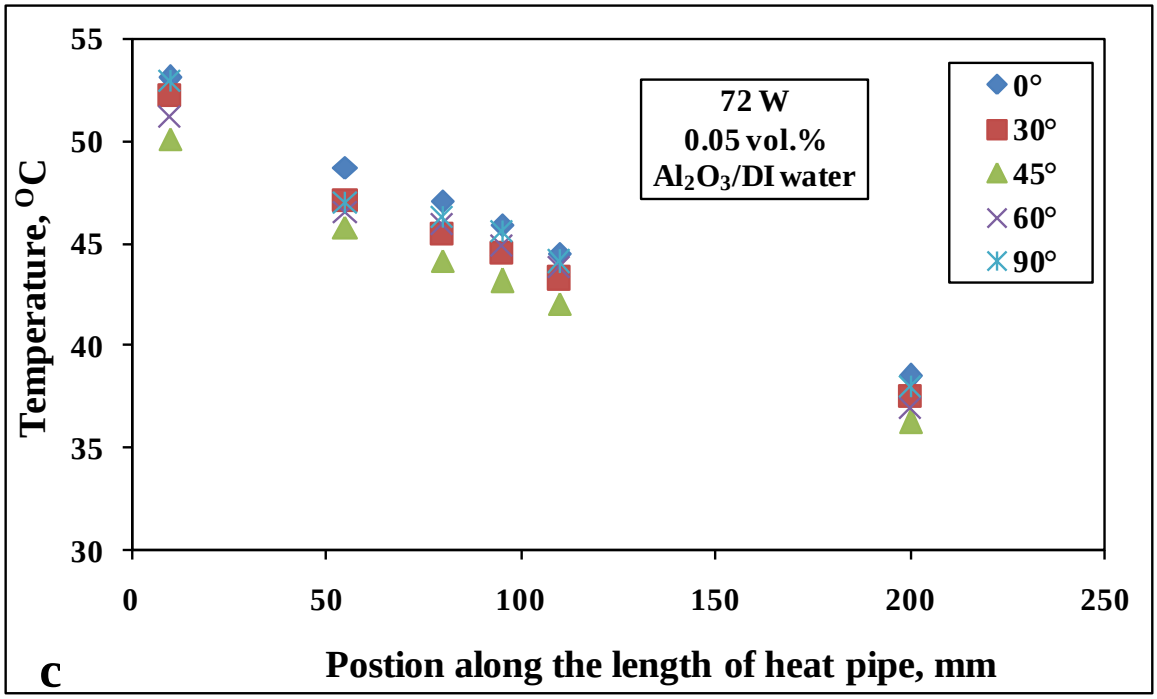

Figure 5.15 **Wall temperature distribution along the length of heat pipe using 0.05 vol.% Al_2O_3/DI water at different favorable tilt angles (a) 12 W, (b) 32 W (c) 72 W**

CHAPTER 6

TEMPORAL EFFECT OF USING NANOFLUIDS IN HEAT PIPE

6.1 Introduction

With the nanofluids prone to sedimentation with the passage of time, it has become important to notify the thermal performance of heat pipe after certain designed durations. Unlike the studies referred in the literature which are limited to hours or days, it has been decided to investigate the same after 3, 6 and 9 months at non-operational standstill condition. The heat pipe is kept non-operational after performing the tests to fully study its sensitivity towards the stability of the working fluid.

6.2 Temporal effect on wall temperature distribution along the length of heat pipe using Al_2O_3 / DI water nanofluids

The wall temperature distribution along the length of heat pipe at different Al_2O_3/DI vol.% concentrations (0.005, 0.05, 0.5, 1) Watts loads of heat inputs (12 W, 32 W, 72 W), and specified time durations of 0, 3, 6, 9 months from the date of manufacturing are obtained and the values are plotted in Figure 6.1 to Figure 6.4.

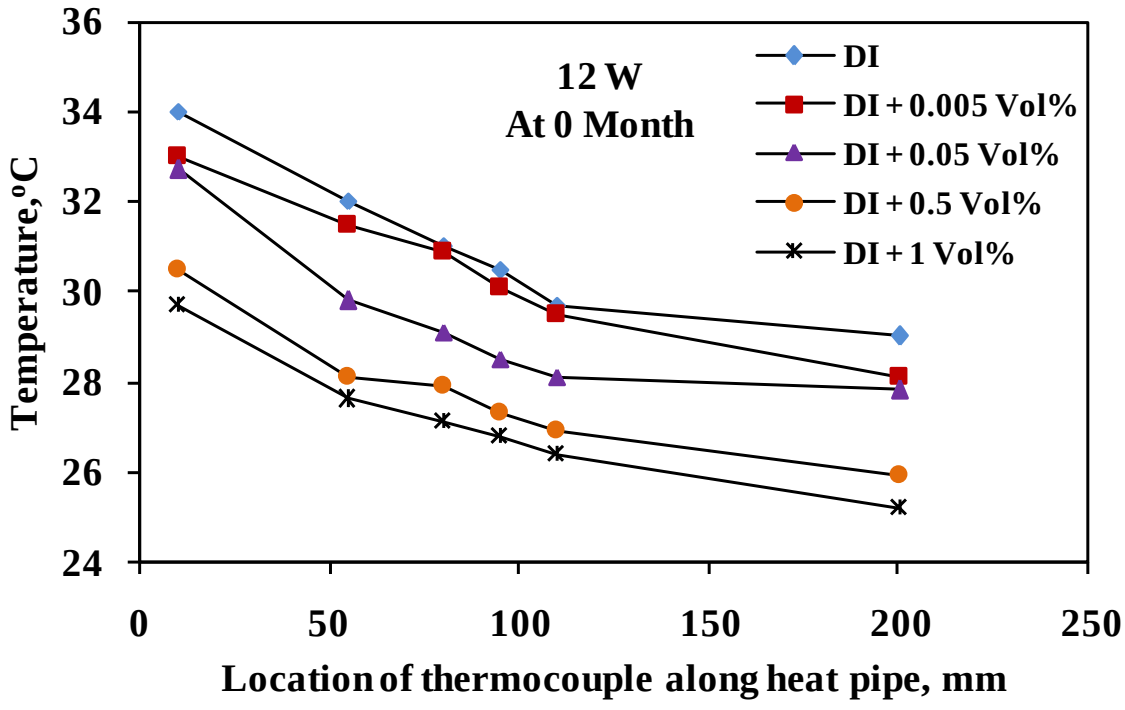

Figure 6.1 Wall temperature distributions at 12 Wheat input at 0 month from manufacturing

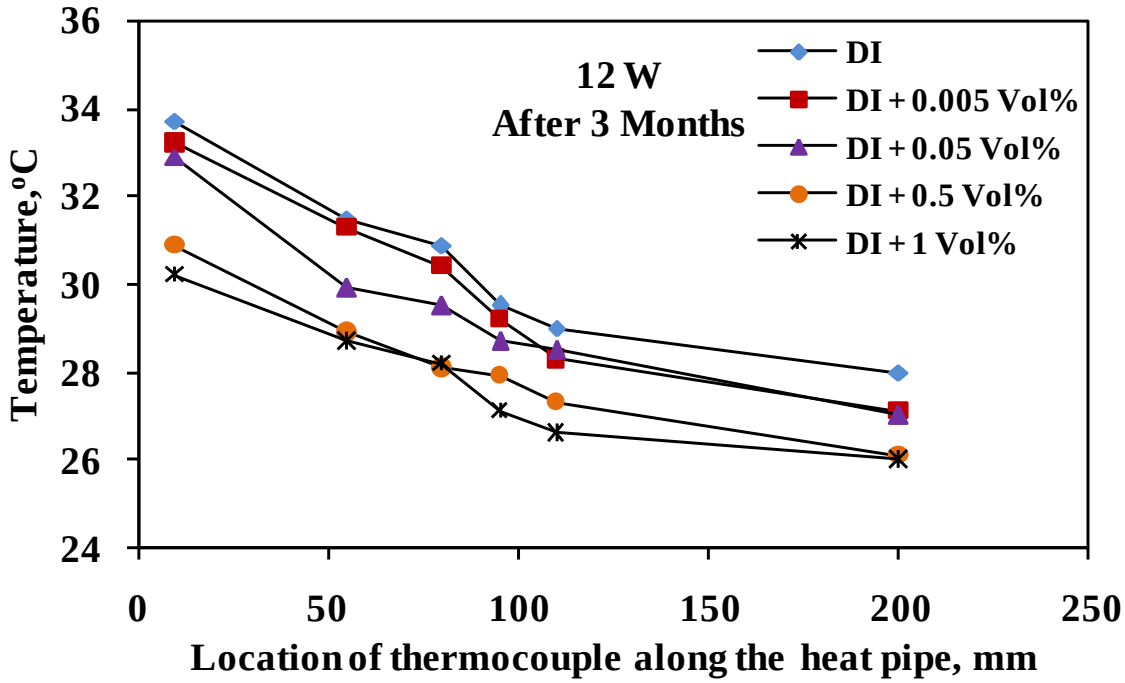

Figure 6.2 **Wall temperature distributions at 12 W heat input after 3 months from manufacturing**

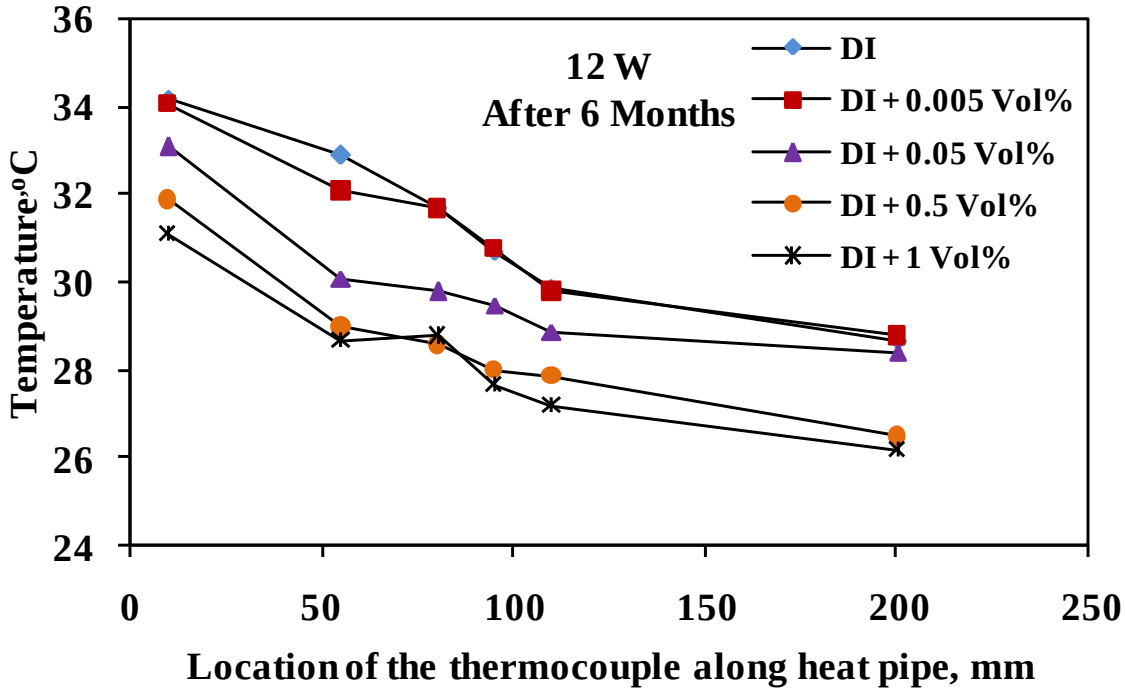

Figure 6.3 **Wall temperature distributions at 12 W heat input after 6 months from manufacturing**

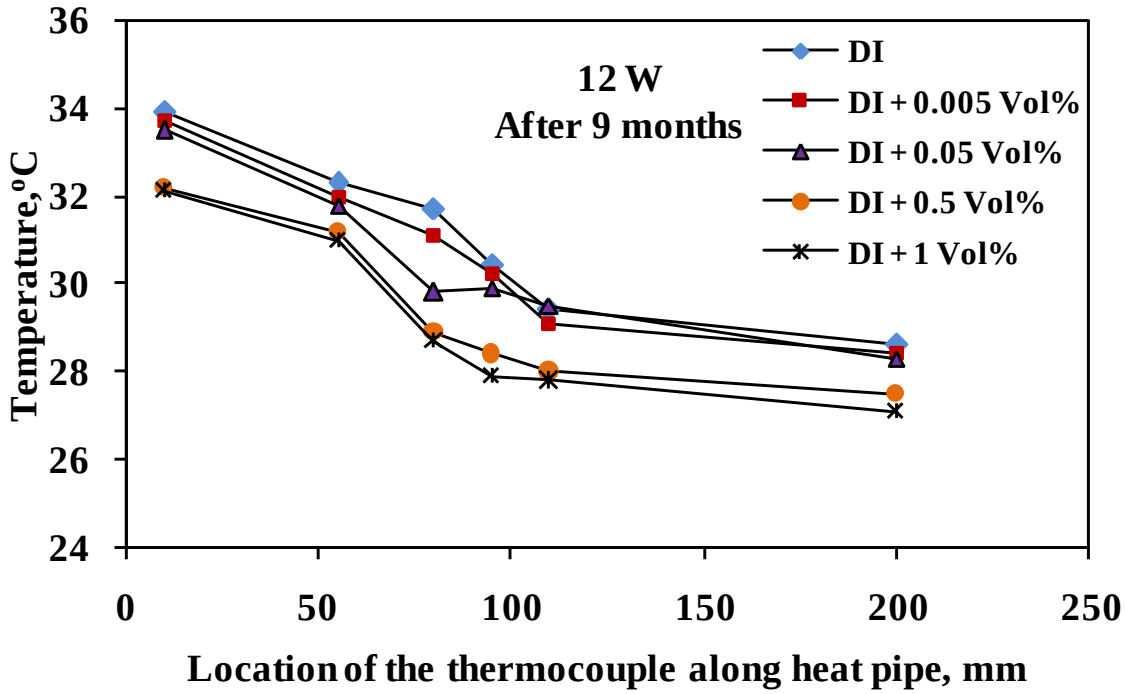

Figure 6.4 Wall temperature distributions at 12 W heat input after 9 months from manufacturing

From the plotted values as shown above, it has been observed that the average wall temperature of modified heat pipe decreases with increase in the nanofluid concentrations in the entire designed temporal time frame of 0 to 9 months. For better observation of the above plotted values, they have been plotted in more consolidated form in Figure 6.5.

Figure 6.5 shows the compiled results of wall temperature distribution of heat pipe using DI water and 1 vol. % concentration of Al_2O_3 / DI water nanofluids tested at 12 W, 32 W and 72 W load of heat input at designed time frames of 0,3,6 and 9 months from the date of manufacturing of heat pipe.

It has been observed from Figure 6.5 that irrespective of the heat input to the evaporator section (12W, 32W and 72W), the average wall temperature of heat pipe using DI water as working fluid does not show any significant drop or rise in the wall temperatures after 0, 3, 6, and 9 months of non-operational standby condition. This shows the high consistency of heat pipe operating characteristics using DI water as working fluid.

From the Figure 6.5, it has been observed that using 1 vol. % of nanofluid concentration , the wall temperature distribution along the length of heat pipe at 12 W load of heat input increases with the increase in the designed time frame of 0, 3, 6 and 9 months. The rise of average temperature with time indicates the temporal deterioration in the thermal performance of heat pipe at low heat input of 12 W.

At 12 W load of heat input, the average temperature of the evaporator and condenser section of heat pipe increases from 28.5^{o}C to 31.5^{o}C and 25.5^{o}C to 27.75^{o}C respectively at 0 and 9 months of non-operational standby time from the date of manufacturing. Using1 vol. % nanofluid concentration, the wall temperature after 9 months tends to approach the values obtained by using DI water as working fluid. It clearly shows reduction in functionality of using heat pipe at 1 vol. % concentration at 12 W load of heat input due to temporal deterioration.

It is suspected that the low vapor pressure generated at low heat input of 12W does not generate enough pressure for the physical movement of nanoparticles through the vapor core section of heat pipe and the nanoparticles entangled with mesh strands do not add value to the latent heat transfer.

At 32W load of heat input to the evaporator section of 200 mm long modified heat pipe, the average wall temperature along its length decreases as compared to that of DI water, thus setting the benefits of using 1 vol.% nanofluids in heat pipe. After performing the temporal test in the designed time frame of 0, 3, 6 and 9 months, the tendency for the average wall temperature to increase with time has been noticed, thus raising the doubt on the consistency of the operating characteristics of heat pipe using nanofluids. But the results were more consistent as compared to 12 W load of heat input. The average temperature of the evaporator and condenser section of heat pipe at 32 W load of heat input increases from 32.5^{o}C to 33.5^{o}C and 28.5^{o}C to 29.5^{o}C, respectively at 0 and 9 month of non-operational standby time.

With further increase in the heat input from 32 W to 72 W to the evaporator section of heat pipe loaded with 1 vol. % of Al_2O_3 /DI water nanofluids, more consistency has been observed in the wall temperatures of heat pipe in the designed time frame of 0,3,6 and 9

months. It gives extreme satisfaction in concluding that there exists a particular heat input and concentration at which the heat pipe under study gives the best temporal results in its thermal performance. At 72 W of heat input subjected to a loading of 1 vol. % of nanofluids concentration, good consistency in the wall temperatures has been observed and the results are well matched with those of DI water from the stability and temporal point of view.

To explore and understand more deeply the reasons for the rise in thermal performance, the modified heat pipe(s) has been dissected to know the morphology and surface characteristics of the mesh. The optical microscope images of the screen mesh wick taken at different stages of experimental study are shown in Figure 6.6 (a - d). It has been seen that the sedimentation and agglomeration of nanoparticles at low heat input tends to block the passage through the mesh and this phenomenon is indicated from the optical microscope images of the used screen mesh wick as shown in Figure 6.6c and Figure 6.6 d. The magnified image shown in Figure 6.6 d shows the complete blockage of the mesh pores obstructing the flow of the condensate back to the evaporator section. Whereas high heat input at 72 W is indicative of high vapor pressure generated in the evaporator section, thus resulting in forceful dragging of Al_2O_3 nanoparticles. The deposition or sticking of the nanopartcles in the longitudinal or transversal direction of the wick may unfold the mystery. This needs an exhaustive study on the deposition of nanoparticles during their flow through the wick at different pressures. The optical microscope image of nanoparticles deposition at 72 W load heat input is shown in Figure 6.6 (b). It clearly shows the nanoparticles deposition on the surface of the strands rather than blocking the space between the strands. Also it worthwhile to mention that the nanoparticles deposition on the mesh wick increases the surface area, its wettability and capillarity action.

The movement of the nanoparticles from the evaporator to the condenser section resulted in the deposition of nanoparticles on the wick surface along the length of the wick. The entrainment of nanoparticles into the vapor phase has been experimentally studied by Dhawan et al. [113] in a vertical pipe using Al_2O_3-water nanofluids of different concentrations at different temperatures. In comparison with pure water, nanofluid resulted in severe entrainment due to the foaming action of the nanoparticles. The degree of entrainment increased with increasing the particle concentration as well as temperature. It indicates the movement of nanoparticles along with vapors.

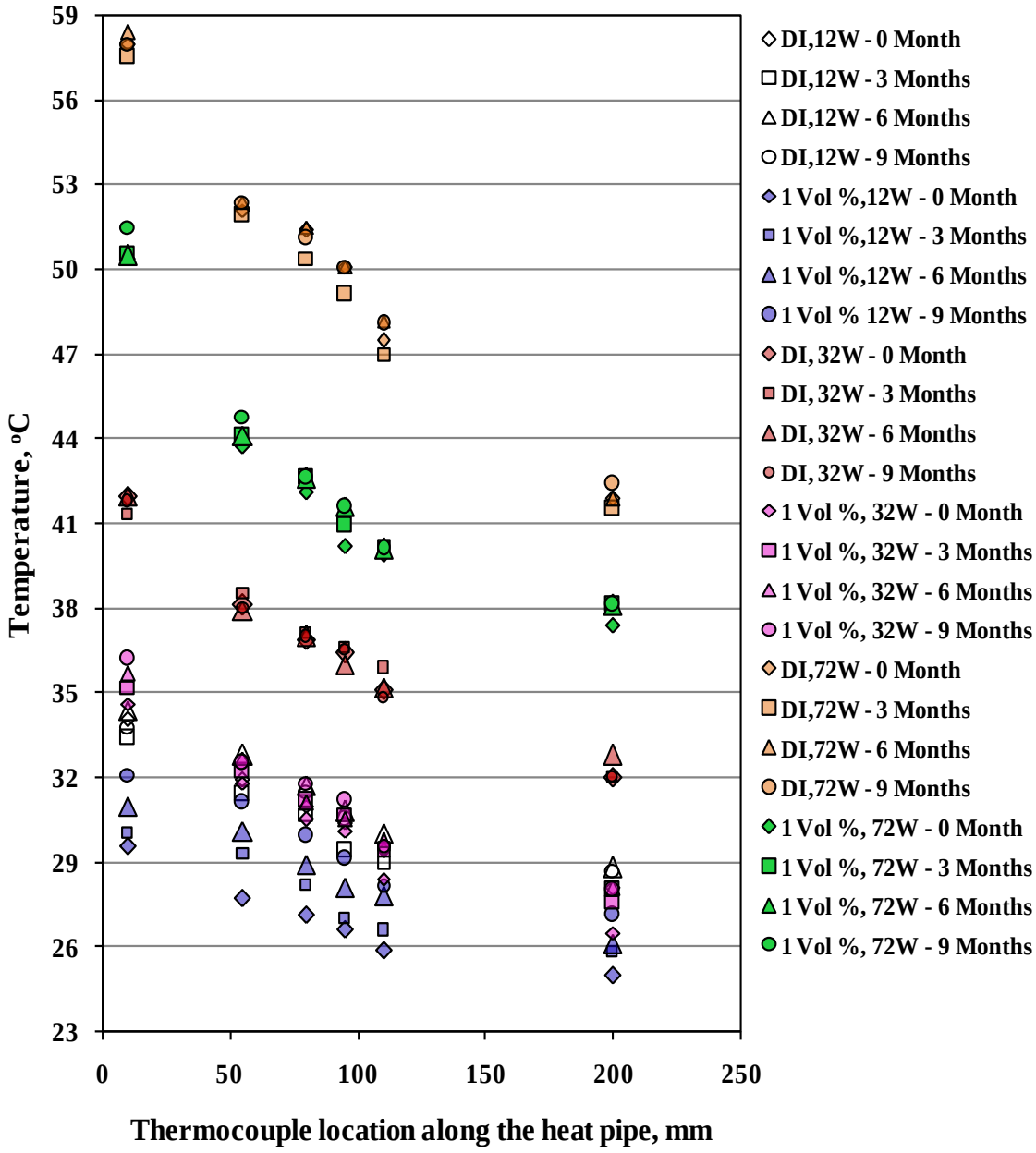

Figure 6.5 **Axial temperature variation of the heat pipe as a function of time interval (0,3, 6, 9 months) at 12W, 32 W and 72 W heat input**

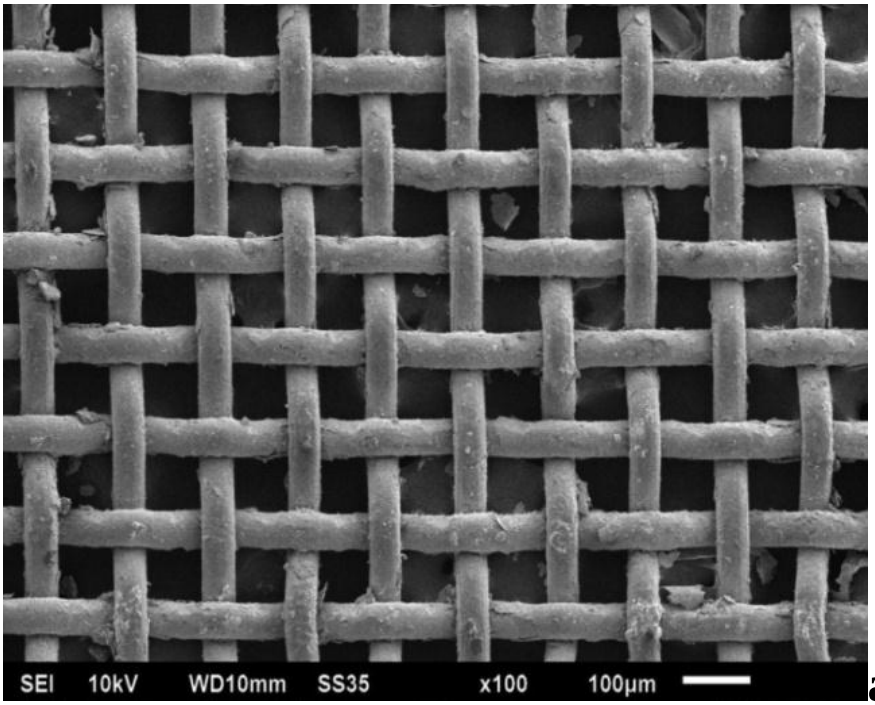

a

Figure 6.6 (a) Optical Microscope images of a screen mesh wick surface using 1 vol.% of Al_2O_3/DI nanofluids as working fluidat 0 month from manufacturing

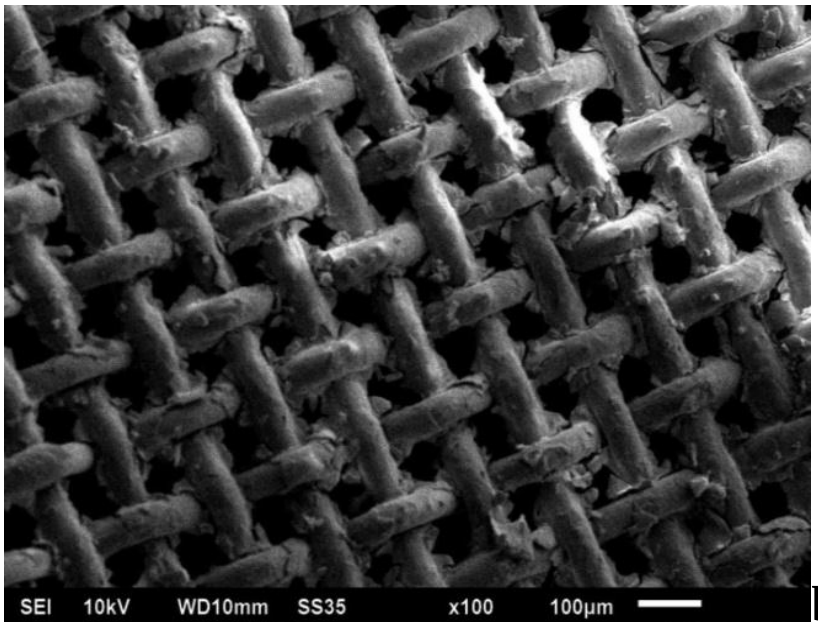

b

Figure 6.6 (b) Optical Microscope images of a screen mesh wick surface using 1 vol.% of Al_2O_3/DI nanofluids as working fluid after 9 months of successive heat input of 72 W

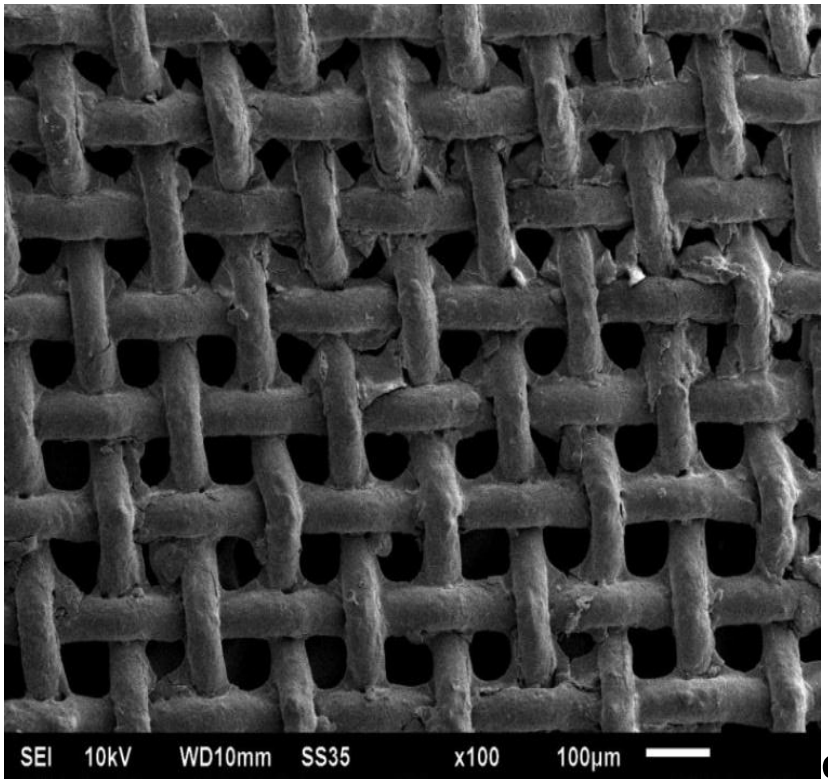

c

Figure 6.6 (c) **Optical Microscope images (x 100) of a screen mesh wick surface using 1 vol.% of Al_2O_3/DI nanofluids as working fluid after 9 months of successive heat input of 12 W**

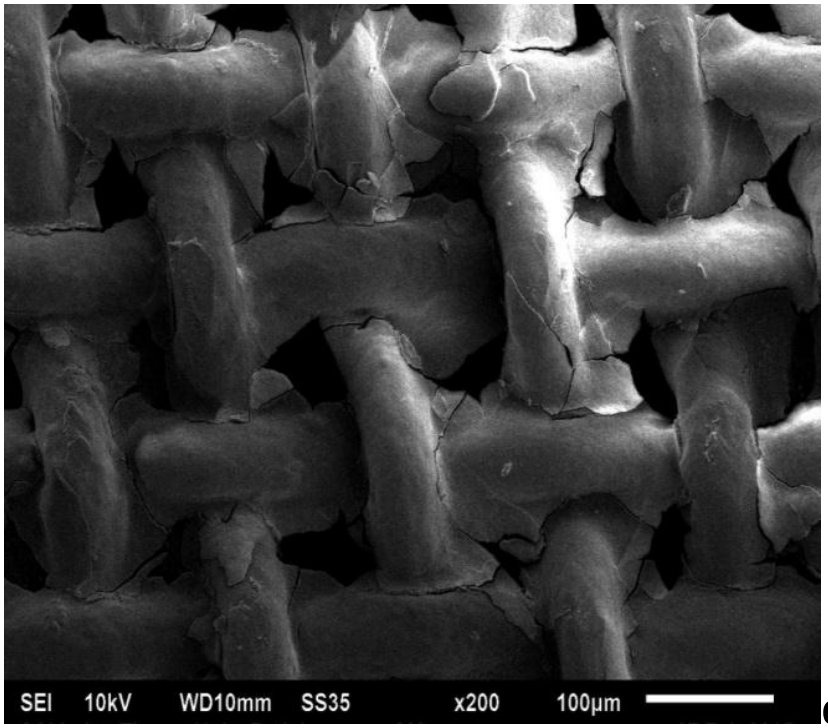

d

Figure 6.6 (d) **Optical Microscope images (x 200) of a screen mesh wick surface using 1 vol.% of Al_2O_3/DI nanofluids as working fluid after 9 months of successive heat input of 12 W**

6.3 Temporal effect on the heat pipe performance indicators

The effective thermal conductivity and thermal resistance of heat pipe are the performance indicators of heat pipe. Taking the practical applicability of modified heat pipe in to consideration, it is necessary to perform the temporal test on the thermal conductivity and thermal resistance of heat pipe at 0, 3, 6 and 9 months of non-operational standby period.

The effective thermal conductivity values as a function of heat flux performed at 0, 3, 6 and 9 months of time frame for the DI water and 1 vol. % concentration are shown graphically in the Figure 6.7.

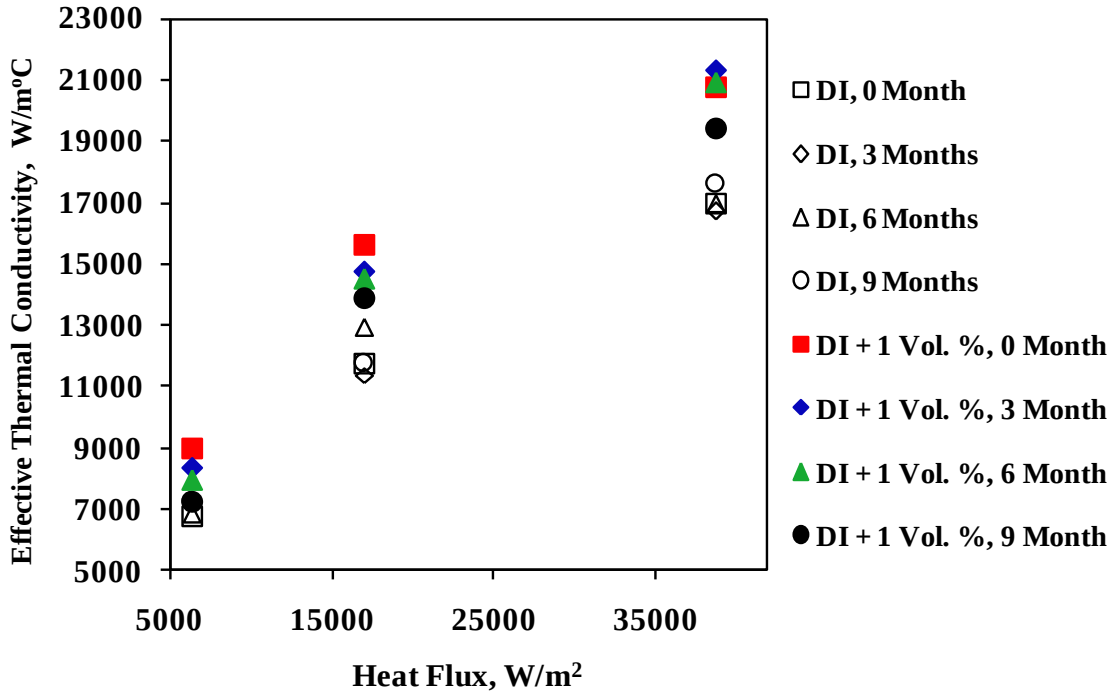

Figure 6.7 Effective thermal conductivity of heat pipe as a function of heat flux and time interval

As compared to DI water, the effective thermal conductivity of modified heat pipe using 1 vol. % of Al_2O_3/DI water nanofluids shows an enhancement of 15.35%, 22.98%, 21.04% obtained at 12W, 32W and 72W heat inputs, respectively after 9 months span of non-operational standby period.

Figure 6.8 shows the thermal resistance of heat pipe at different heat flux rates for DI water and 1 vol. % Al_2O_3/DI water nanofluids concentration at 0,3,6 and 9 months.It is observed

that the use of nanofluids decreases the thermal resistance of heat pipe. Compared to DI water, the use of 1 vol. % concentration of Al_2O_3/DI water nanofluids decreases the thermal resistance by 12.89%, 18.72%, 17.14% at 12W (Heat Flux 6382 W/m^2), 32W (Heat Flux 17021 W/m^2) and 72W (Heat Flux 38829 W/m^2) heat input respectively in the entire test span of 9 months period.

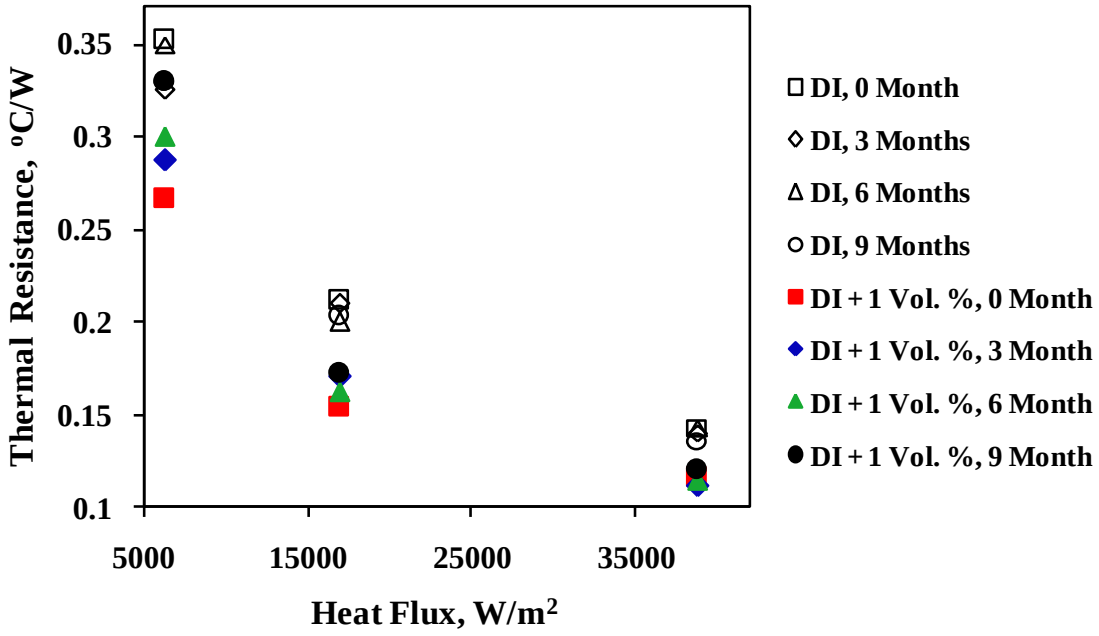

Figure 6.8 Thermal resistance of heat pipe as a function of heat flux and time interval

CHAPTER 7
CONCLUSIONS AND FUTURE SCOPE

The present work investigates the thermophysical properties of Al_2O_3/ DI water nanofluids prepared by two step method. The thermal conductivity of surfactant free nanofluids are investigated thoroughly at selected volume concentrations and temperatures using the Transient hot wire method. The stabilized nanofluids are used as working fluids in heat pipe. The thermal performance of heat pipe has been investigated at different tilt angles, volume concentrations and heat inputs. The significant observation and the conclusion obtained from the present investigation are summarized in the following paragraph.

1. The thermal conductivity ofAl_2O_3/ DI water nanofluids increases with the increase in nanoparticles concentration and temperature. An optimum enhancement of 15 % is achieved at 1 vol. % concentration of Al_2O_3/ DI measured at 70^oC.
2. The operating characteristics of heat pipe are investigated at selected favorable tilt angles (0^o, 30^o, 45^o, 60^o, 90^o) and at different volume concentration of Al_2O_3/ DI water nanofluids (0.005, 0.05, 0.5 & 1 vol. %) and heat inputs (12 W to 72 W).The wall temperature along the length of the heat pipe decreases with the increase in the concentration of nanofluids in the selected heat input range. The thermal resistance decreases with the increase in the nanofluids concentration and heat input. This results due to partial contribution of thermal conductivity along with thermophoresis, shear induced migration and particle drag present during convective transport of nanofluids.
3. An optimum heat pipe angle of 30^o and 45^o has been found for DI water and 1 vol. % Al_2O_3/DI water nanofluids, respectively. This indicates dependency of heat pipe orientation with the nanofluids concentration thus resulting in a shift in the optimum tilt angle of modified heat pipe.
4. Using 1 vol. % concentration of nanofluids, deterioration in the thermal performance of heat pipe is observed at low Watt heat input of 12W and a nearly consistent performance is observed at high Watt load of 72 W. The reduced vapor pressure generated in the heat pipe at low heat input leads to agglomeration and sedimentation of the nanoparticles, thus blockage the porous wick. At high heat loads, pressure gradient across the heat pipe develop convective and capillarity transport phenomenon to

overcome the enhanced tortuosity of the wick, and finally resulting in the consistent performance. Keeping the practicality in to consideration, the findings strongly recommend for the optimization test at specified heat input and nanofluid concentration in heat pipe.

Future Scope

1. The heat pipe known to extract heat from the intricate parts needs to be further investigated with complex geometrical shapes, volume concentration levels, wick designs and high heat loads.
2. Different combinations of metallic and oxide nanoparticles with different mixing ratio and base fluids need to be explored as working fluid in heat pipe.
3. Heat pipe being sensitive to orientation needs to be tested for its thermal performance using nanofluids at adverse tilt.
4. Operating characteristics of heat pipe at different filling ratio of working fluids needs attempted observation.
5. Temporal performance of heat pipe after longer operational times may indicate better performance and needs structured study.

APPENDIX A

Thermophysical Properties of Al_2O_3 DI water nanofluids

Density of Al_2O_3 / DI Water Nanofluids (kg/m^3)

Temperature (^oC)	DI water	0.005 vol. %	0.05 vol. %	0.5 vol. %	1 vol. %
30	995.0	995.6	1000.3	1020.2	1038.2
40	992.4	993	998	1019.2	1037.2
50	989.0	992	994.5	1016.6	1036.0
60	984.2	984.3	991	1013.8	1034.4
70	978.2	980	989	1010.2	1033.6
80	973.6	976	983	1003.6	1032.2
90	967.4	970	978	998.4	1025.6

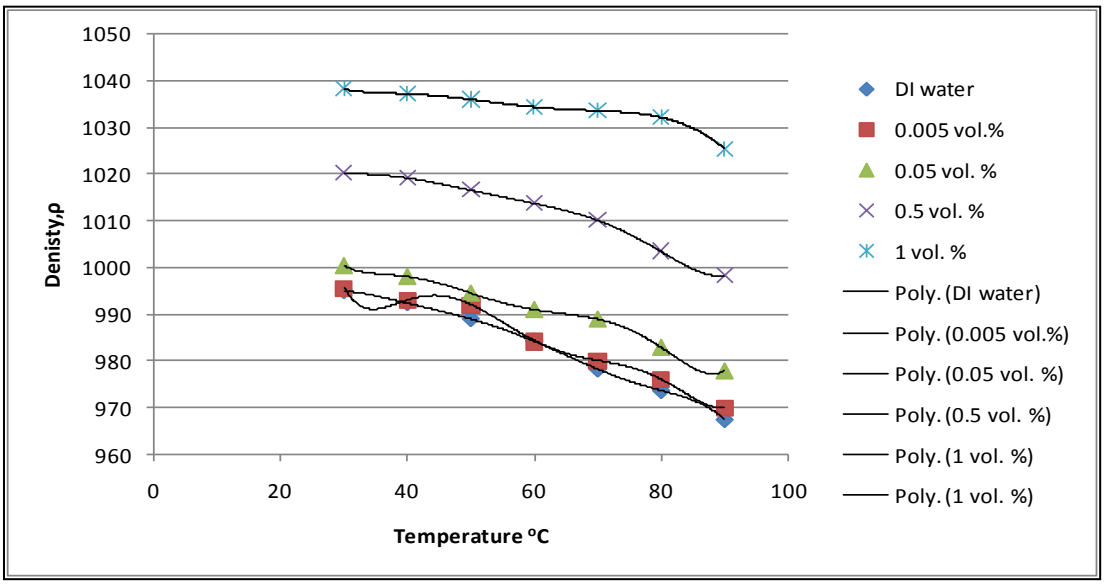

$\rho = 713.6 + 34.81\,\mathbf{T} - 1.729\,\mathbf{T^2} + 0.044\,\mathbf{T^3} - 0.000\,\mathbf{T^4} + 5 \times 10^{-6}\,\mathbf{T^5} - 1 \times 10^{-8}\,\mathbf{T^6}$ **DI water**

$\rho = 3312 - 261.5\,\mathbf{T} + 11.87\,\mathbf{T^2} - 0.278\,\mathbf{T^3} + 0.003\,\mathbf{T^4} - 2 \times 10^{-5}\,\mathbf{T^5} + 6 \times 10^{-8}\,\mathbf{T^6}$ **0.005 vol. %**

$\rho = 1840 - 100.6\,\mathbf{T} + 4.886\,\mathbf{T^2} - 0.122\,\mathbf{T^3} + 0.001\,\mathbf{T^4} - 1 \times 10^{-5}\,\mathbf{T^5} + 3 \times 10^{-8}\,\mathbf{T^6}$ **0.05 vol. %**

$\rho = 1179 - 21.27\,\mathbf{T} + 1.142\,\mathbf{T^2} - 0.031\,\mathbf{T^3} + 0.000\,\mathbf{T^4} - 4 \times 10^{-6}\,\mathbf{T^5} + 1 \times 10^{-8}\,\mathbf{T^6}$ **0.5 vol. %**

$\rho = 1242 - 22.95\,\mathbf{T} + 1.038\,\mathbf{T^2} - 0.024\,\mathbf{T^3} + 0.000\,\mathbf{T^4} - 2 \times 10^{-6}\,\mathbf{T^5} + 5 \times 10^{-9}\,\mathbf{T^6}$ **1 vol. %**

Viscosity of Al_2O_3 / DI Water Nanofluids (cP) [102]

Temperature (^oC)	DI water	0.005 vol. %	0.05 vol. %	0.5 vol. %	1 vol. %
30	0.798	0.8	0.885	1.107	1.277
40	0.653	0.699	0.735	0.866	0.972
50	0.547	0.555	0.595	0.721	0.828
60	0.467	0.483	0.53	0.637	0.701
70	0.404	0.415	0.435	0.518	0.595
80	0.355	0.365	0.39	0.461	0.513
90	0.315	0.32	0.35	0.386	0.438

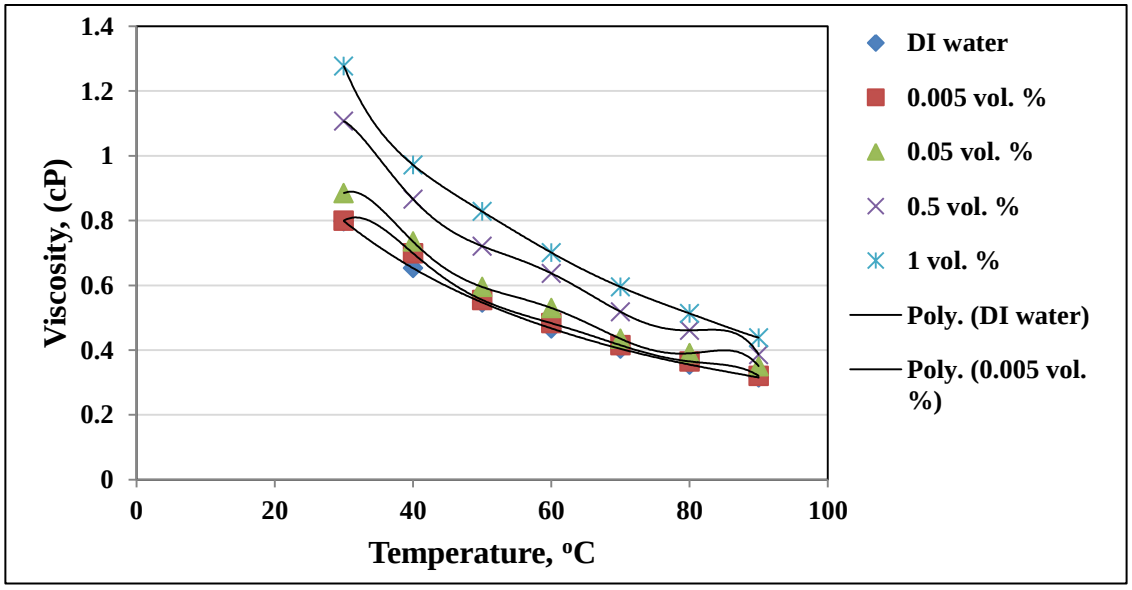

$\mu = 1.335 - 0.005\,\mathbf{T} - 0.001\,\mathbf{T^2} + 4 \times 10^{-05}\,\mathbf{T^3} - 6 \times 10^{-07}\,\mathbf{T^4} + 5 \times 10^{-09}\,\mathbf{T^5} - 1 \times 10^{-11}\,\mathbf{T^6}$ **DI water**

$\mu = -19.08 + 2.239\,\mathbf{T} - 0.100\,\mathbf{T^2} + 0.002\,\mathbf{T^3} - 3 \times 10^{-05}\,\mathbf{T^4} + 2 \times 10^{-07}\,\mathbf{T^5} - 5 \times 10^{-10}\,\mathbf{T^6}$ **0.005 vol. %**

$\mu = -27.88 + 3.357\,\mathbf{T} - 0.156\,\mathbf{T^2} + 0.003\,\mathbf{T^3} - 5 \times 10^{-05}\,\mathbf{T^4} + 3 \times 10^{-07}\,\mathbf{T^5} - 9 \times 10^{-10}\,\mathbf{T^6}$ **0.05 vol. %**

$\mu = -20.96 + 2.712\,\mathbf{T} - 0.132\,\mathbf{T^2} + 0.003\,\mathbf{T^3} - 4 \times 10^{-5}\,\mathbf{T^4} + 3 \times 10^{-07}\,\mathbf{T^5} - 9 \times 10^{-10}\,\mathbf{T^6}$ **0.5 vol. %**

$\mu = 13.58 - 1.195\,\mathbf{T} + 0.047\,\mathbf{T^2} - 0.001\,\mathbf{T^3} + 1 \times 10^{-5}\,\mathbf{T^4} - 7 \times 10^{-8}\,\mathbf{T^5} + 2 \times 10^{-10}\,\mathbf{T^6}$ **1 vol. %**

Thermal Conductivity of Nanofluids, W/(m.K) [THW Method]

Temperature, ^{o}C	DI water	0.005 vol. %	0.05 vol. %	0.5 vol. %	1 vol. %
20	0.5926	0.6109	0.6176	0.6281	0.634
30	0.6156	0.6414	0.65	0.658	0.6716
40	0.626	0.656	0.66	0.6725	0.6904
50	0.6438	0.6798	0.6888	0.6965	0.721
60	0.6512	0.6891	0.7023	0.7143	0.7417
70	0.6662	0.7088	0.72	0.7348	0.7667

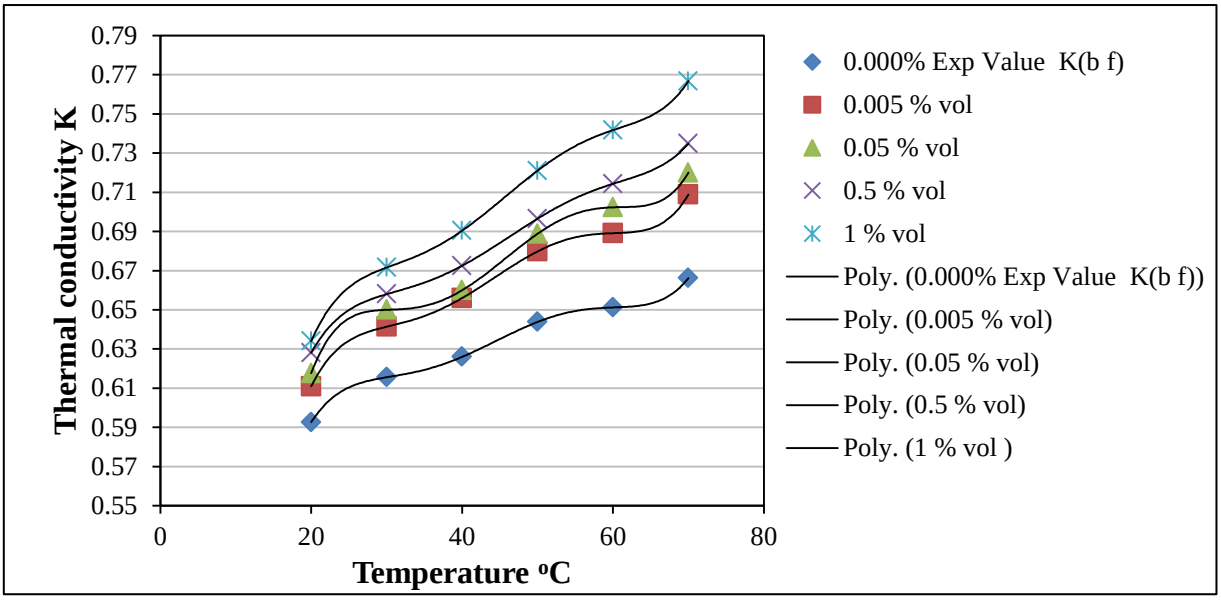

$k = - 0.201 + 0.102\,\mathbf{T} - 0.005\,\mathbf{T^2} + 0.000\,\mathbf{T^3} - 1 \times 10^{-6}\,\mathbf{T^4} + 6 \times 10^{-9}\,\mathbf{T^5}$ **DI water**

$k = - 0.829 + 0.187\,\mathbf{T} - 0.009\,\mathbf{T^2} + 0.000\,\mathbf{T^3} - 2 \times 10^{-6}\,\mathbf{T^4} + 1 \times 10^{-8}\,\mathbf{T^5}$ **0.005 vol. %**

$k = - 0.426 + 0.134\,\mathbf{T} - 0.006\,\mathbf{T^2} + 0.000\,\mathbf{T^3} - 2 \times 10^{-6}\,\mathbf{T^4} + 8 \times 10^{-9}\,\mathbf{T^5}$ **0.05 vol. %**

$k = - 0.171 + 0.100\,\mathbf{T} - 0.004\,\mathbf{T^2} + 0.000\,\mathbf{T^3} - 1 \times 10^{-6}\,\mathbf{T^4} + 5 \times 10^{-9}\,\mathbf{T^5}$ **0.5 vol. %**

$k = - 0.410 + 0.132\,\mathbf{T} - 0.006\,\mathbf{T^2} + 0.000\,\mathbf{T^3} - 2 \times 10^{-6}\,\mathbf{T^4} + 7 \times 10^{-9}\,\mathbf{T^5}$ **1 vol. %**

Surface Tension of Al_2O_3 / DI Water Nanofluids σ (mN/m) [103]

Temperature, ^oC	DI water	0.005 vol. %	0.05 vol. %	0.5 vol. %	1 vol. %
40	69.6	69.8	70.1	70.9	71.2
50	68.3	68.5	69.2	69.5	69.7
60	67.5	67.8	68	68.5	68.7
70	67.0	67.2	67.5	67.7	68.0
80	66.4	66.5	66.8	67	67.5

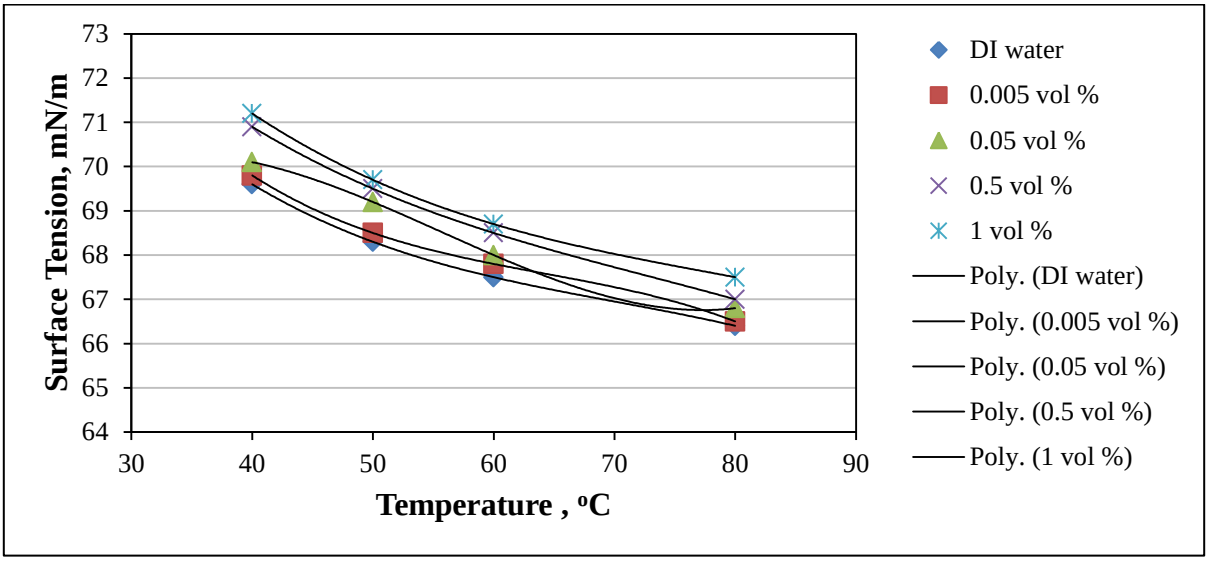

$\sigma = 85.7 - 0.590\ T + 0.006\ T^2 - 3 \times 10^{-05}\ T^3$ **DI water**

$\sigma = 84 - 0.535T + 0.006\ T^2 - 3 \times 10^{-05} T^3$ **0.005 vol. %**

$\sigma = 60.2 + 0.692T - 0.014\ T^2 + 9 \times 10^{-05}\ T^3$ **0.05 vol. %**

$\sigma = 89.5 - 0.924\ T + 0.013\ T^2 - 7 \times 10^{-05}\ T^3$ **0.5 vol. %**

$\sigma = 84.8 - 0.663\ T + 0.008\ T^2 - 4 \times 10^{-05}\ T^3$ **1 vol. %**

Latent Heat of Vaporization λ, kJ/kg [104, 105]

Temperature, ^{o}C	DI water	0.005 vol.%	0.05 vol.%	0.5 vol.%	1 vol.%
40	2410	------	2425	2565	2740
50	2380	2374	------	------	------
60	----	------	2375	2520	2715
70	2338	2340	------	------	------
80	------	2313	2350	2475	2650
90	2292	------	------	------	------
100	2248	2259	2275	2414	2595

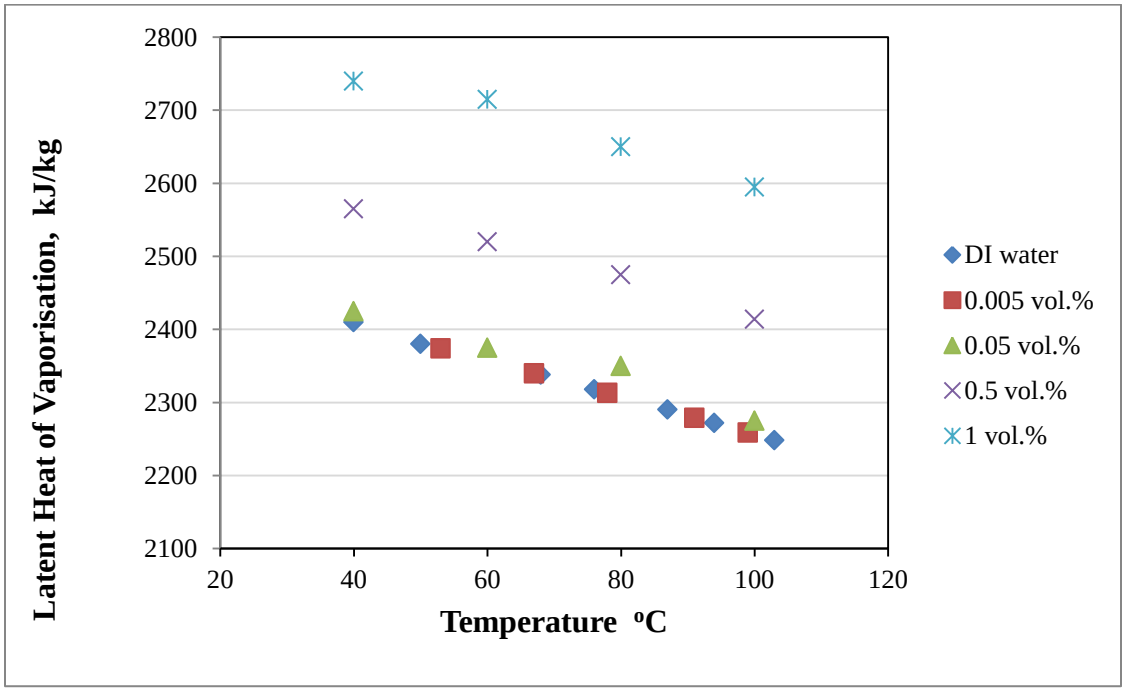

$\lambda = 2767 + 0.125T - 0.018T^2$ **DI water**

$\lambda = 2623 - 1.09T - 0.01T^2$ **0.005 vol. %**

$\lambda = 2453 - 0.187T - 0.015T^2$ **0.05 vol. %**

$\lambda = 2830 - 20.96T + 0.384T^2 - 0.003T^3 + 1x10^{-05}T^4$ **0.5 vol. %**

$\lambda = 3865 - 115.2\,T + 3.810\,T^2 - 0.067\,T^3 + 0.000\,T^4 - 3x\,10^{-06}\,T^5 + 7 \times 10^{-09}\,T^6$ **1 vol. %**

Specific Heat of Al_2O_3/DI Water Nanofluids, kJ/kg ^oC [106]

Temperature,^oC	DI water	0.005 vol.%	0.05 vol.%	0.5 vol.%	1 vol.%
40	2410	------	2425	2565	2740
50	2380	2374	------	------	------
60	----	------	2375	2520	2715
70	2338	2340	------	------	------
80	------	2313	2350	2475	2650
90	2292	------	------	------	------
100	2248	2259	2275	2414	2595

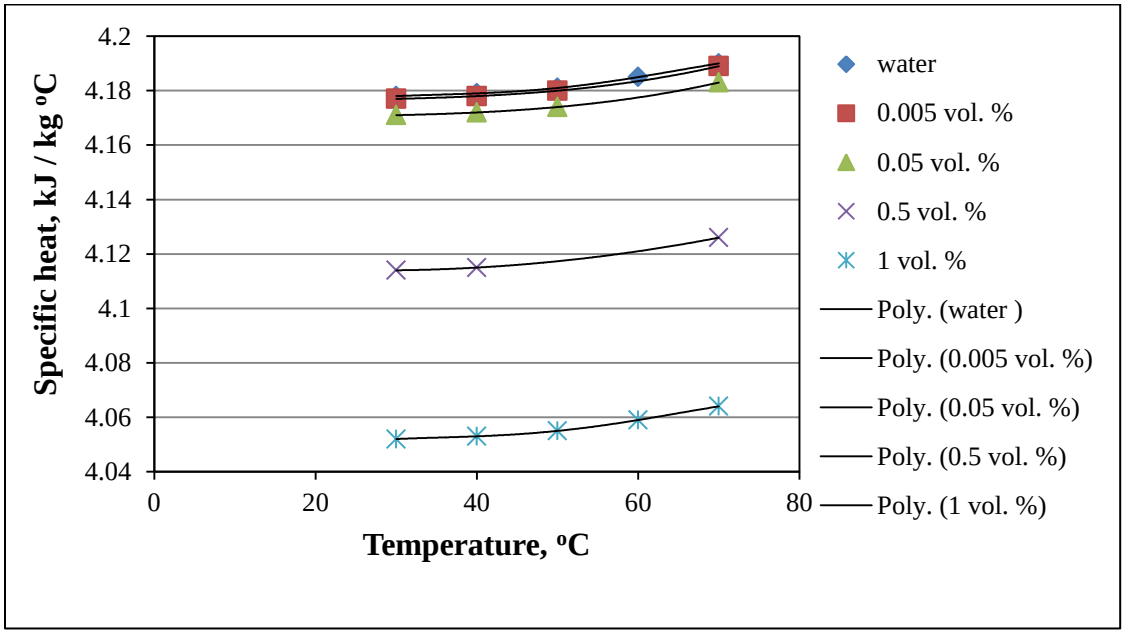

$C_{p,nf} = 4.015 + 0.003T - 0.000T^2 + 2x\ 10^{-06}T^3 - 8x\ 10^{-09}T^4$ **1 vol. %**

$C_{p,nf} = 4.119 - 0.0000T + 7\ x\ 10^{-06}T^2$ **0.5 vol. %**

$C_{p,nf} = 4.169 + 0.000T - 5x\ 10^{-06}T^2 + 8x\ 10^{-08}T^3$ **0.05 vol. %**

$C_{p,nf} = 4.175 + 0.000T - 5\ x\ 10^{-06}T^2 + 8x\ 10^{-08}T^3$ **0.005 vol. %**

$C_{p,nf} = 4.141 + 0.003T - 0.000T^2 + 2\ x10^{-06}T^3 - 8x\ 10^{-09}T^4$ **DI water**

Dynamic Viscosity of Water Vapor μ_{wv} (kg/m.s)

Temp.^{o}C	Base Fluid	0.005 % vol.	0.05 % vol.	0.5 % vol.	1 % vol.
24.10	0.000010000	0.000010050	0.000010052	0.000010125	0.000010150
32.9	0.000010042	0.000010092	0.000010094	0.000010117	0.000010141
41.53	0.000010277	0.000010328	0.000010330	0.000010353	0.000010379
60	0.000010957	0.000011011	0.000011014	0.000011038	0.000011066
69.1370	0.000011187	0.000011242	0.000011245	0.000011265	0.000011298

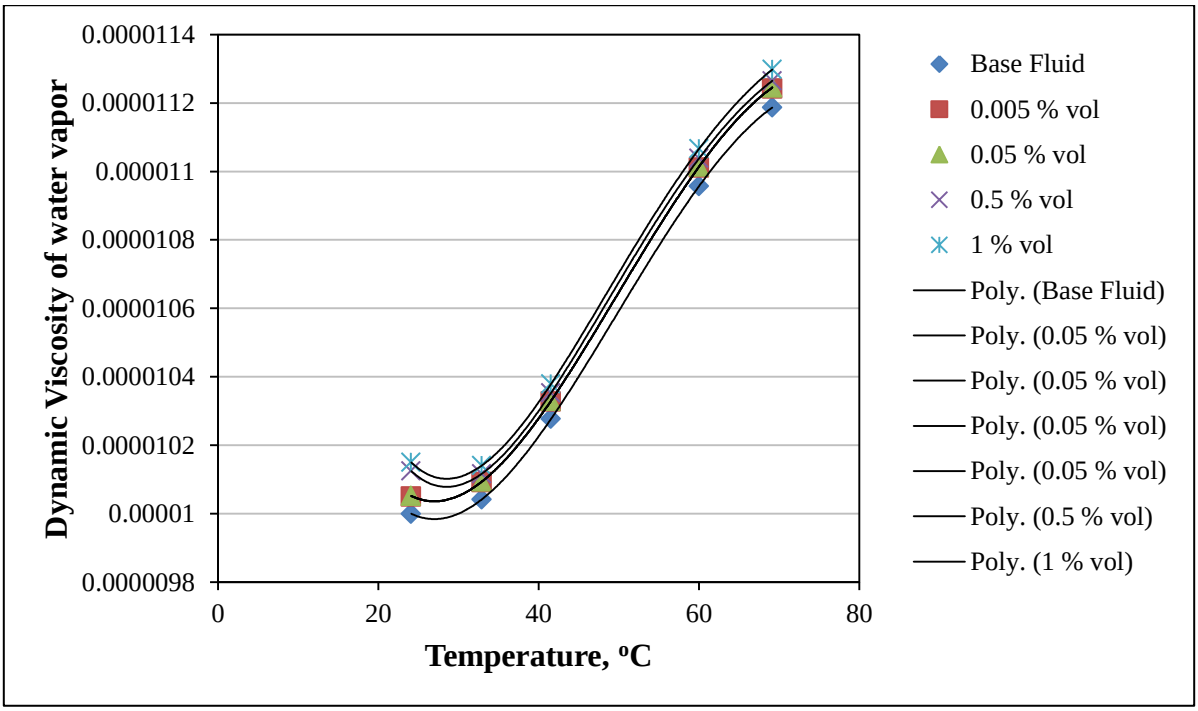

$\mu_{wv} = 1x\ 10^{-05} - 3\ x\ 10^{-07}T + 8\ x\ 10^{-09}T^2 - 9\ x\ 10^{-11}T^3 + 3\ x\ 10^{-13}T^4$ **I vol. %**

$\mu_{wv} = 1x10^{-05} - 2x10^{-07}T + 5\ x\ 10^{-09}T^2 - 4\ x10^{-11}T^3 + 1\ x\ 10^{-13}T^4$ **0.05 vol.%**

$\mu_{wv} = 1x10^{-05} - 2x10^{-07}T + 5\ x\ 10^{-09}T^2 - 4\ x10^{-11}T^3 + 1\ x\ 10^{-13}T^4$ **0.005 vol. %**

$\mu_{wv} = 1\ x\ 10^{-05} - 3\ x\ 10^{-07}T + 8x\ 10^{-09}T^2 - 8\ x\ 10^{-11}T^3 + 3\ x\ 10^{-13}T^4$ **0.5 vol %**

$\mu_{wv} = 1\ x\ 10^{-05} - 2\ x\ 10^{-07}T + 5\ x\ 10^{-09}T^2 - 4\ x\ 10^{-11}T^3 + 1x\ 10^{-13}T^4$ **DI water**

Density of Vapor, ρ_{wv} (kg/m^3)

Density of vapor	30°C	40 °C	60 °C	70 °C
0.005 vol. %	0.2244	0.2384	0.3204	0.3804
0.05 vol. %	1.929	1.943	2.025	2.085
0.5 vol. %	18.98	18.99	19.11	19.14
1 vol. %	37.93	37.94	38.02	38.08
DI water	0.035	0.049	0.131	0.191

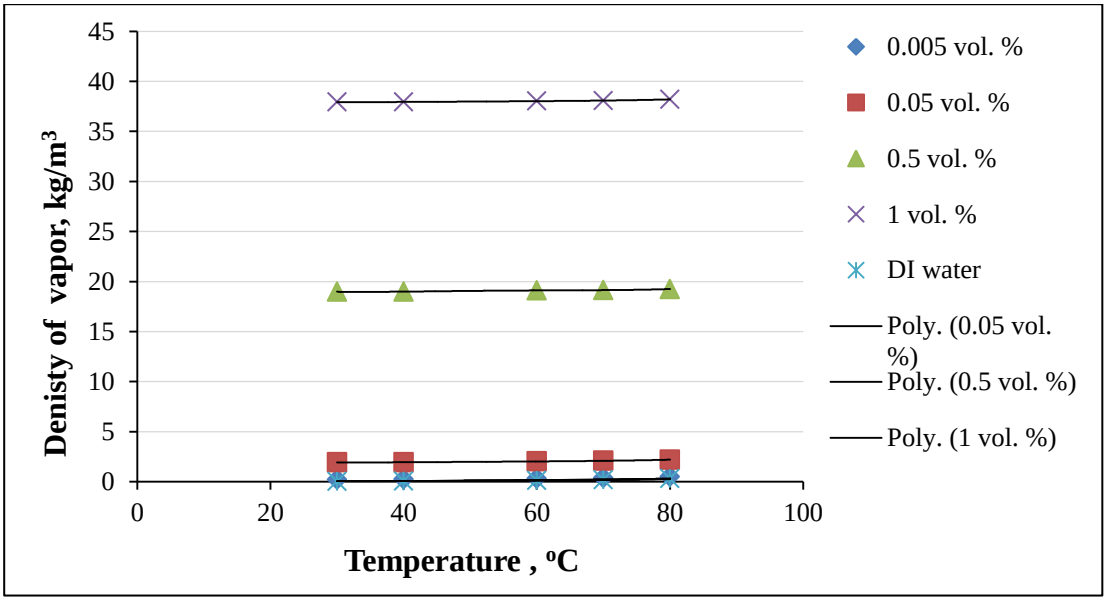

$\rho_{wv} = 38.75 - 0.070T + 0.002T^2 + 1 \times 10^{-07}T^4 - 3 \times 10^{-05}T^3$ **1 vol. %**

$\rho_{wv} = 21.56 - 0.219T + 0.006T^2 - 8 \times 10^{-05}T^3 + 4 \times 10^{-07}T^4$ **0.5 vol. %**

$\rho_{wv} = 2.681 - 0.065T + 0.002T^2 - 3 \times 10^{-05}T^3 + 1 \times 10^{-07}T^4$ **0.05 vol. %**

$\rho_{wv} = 0.787 - 0.065T + 0.002T^2 - 3 \times 10^{-05}T^3 + 1 \times 10^{-07}T^4$ **0.005 vol. %**

$\rho_{wv} = 0.787 - 0.065T + 0.002T^2 - 3 \times 10^{-05}T^3 + 1 \times 10^{-07}T^4$ **DI water**

REFERENCES

1. McWilliams A., "The market for thermal management technologies", BCC Research Report Code SMC024J, 2014.
2. Gordon E. Moore., "Cramming more components onto integrated circuits", Electronics, pp. 114-117, 1965.
3. Abraham V. and Iyer G., "Semiconductor Industry: Rising up the value chain", Wipro council for Industrial Research, 2012.
4. "International Technology Roadmap for Semiconductors (ITRS)", Assembly and Packaging, SIA, 2013.
5. Koch G., "Discovering Multi Core: Extending the benefits of Moore's law", Intel White Paper, Technology Intel Magazine, 2005.
6. Kakac S., "Introduction to ASI on cooling of electronic systems", edited by Kakac S., Yuncu H. and Hijikata K., 1994, pp.1-15, Kulwar Academic Publishers, 1994.
7. Lin S., Sefiane K. and Christy J.,"Prospects of confined flow boiling in thermal management of Microsystems", Applied Thermal Engineering, vol. 22, No. 7, pp. 825-837, 2002.
8. Cengel Y. A., "Heat Transfer– A practical approach", McGraw Hill, 1998.
9. Moffat R. J., "Air cooling of electronic components, and advances in thermal modeling of electronic components and systems", vol. 1, (edited by Bar-Cohen A. and Kraus A.D), Hemisphere Publishing Corporation, New York, USA, 1998.
10. Chu R. C., "A review of IBM sponsored research and development Projects for computer cooling", Proc. of 15th IEEE Semi-Therm Symposium, pp. 151-165, 1999.
11. Khandekar S., Groll M. and Luckchoura V., "An introduction to pulsating heat pipes", Electronics Cooling Magazine, vol. 9, no.2, pp. 38-41, 2003.
12. Khandekar S.,"Thermo hydrodynamics of closed loop pulsating heat pipes", Doctoral Dissertation, University of Stuttgart, Germany 2004. (Retrieved fromhttp://elib.uni-stuttgart.de/opus/volltexte/2004)
13. Reid R. S. and Merrigan M. A., "Heat pipe activity in the Americas – 1990 to 1995", Los Alamos National Laboratory, New Mexico, 1997.

14. Lee S., Choi S. U. S., Li S. and Eastman J. A.,"Measuring thermal conductivity of fluids containing oxide nanoparticles", Journal of Heat Transfer,vol. 121, pp. 280-289, 1999.
15. Eastman J. A., Choi S. U. S., Li S., Yu W. and Thompson L. J., "Anomalously increased effective thermal conductivities of ethylene glycol-based nanofluids containing copper nanoparticles", Applied Physics Letters, vol. 78, no. 6, pp. 718-720, 2001.
16. Yatsuya S., Tsukasaki Y., Mihama K. and Uyeda R., "Preparation of extremely fine particles by vacuum evaporation onto a running oil substrate",Journal of Crystal Growth,vol. 45, pp.490-494, 1978.
17. Zhu H., Lin Y. S. and Yin Y.S.,"A novel one-step chemical method for preparation of copper nanofluids", Journal of Colloid and Interface Science, vol. 277,pp. 100 -103, 2004.
18. Lo C. H., Tsung T. T., Chen L. C., Su C. H. and Lin H. M., "Fabrication of copper oxide nanofluid using submerged arc nanoparticle synthesis system (SANSS)", Journal of Nanoparticle Research, vol. 7, no. 2-3, pp. 313-320, 2005.
19. Patel H. E., Das S. K., Sundararajan T., Sreekumaran A., George B. and Pradeep T., "Thermal conductivity of naked and monolayer protected metal nanoparticle based nanofluids: Manifestation of anomalous enhancement and chemical effects", Applied Physics Letters, vol.83, no.14, pp. 2931-2933, 2003.
20. Zhang X., Gu H. and Fujii M., "Effective thermal conductivity and thermal diffusivity of nanofluids containing spherical and cylindrical nanoparticles", Journal of Applied Physics, vol. 100, no. 4, Article ID 044325,2006.
21. Liu M., Lin M. C., Tsai C. Y. and Wang C., "Enhancement of thermal conductivity with Cu for nanofluids using chemical reduction method", International Journal of Heat and Mass Transfer, vol.49, pp 3028-3033, 2006.
22. Phuoc T. X., Soong Y. and Chyu M. K., "Synthesis of Ag-deionized water nanofluids using multi-beam laser ablation in liquids", Optics and Lasers in Engineering, vol. 45,pp. 1099-1106, 2007.

23. Tamjid E. and Guenther B.H., "Rheology and colloidal structure of silver nanoparticles dispersed in diethylene glycol", Powder Technology, vol. 197, no.1, pp.49-53, 2010.
24. Han, Z. H., Cao F.Y. and Yang B., "Synthesis and thermal characteristics of phase changeable indium/polyalphaoefin nanofluids", Applied Physics Letters, vol. 92,pp. 243104, 2008.
25. Zhu H. T., Zhang C. Y., Tang Y. M. and Wang J. X., "Novel synthesis and thermal conductivity of CuO nanofluids", Journal of Physical Chemistry C, vol. 3, no. 4, pp. 1646-1650, 2007.
26. Chen Y. and Wang X., "Novel phase transfer preparation of mono disperse silver and gold nanoparticles at room temperature", Materials Letters, vol. 62, no. 15, pp. 2215-2218, 2008.
27. Wang L. and Fan J., "Nanofluids research: key issues", Nanoscale Research Letters, vol. 5, no. 8, pp. 1241-1252, 2010.
28. Timofeeva E. V., Gavrilov A. N., McCloskey J. M., Tolmechev Y. V.,Sprunt S.,Lopatina.and Selinger J. V., "Thermal conductivity and particle agglomeration in alumina nanofluids", Experiment and Theory, Physical Review Letters, E-76 (6) 061203, 2007.
29. Hiemenz P. C. and Dekker M., "Principles of colloid and surface chemistry", Second ed., Marcel Dekker, New York, 1986.
30. Wu D., Zhu H., Wang L. and Liua L., "Critical issues in nanofluids preparation, characterization and thermal conductivity", Current Nanoscience, vol. 5, pp. 103-112, 2009.
31. Hwang Y., Lee J. K., Lee C. H., Jung Y. M., Cheong S. I, Lee C. G., Ku B. C. and Jang S. P., "Stability and thermal conductivity characteristics of nanofluids", Thermochimica Acta,vol. 455,Issue 1-2, pp. 70-74, 2007.
32. Hwang Y. J., Ahn Y. C., Shin H.S., Lee C.G., Kim G.T., Park H.S. and Lee J.K., "Investigation on characteristics of thermal conductivity enhancement of nanofluids", Current Applied Physics, vol. 6, no. 6,pp. 1068-1071, 2006.
33. Ding Y., Chen H., He Y., Lapkin A., Yeganeh M.,Siller L. and Butenko Y. V., "Forced convective heat transfer of nanofluids", Advanced Powder Technology, vol. 18, no. 6, pp. 813-824, 2007.

34. Assael M. J., Metaxa I. N., Arvanitidis J., Christofilos D. and Lioutas C.,"Thermal conductivity enhancement in aqueous suspensions of carbon multi-walled and double-walled nanotubes in the presence of two different dispersants", International Journal of Thermophysics, vol. 26, no. 3,pp. 647-664, 2005.

35. Madni I., Hwang C.Y., Park S. D, Choa Y. H. and Kim H. T., "Mixed surfactant system for stable suspension of multiwalled carbon nanotubes", Colloids and Surface A: Physicochemical and Engineering Aspects, vol. 358, no 1-3, pp. 101-107, 2010.

36. Zhu H., Zhang C., Tang Y., Wang J., Ren B. and Yin Y., "Preparation and thermal conductivity of suspensions of graphite nanoparticles", Carbon, vol. 45, no. 1, pp. 226-228, 2007.

37. Li X. F., Zhu D. S.,Wang X. J., Wang N., Gao, J. W. and Li H., "Thermal conductivity enhancement dependent pH and chemical surfactant for Cu–H_2O nanofluids". Thermochimica Acta, vol. 469, Isss 1, pp. 98-103, 2008.

38. Wen D., Lin G., Vafaei S. and Zhang K., "Review of nanofluids for heat transfer applications", Particuology, vol. 7, no. 2, pp. 141-150, 2009.

39. Wang X. Q. and Mujumdar A. S., "A review on nanofluids", Part II: Experiments and Applications, Brazilian Journal of Chemical Engineering, vol. 25, pp. 631-648, 2008.

40. Murshed S. M. S., Leong K. C. and Yang C., "Investigations of thermal conductivity and viscosity of nanofluids", International Journal of Thermal Science, vol. 47, pp 560-568, 2008.

41. Wang X. Q. and Mujumdar A. S., "Heat transfer characteristics of nanofluids: a review", International Journal of Thermal Science, vol. 46, no. 1, pp. 1-19, 2007.

42. Chang H., Wu Y. C., Chen X. Q. and Kao M. J., "Fabrication of Cu based nanofluid with superior dispersion", National Taipei University of Technology, Taipei, Taiwan, 2000.

43. Wei X., Zhu H., Kong T. and Wang L., "Synthesis and thermal conductivity of Cu_2O nanofluids", International Journal of Heat Mass Transfer, vol. 52 no. 19- 20, pp. 4371-4374, 2009.

44. Lee D., Kim J. W. and Kim B .G.,"A new parameter to control heat transport in nanofluids: surface charge state of the particle in suspension", Journal of Physical Chemistry B, vol. 110, no. 9, pp. 4323-4328, 2006.

45. Xie H., Lee H., Youn W. and Choi M., "Nanofluids containing multiwalled carbon nanotubes and their enhanced thermal conductivities", Journal of Applied Physics, vol. 94, no. 8, pp. 4967-4971, 2003.

46. Chang H., Jwo C., Fan P. and Pai S., "Process optimization and material properties for nanofluid manufacturing", International Journal of Advanced Manufacturing Technology, vol. 34, no. 3, pp. 300-306, 2007.

47. Missana T. and Adell A., "On the applicability of DLVO theory to the prediction of clay colloids stability", Journal of Colloid and Interface Science, vol. 230, no. 1, pp. 150-156, 2000.

48. Popa I., Gillies G., Papastavrou G. and Borkovec M.,"Attractive and repulsive electrostatic forces between positively charged latex particles in the presence of anionic linear polyelectrolytes", Journal of Physical Chemistry B, vol. 114, no. 9, pp. 3170-3177, 2010.

49. Lee J. H., Hwang K. S., Jang S. P., Lee B. H., Kim J. H., Choi S. U. S. and Choi C.J., "Effective viscosities and thermal conductivities of aqueous nanofluids containing low volume concentrations of Al_2O_3 nanoparticles". International Journal of Heat and Mass Transfer, vol. 51, pp. 2651-2656, 2008.

50. Wang X. J. and Li X. F., "Influence of pH on nanofluids viscosity and thermal conductivity", Chinese Physics Letters, vol. 26, no. 5, 056601, 2009.

51. Munson B. R., Young D. F. and Okiishi T. H., "Fundamentals of Fluid Mechanics", John Wiley & Sons Inc, 1998.

52. Buongiorno, J., Venerus, D. C., Prabhat, N., McKrell, T., Townsend, J., Christianson, R., Tolmachev, Y. V., Keblinski, P., L.-W Hu, L. W., Alvarado, J. L., Bang, I. C., Bishnoi, S. W., Bonetti, M., Botz, F., Cecere, A., Chang, Y., Chen, G., Chen, H., Chung, S. J., M. Chyu, M. K., Das, S. K., Paola, R. D., Ding, Y., Dubois, F., Dzido, G., Eapen, J., Escher, W., Funfschilling, D., Galand, Q., Gao, J., Gharagozloo, P. E., Goodson, K. E., Gutierrez, J. G., Hong, H., Horton, M., Hwang, K.

S., Iorio, C. S., Jang, S. P., Jarzebski, A. B., Jiang, Y., Jin, L., Kabelac, S., Kamath, A., Kedzierski, M. A., L. G. Kieng, Kim, C., Kim, J. H., S. Kim, S., Lee, S. H., Leong, K. C., Manna, I., Michel, B., NI, R., Patel, H. E., Philip, J., Poulikakos, D., Reynaud, C., Savino, R., Singh, P. K., Song, P., Sundararajan, T., Timofeeva, E., Tritcak, T., Turanov, A. N., Vaerenbergh, S. V., Wen, D., Witharana, S., Yang, C., Yeh, W. H., Zhao, X. Z., and Zhou, S. Q.,"A Benchmark Study on the Thermal Conductivity of Nanofluids", Journal of Applied Physics, vol.106, 094312, 2009.

53. Sommers A. and Yerkes K., "Experimental investigation into the convective heat transfer and system level effects of Al_2O_3propanol nanofluids", Journal of Nanoparticle Research, vol. 12, no. 3, pp. 1003-1014, 2009.

54. Zhou M. Z., Xia G. D, Li J, Chai L. and Zhou L. J., "Analysis of factors influencing thermal conductivity and viscosity in different kinds of surfactant solutions", Experimental Thermal and Fluid Science, vol. 36, pp. 22-29, 2012.

55. Hong K. S., Hong T. K. and Yang H. S., "Thermal conductivity of Fe nanofluids depending on the cluster size of nanoparticles", Applied Physics Letters, vol. 88, no. 3, pp. 1-3, 2006.

56. Ozerinc S., Kakac S. and Yazicioglu A. G., "Enhanced thermal conductivity of nanofluids: a state of the art review", Microfluidics and Nanofluidics, vol. 8, no. 2, pp 145-170, 2010.

57. Timofeeva E. V., Routbort J. L. and Singh D., "Particle shape effects on thermophysical properties of alumina nanofluids", Journal of Applied Physics, vol.106,no.1, Article ID 014304, 2009.

58. Xie H., Wang J., Xi T. and Y. Liu Y.,"Thermal conductivity of suspensions containing nanosized SiC particles". International Journal of Thermophysics vol. 23, no. 2, pp. 571-580, 2002.

59. Murshed S., Leong K. and Yang C., "Enhanced thermal conductivity of TiO_2–water based nanofluids", International Journal of Thermal Sciences, vol. 44, no.4, pp. 367-373, 2005.

60. JeongJ., Li C., Kwon Y., Lee J., Kim S. H. and Yun R., "Particle shape effect on the viscosity and thermal conductivity of ZnO nanofluids", International Journal of Refrigeration**, v**ol. 6, Issue 8, pp. 2233-2241, 2013.

61. Singh D., Timofeeva E., Yu W., Routbort J., France D., Smith D. and Lopez-Cepero J., "An investigation of silicon carbide–water nanofluid for heat transfer applications", Journal of Applied Physics, vol. 105, pp. 6, Article ID 064306, 2009.

62. Zhou X.F. and Gao L., "Effective thermal conductivity in nanofluids of non-spherical particles with interfacial thermal resistance: Differential effective medium theory", Journal of Applied Physics, vol. 100, Article ID 024913, 2006.

63. Das S.K., Putra N., Thiesen P. and Roetzel W., "Temperature dependence of thermal conductivity enhancement for nanofluids", Journal of Heat Transfer, vol. 125, pp**.** 567–574, 2003.

64. Xie H., Wang J., Xi T., Liu Y. and Ai F., "Thermal conductivity enhancement of suspensions containing nanosized alumna particles", Journal of Applied Physics, vol. 91, pp. 4568-4572, 2002.

65. Wang X., Xu X. and Choi S.U.S., "Thermal conductivity of nanoparticle-fluid mixture", Journal of Thermophysics Heat Transfer, vol.13, pp**.** 474-480, 1999.

66. Murshed S.M.S., Leong K.C. and Yang C**., "**Investigation of thermal conductivity and viscosity of nanofluids", International Journal of Thermal Sciences, vol. 47, pp**.** 560-568, 2008.

67. Beck M.P., Sun T. and Teja A.S., "The thermal conductivity of alumina nanoparticles dispersed in ethylene glycol", Fluid Phase Equilibria, vol. 260, pp. 275-278, 2007.

68. Timofeeva E.V., Gavrilov A. N., McCloskey J. M. and Tolmachev Y.V., "Thermal conductivity and particle agglomeration in alumina nanofluids: experiment and theory"**.** Physical Review E, vol. 76, Article ID061203, 2007.

69. Masuda H., Ebata A., Teramae K. and Hishinuma N., **"**Alteration of thermal conductivity and viscosity of liquid by dispersing ultra-fine particles (dispersion of γ-Al_2O_3, SiO_2, and TiO_2 ultra-fine particles)".Netsu Bussei Japan, vol.**7**, pp.227-233,1993.

70. Li C. H. and Peterson G. P., **"**Experimental investigation of temperature and volume fraction variations on the effective thermal conductivity nanoparticle suspensions (nanofluids)", Journal of Applied Physics, vol. 99, Article ID 084314, 2006.

71. Hwang D., Hong K. S. and Yang H. S., **"**Study of thermal conductivity of nanofluids for the application of heat transfer fluids", Thermochimica Acta, vol. 455, pp**.** 66-69, 2007.

72. Sexena R., Gangacharyulu D. and Bulasara V. K., "Heat transfer and pressure drop characteristics of dilute alumina–water nanofluids in a pipe at different power inputs", Heat Transfer Engineering, vol. 37,Issue 18, 2016.

73. Xia G., Jiang H., Liu R., Zhai Y., "Effects of surfactant on the stability and thermal conductivity of Al_2O_3 /Deionised water nanofluids", International Journal of Thermal Sciences, vol. 84, pp.118–124, 2014.

74. Chen L. and Xie H., "Properties of carbon nanotube nanofluids stabilized by cationic gemini surfactant", Thermochimica Acta, vol. 506, pp. 62-66, 2010.

75. Yang L., Du K., Zhang X. S. and Cheng B., "Preparation and stability of Al_2O_3 nanoparticle suspension of ammonia water solution", Applied Thermal Engineering, vol. 31, no.17, pp. 3643-3647, 2011.

76. Das S.K., Putra N. and Roetzel W., "Pool boiling characteristics of nano-fluids", International Journal of Heat and Mass Transfer, vol. 46, pp. 851-862, 2003.

77. Liu M. S., Lin M C., Huang I.T. and Wang C C., "Enhancement of thermal conductivity with CuO for nanofluids", Chemical Engineering and Technology, vol. 29, pp. 72-77, 2006.

78. Wang X., Xu X. and Choi S. U. S.,"Thermal conductivity of nanoparticle–fluid mixture", Journal of Thermophysics and Heat transfer, vol.13, no.4, pp. 474-480, 1999.

79. Kole M. and Dey T. K., "Thermal conductivity and viscosity of Al_2O_3 nanofluid based on car engine coolant", Journal of Physics D, vol. 43, no.31, Article ID 315501, 2010.

80. Oh D.W., Jain A., Eaton J. K., Goodson K. E. and Lee J. S., "Thermal conductivity measurement and sedimentation detection of aluminum oxide nanofluids by using the 3-omega method", International Journal of Heat Fluid Flow, vol. 29, no. 5, pp. 1456-1461, 2008.

81. Wei W. C., Tsai S. H., Shih-Yu., Yang S. Y. and Kang S. W., "Effect of nanofluid concentration on heat pipe thermal performance", IASME Trans. 2, vol.8, pp. 1432-1439, 2005.

82. Naphon P., Pichai A. and Teerapong B., "Experimental investigation of titanium nanofluids on the heat pipe thermal efficiency", International Communications in Heat and Mass Transfer, vol. 35, pp. 1316-1319, 2008.

83. Kang S. W., Wei W C., Tsai S H. and Yang S. Y., "Experimental investigation of silver nanofluid on heat pipe thermal performance", Applied Thermal Engineering, vol. 26, no.17, pp. 2377-2382, 2006.

84. Chen Y. T., Wei W. C.,Kang S. W. and Yu C. S., "Effect of nanofluids on flat heat pipe thermal performance", 24th IEEE Semi-Therm Symposium, pp 16-19, 2008.

85. Mousa M. G., "Effect of nanofluid concentration on the performance of circular heat pipe", Ain Shams Engineering Journal, vol. 2, no. 1, pp. 63- 69, 2011.

86. Hajian R., Layeghi M. and Sani K. A., "Experimental study of nanofluid effects on the thermal performance with response time of heat pipe", Energy Conversion and Management, vol. 56, pp. 63-68, 2012.

87. Tsai C. Y., Chien H. T., Ding P.P., Chan B., Luh T. Y. and Chen P. H., "Effect of structural character of gold nanoparticles in nanofluid on heat pipe thermal performance", Material Letters, vol. 58, no. 9, pp. 1461-1465, 2004.

88. Do K. H., Ha H. J. and Jang S. P., "Thermal resistance of screen mesh wick heat pipes using the water based Al_2O_3 nanofluids", International Journal Of Heat and Mass Transfer, vol. 53, no.25, pp. 5888-5894, 2010.

89. Ghanbarpour M., Nikkam N. Khodabandeh R, Toprak M. S. and Muhammed M., "Thermal performance of screen mesh heat pipe with Al_2O_3 nanofluid", Experimental Thermal and Fluid Science, vol. 66, pp. 213-220, 2015.

90. Moraveji M. K. and Razvarz S., "Experimental investigation of aluminum oxide nanofluid on heat pipe thermal performance", International Communications in Heat and Mass Transfer, vol. 39, pp. 1444-1448, 2012.

91. Putra N., Septiadi W. N., Rahman H. and Irwansyah R., "Thermal performance of screen mesh wick heat pipes with nanofluids", Experimental Thermal and Fluid science, vol.40, pp. 10-17, 2012.

92. Kole M. and Dey T. K., "Thermal performance of screen mesh wick heat pipes using water based copper nanofluids", Applied Thermal Engineering vol. 50, pp. 763-770, 2013.

93. Asirvatham L. G., Nimmagadda R. and Wongwises S, "Heat transfer performance of screen mesh wick heat pipes using silverwater nanofluids", International Journal of Heat and Mass transfer, vol. 60, pp. 201-209, 2013.

94. Liu Z. H. and Shu T., "Application of nanofluids in thermal performance enhancement of horizontal screen heat pipe", Journal of Aerospace Power, vol. 23, pp. 1623-1627, 2008.

95. Hung Y. H., Teng T. P. and Lin B. G., "Evaluation of the thermal performance of a heat pipe using alumina nanofluids", Experimental Thermal and Fluid Science, vol. 44, pp. 504-511, 2013.

96. Do K. H. and Jang S P., "Effect of nanofluids on the thermal performance of a flat micro heat pipe with a rectangular grooved wick", International Journal of Heat and Mass Transfer, vol. 53, no. 9, pp. 2183-2192, 2010.

97. Shafahi M., Bianco V., Vafai K. and Manca O., "An investigation of the thermal performance of cylindrical heat pipes using nanofluids", International Journal of Heat and Mass Transfer, vol. 53, no. 1, pp. 376-383, 2010.

98. Suresh S., Venkitaraj K. P., Selvakumar P. and Chandrasekar M., "Effect of Al_2O_3–Cu/ water hybrid nanofluid in heat transfer", Experimental Thermal and Fluid Science, vol. 38, pp. 54-60, 2012.

99. Brusly Solomon A., Ramachandran K. and Pillai BC., "Thermal performance of a heat pipe with nanoparticles coated wick", Applied Thermal Engineering, vol. 36, pp.106-112, 2012.

100. Saleh R., Putra N., Prakoso S. and Septiadi W., "Experimental investigation of thermal conductivity and heat pipe thermal performance of ZnO nanofluids", International Journal of Thermal Sciences, vol. 63, pp.125-132, 2013.

101. Utomo AdiT., Poth H., Robbins Phillip T, and Pacek AndrzejW. "Experimental and theoretical studies of thermal conductivity, viscosity and heat transfer coefficient of titania and alumina nanofluids", International Journal of Heat and Mass Transfer, vol. 55, 7772-7781, 2012.

102. Senthilkumar R., Vaidyanathan S. and Sivaraman B., "Effect of inclination angle in heat pipe performance using copper nanofluids", Procedia Engineering, vol.38, pp. 3715-3721,2012.

103. Peterson G. P., "An Introduction to Heat Pipes", John Wiley, Inc., New York, 1994.

104. JCPDS–ICDD, "The International Centre for Diffraction Data", PCPDFWIN version 2.4, Newtown Square, PA, USA, 2003

105. Nagasaka Y. and Nagashima A., Absolute measurement of the thermal conductivity of electrically conducting liquids by transient hot wire method., Journal of Physical Scientific Instruments , vol. 14, pp. 1435-1440, 1981.

106. VDI Wärmeatlas (Heat Atlas), "Berechnungsblätter für den Wärmeübergang (Calculation sheets for heat transfer)", VDI-GVC, 9 Auflage (Edition), Springer, Berlin, Heidelberg, New York, 2002.

107. Reay D., McGlen R. and Kew P., "Heat Pipes, Theory, Design and Applications", 6th Edition. Kidlington, Oxford, UK: Butterworth-Heinemann, an imprint of Elsevier, 2014.

108. Anoop K.B., Sundararajan T. and Das S. K., "Effect of particle size on the convective heat transfer in nanofluids in the developing region", International Journal of Heat and Mass Transfer, vol. 52, No. 9, pp. 2189-2195, 2009.

109. Kumar V., D. Gangacharyulu. and Tathgir R G., “Heat Transfer studies of a heat pipe”, Heat Transfer Engineering, vol.28, no. 11,pp. 964-965,2007.

110. Hung Y H., Teng T P. and Lin B G., “Evaluation of the thermal performance of a heat pipe using alumina nanofluids”, Experimental Thermal and Fluid Science**,** vol 44, pp. 504-511, 2013.

111. Kumaresan G., Venkatachalapathy S. and Asirvatham L G., “Experimental investigation on enhancement in thermal characteristics of sintered wick heat pipe using CuO nanofluids”, International Journal og Heat and Mass Transfer, vol. 72, pp. 507-516, 2014.

112 Kumar D.H., Patel H E., Kumar V R.R., Sundararajan T. Pradeep T. and Das S. K., “Model for heat conduction in nanofluids” Physical Review Letters, vol 93, No 14, 2004.

113 Dhawan, N., Gangacharyulu, D., and Bulasara, V.K., “Experimental studies on entrainment characteristics of alumina-water nanofluids”, M.Tech. Thesis, Department of Chemical Engineering, Thapar University, Patiala, India, 2015, http://dspace.thapar.edu:8080/dspace/handle/10266/3678).

PUBLICATIONS BASED ON THE RESEARCH WORK

1 Bhullar B. S, Gangacharyulu D, Das S.K, "Augmented Thermal Performance of Straight Heat Pipe Employing Annular Screen Mesh Wick and Surfactant Free Stable Aqueous Nanofluids", **Heat Transfer Engineering**,vol.38, Issue 1, 2017.

2 Bhullar B. S, Gangacharyulu D, Das S.K, 'Temporal deterioration in thermal performance of screen mesh wick straight heat pipe using surfactant free aqueous nanofluids", **Heat and Mass Transfer,** DOI: 10.1007/s00231-016-1785-6

International/National Conferences

1 Bhullar B. S, Gangacharyulu D, "Thermal Performance of Mesh wicked heat pipe using Al_2O_3 nanofluids ,17^{th} International Heat Pipe Conference , IIT Kanpur, Oct 13 -14, 2013.

2 Bhullar B. S, Gangacharyulu D, Thermal performance optimization of heat pipe using surfactant free Al_2O_3 nanofluids, 14th International Conference on Simulation and Experiments in Heat Transfer and its Applications, Ancona, Italy, 7 - 9 September, 2016.